Pathology of Infectious Diseases

Histopathological diagnosis of infectious diseases is as important as the diagnosis of malignancies, because the detection of pathogens in the pathology specimens is crucially valuable for appropriate patients' treatment. Immunohistochemical and molecular approaches can be applied using formalin-fixed, paraffin-embedded samples. In case of transmissible disorders including sexually transmitted diseases, the prompt and appropriate diagnosis will avoid avoidable transmission of infectious agents among people and eventually contribute to the safety of the human society.

Ref.-1: Tsutsumi Y. Atlas of Infectious Disease Pathology, 2000, Bunkodo, Tokyo (in Japanese). https://pathos223.com/atlas/index.htm
Ref.-2: Tsutsumi Y. Pathology of infectious diseases. 2003. https://pathos223.com/en/

References:

1) Tsutsumi Y. Atlas of Infectious disease pathology, Bunkodo, Tokyo, 2000 (in Japanese). https://pathos223.com/atlas/index.htm

2) Tsutsumi Y. Pathology of Infectious Diseases (online), 2004. https://pathos223.com/en/

3) Tsutsumi Y. Pathology of Skin Infections. NY, USA. Nova Science Publishers; 2013, pp. 1-378.

4) Tsutsumi Y. Cytological diagnosis of infectious diseases: identification of pathogens and recognition of cellular reactions. IntechOpen: Innate Immunity in Health and Disease (eds. Saxena SK, Prakash H). 2020. doi: 10.5772/intechopen.95578

5) Tsutsumi Y. Pathology of gangrene. IntechOpen: Pathogenic Bacteria (eds. Edited by Kırmusaoğlu S, Bhardwaj SB). 2020. doi: 10.5772/intechopen.93505

6) Tsutsumi Y. Tsutsumi, Y. Pitfalls and caveats in applying chromogenic immunostaining to histopathological diagnosis. Cells 2021, 10: 1501. doi: 10.3390/cells10061501

7) Tsutsumi Y. Pathology of streptococcal infections. IntechOpen: Antibiotic Resistance - New Insights (eds. Mustafa G, Saxena SK), 2022. doi: 10.5772/intechopen.105814

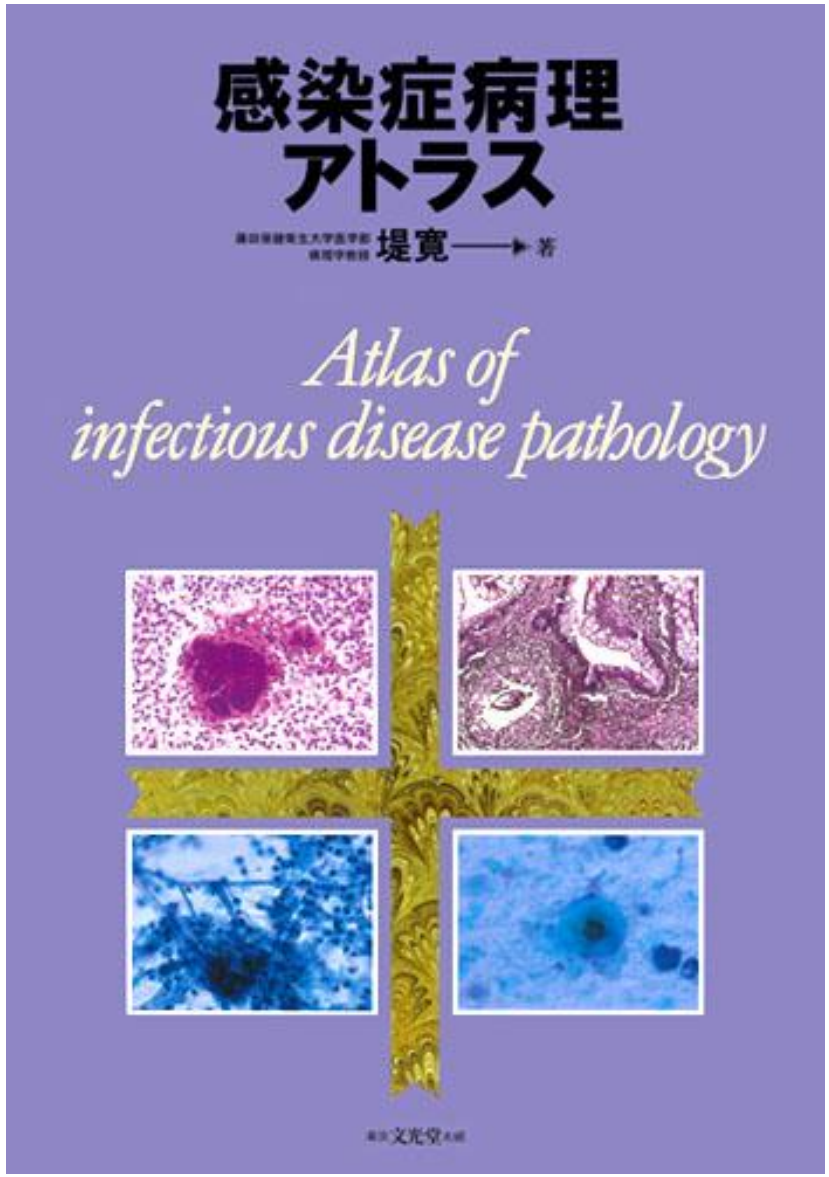

You can access my URL site.

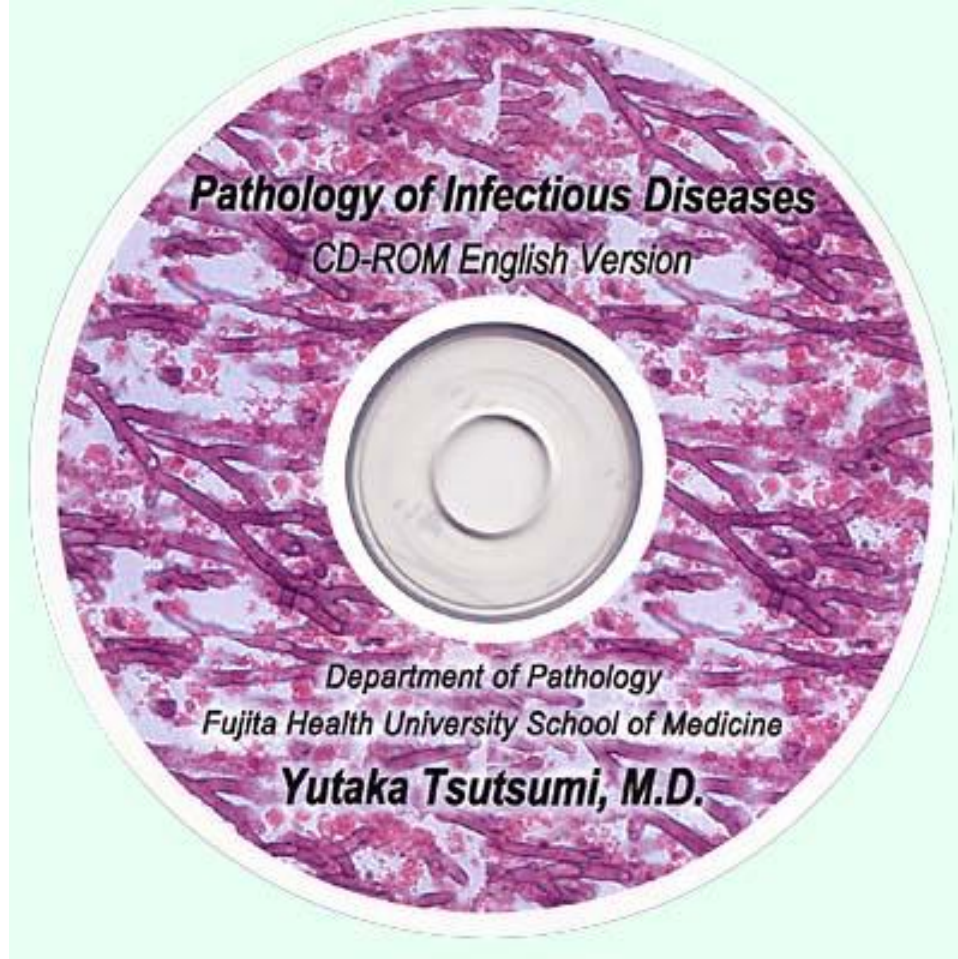

https://pathos223.com/en/

https://pathos223.com/atlas/index.htm

https://pathos223.com/atlas2017/book/index.html#target/page_no=1

PATHOS TSUTSUMI PROJECT

”Tsutsumi Pathology Library”

Yutaka Tsutsumi M.D

https://pathos223project.com

Presentation of virtual microscopic slides of infectious diseases

a) histologic sections series (H&E and special stains/immunostains

b) cytology specimens series (Papanicolaou/Giemsa/Gram stains)

Inflammatory cells

Cell	Function	Growth potential
Granulocyte		
Neutrophil	phagocytosis (mycetophagy)	no
Eosinophil	allergy, anti-parasite	no
Basophil	histamine production	no
Mast cell	histamine production	yes
Monocyte	phagocytosis	yes
Macrophage	phagocytosis, granuloma	yes
Lymphocyte	humoral/cellular immunity	yes
NK cell	nonspecific immunity	yes
Plasma cell	antibody production	no
Dendritic cell	antigen presentationno	yes

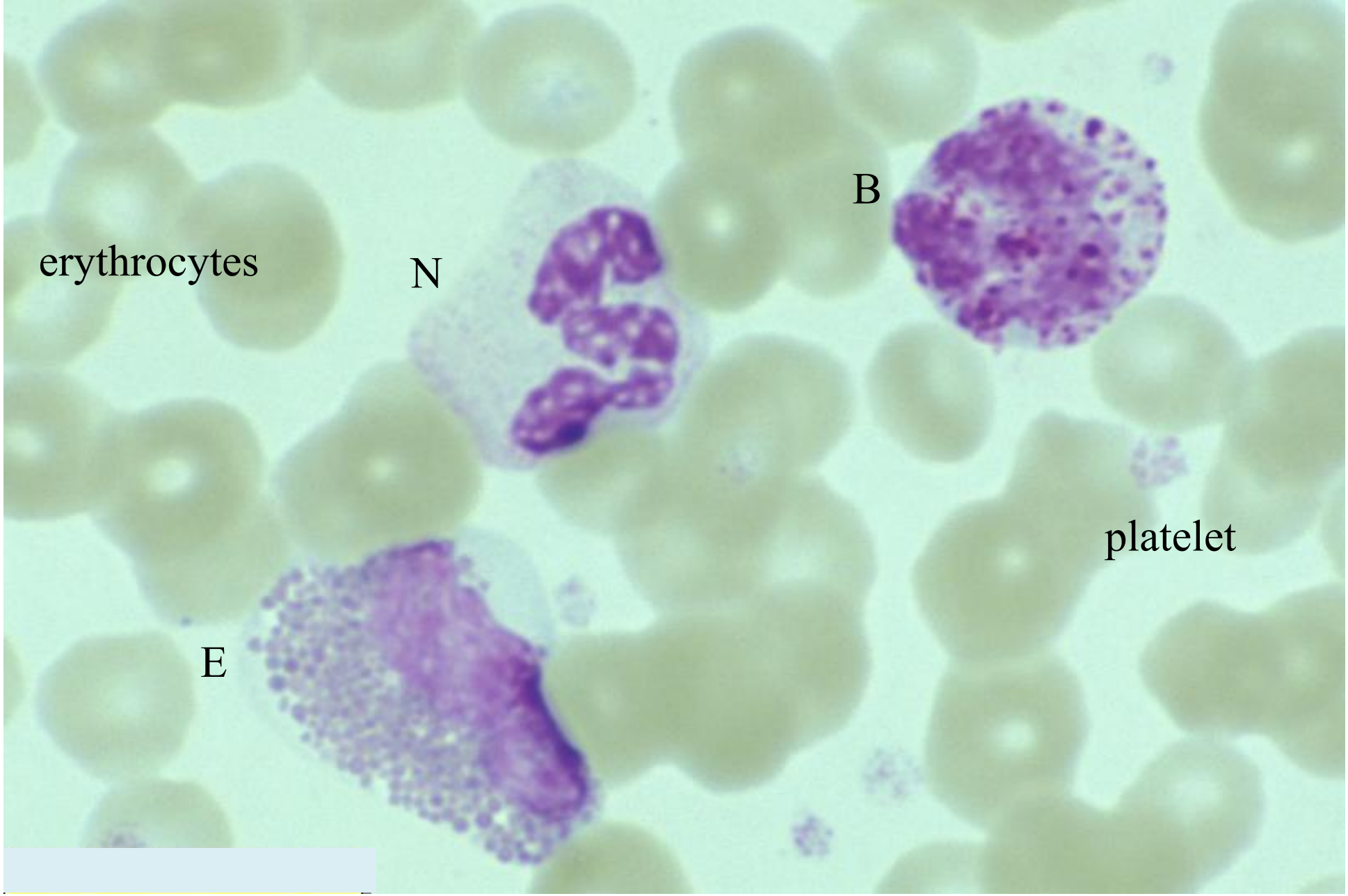

Three kinds of **granulocytes**: neutrophil (N), eosinophil (E) and basophil (B) (May-Giemsa)

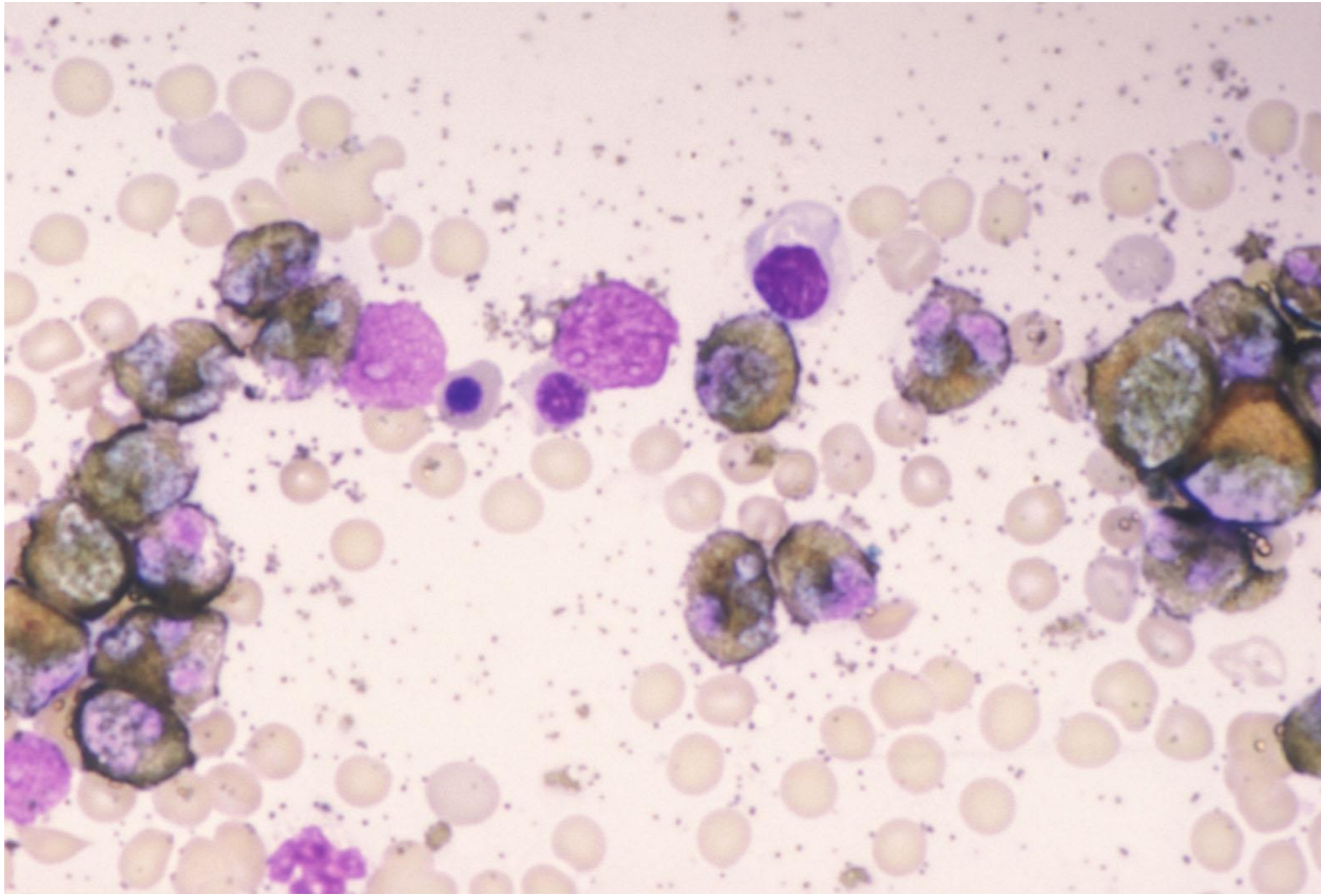

Myeloperoxidase activity of neutrophils with brown-colored reaction products

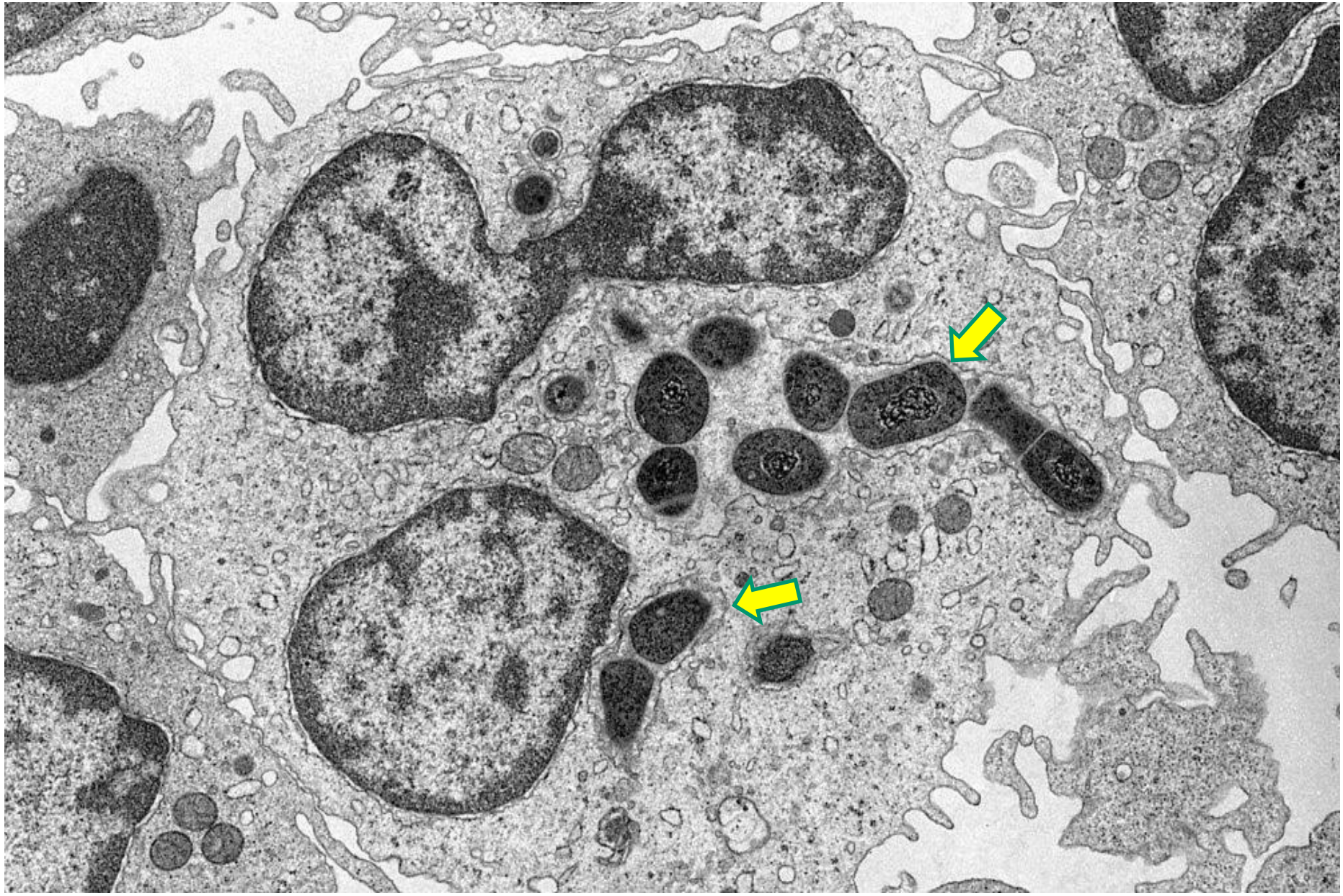

EM features of a neutrophil phagocytizing bacilli. Arrows indicate rods.

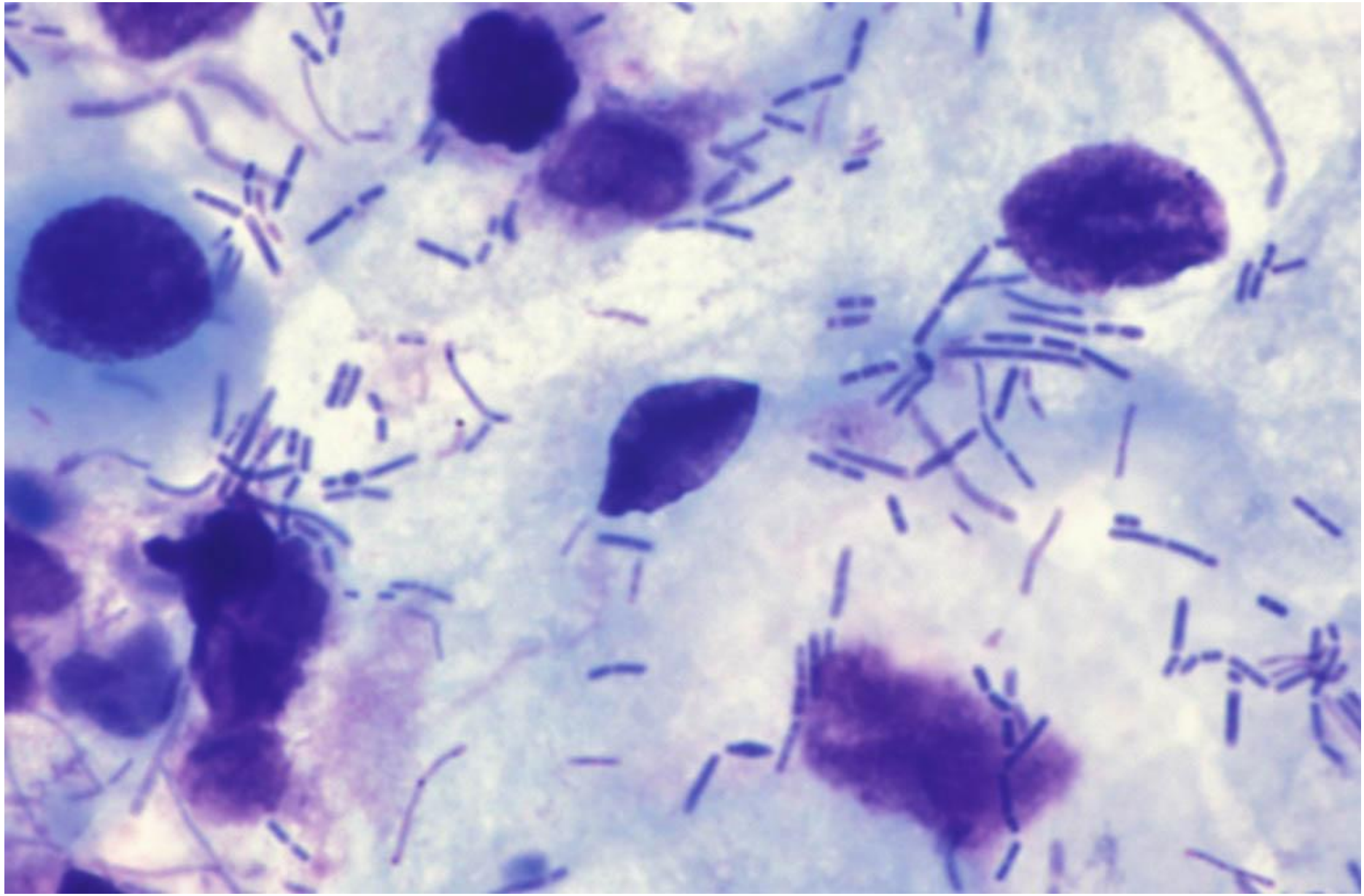

Pyruria (urine sediment: Gram-negative bacilli and neutrophils, Giemsa). Acute cystitis, common in ladies, are most frequently caused by *E. coli* infection.

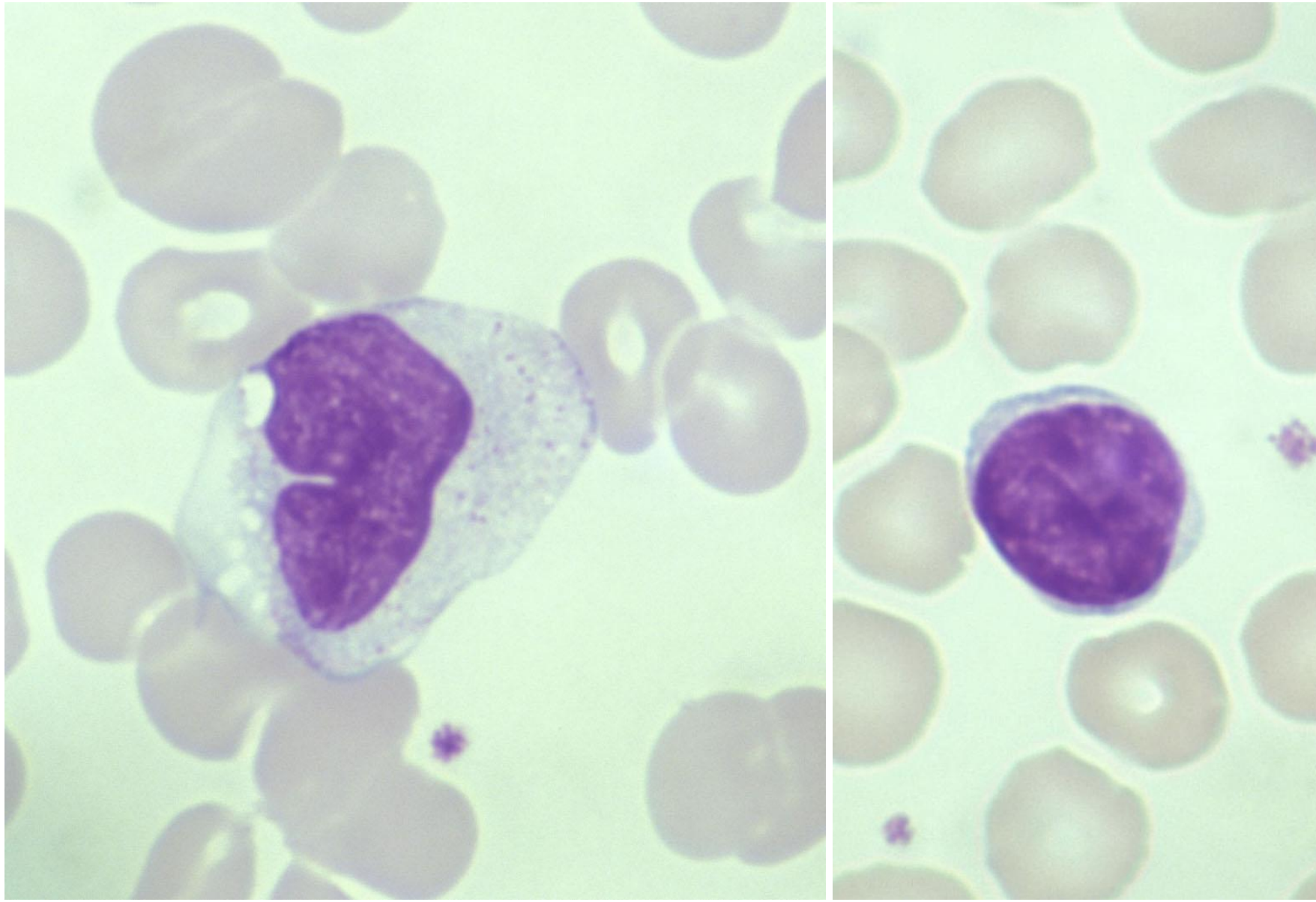

Monocyte (left) and **small lymphocyte** (right)
in the peripheral blood smear (May-Giemsa)

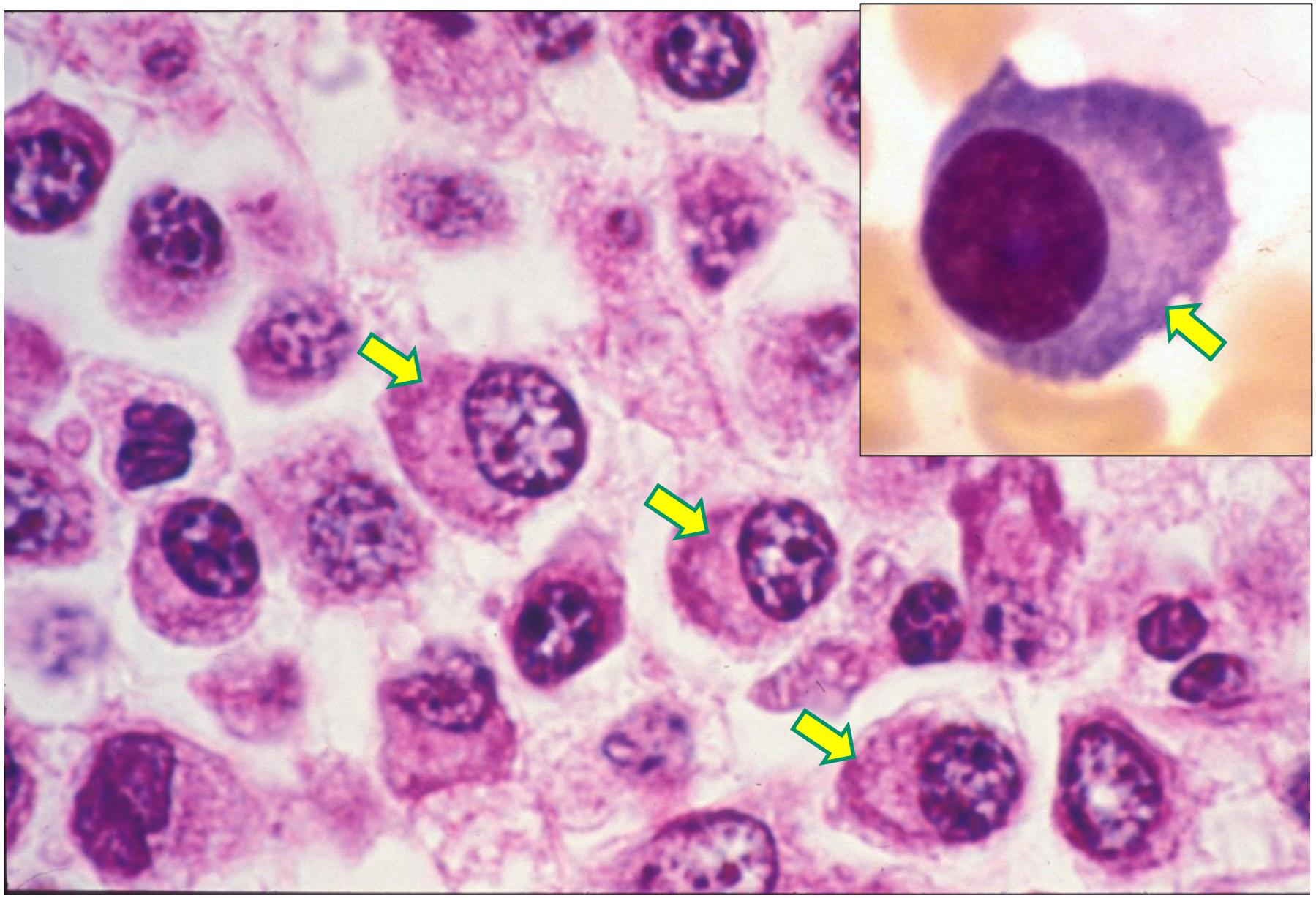

Plasma cells in granulation tissue (H&E), inset: May-Giemsa. Arrows indicate the Golgi area (“perinuclear haloe”)

Plasma cells

（Immunoelectron microscopy for IgG）

N＝nucleus

G＝Golgi apparatus

Arrows＝rER (rough endoplasmic reticula)

Plasma cells secrete immunoglobulins. rER is positive for the signals, while the Golgi apparatus is negative in the normal state.

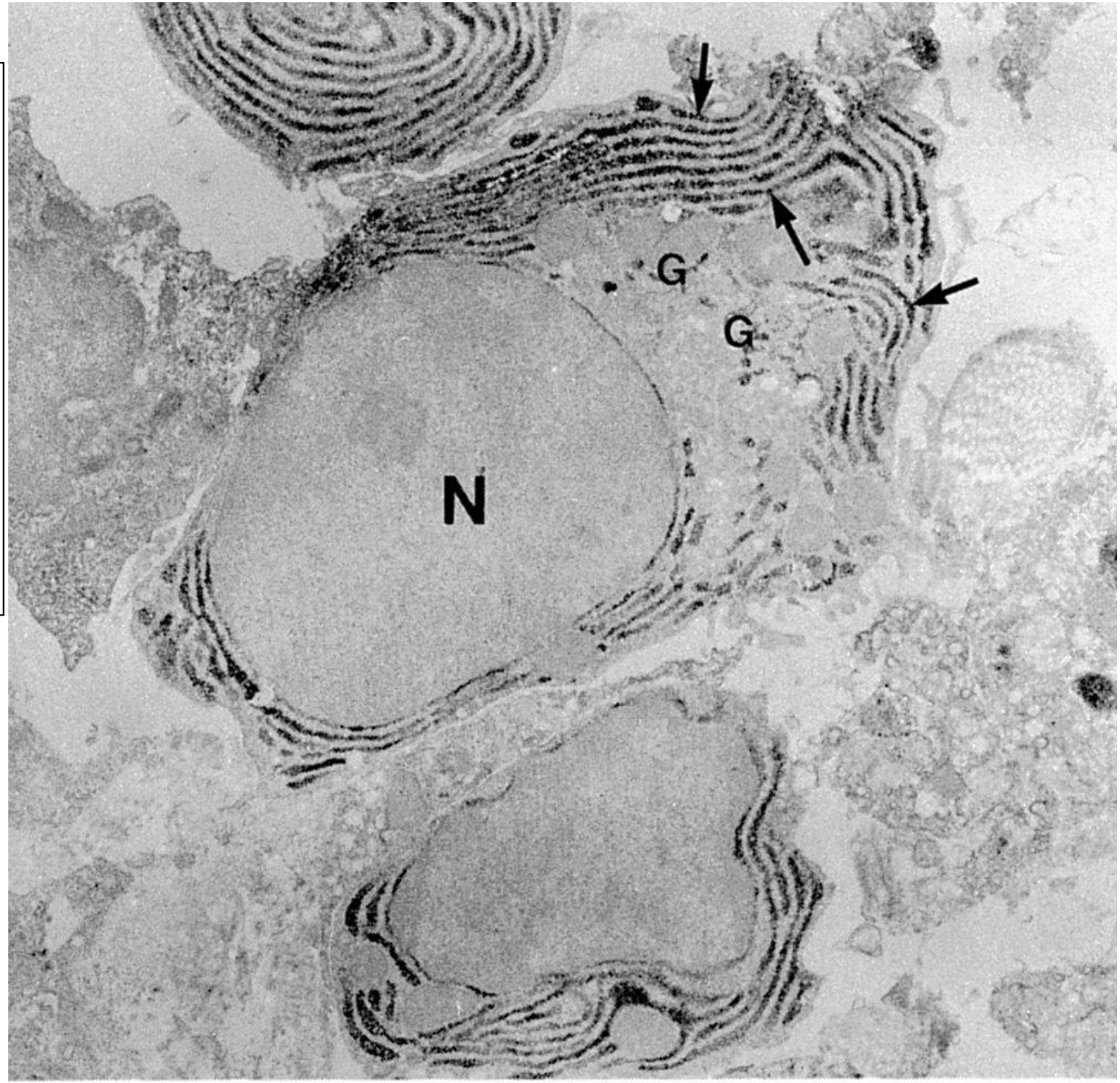

Inflammatory cellular reactions

Tissue reaction	Inflammatory cell	Pathological features
Abscess	Neutrophil	Localized lesion（acute inflammation）
Phlegmone	Neutrophil	Diffuse lesion（acute inflammation）
Eosinophilic phlegmone	Eosinophil	Allergy, Parasite infection
Lymphocytic infiltration	T/NK-lymphocyte	Chronic inflammation, viral infection
Lymphoid follicle formation	B-lymphocyte	Chronic inflammation, autoimmunity
Plasma cell infiltration	Plasma cell	Subacute inflammation, syphilis
Granuloma	Macrophage	Cellular immunity
Caseous		Tuberculosis
Foreign body		Foreign body reaction
Xanthogranuloma		Lipid metabolism
Granulation tissue	Endothelial cell	Tissue repair reaction
Acellular reaction	Red cell	Immunodeficiency

Pathogen, defense mechanism and tissue reactions

Defense cell	Causative pathogen	Features	Tissue reaction	Compromised state
Neutrophil	Aspergillus, Candida (deep-seated), Suppurative bacteria, Enterobacteria	Extracellular infection	Abscess	Bone marrow suppression
T-lymphocyte/ macrophage	Candida (surface), Cryptococcus, *Mycobacterium tuberculosis*, Protozoa, Herpesvirus	Intracellular infection	Granuloma	AIDS, steroid therapy
Neutralizing antibody/ complement	Meningococcus, Pneumococcus, *Haemophilus influenzae*, Varicella, Measles, Hepatitis B virus	Capsule-forming bacteria, Persistent infection	Phlegmonous inflammation, viral inclusion bodies	Complement deficiency, Specialized immune suppression

Status post BMT: neutropenia in early stage, suppressed cellular immunity in mid-stage, and defective antibody production in late stage

Extracellular (exogenous) pathogens

Pyogenic bacteria (Gram−negative rods, Gram−positive cocci)

Aspergillus, Candida, Mucor

→cellular reaction = neutrophils (abscess formation)

(Neutropenia provokes opportunistic infection)

Intracellular (endogenous) pathogens

Mycobacterium tuberculosis, non−tuberculous mycobacteria,

Cryptococcus, Histoplasma, Toxoplasma

→cellular reaction = macrophages + T−cells (granuloma)

Legionella, Virus, Protozoa (without granuloma reaction)

(Cellular immunodeficiency provokes opportunistic infection)

Immunity does not necessarily induce "Never Again"

- Neutralizing antibody production＝effective vaccination

  Hepatitis A, Hepatitis B, Polio, Yellow fever,

  Exanthematous viral diseases

  (Measles, Rubella, Varicella, Mumps)

  Toxin-producing bacteria (Diphtheria, Pertussis, Tetanus)

  Capsule-forming bacteria

  (Pneumococcus, Meningococcus, *Haemophilus influenzae*)

  SARS-CoV-2

- Non-neutralizing antibody production＝evidence of infection

  Hepatitis C, AIDS, EB virus, *Helicobacter pylori*, syphilis

  SARS-CoV-2

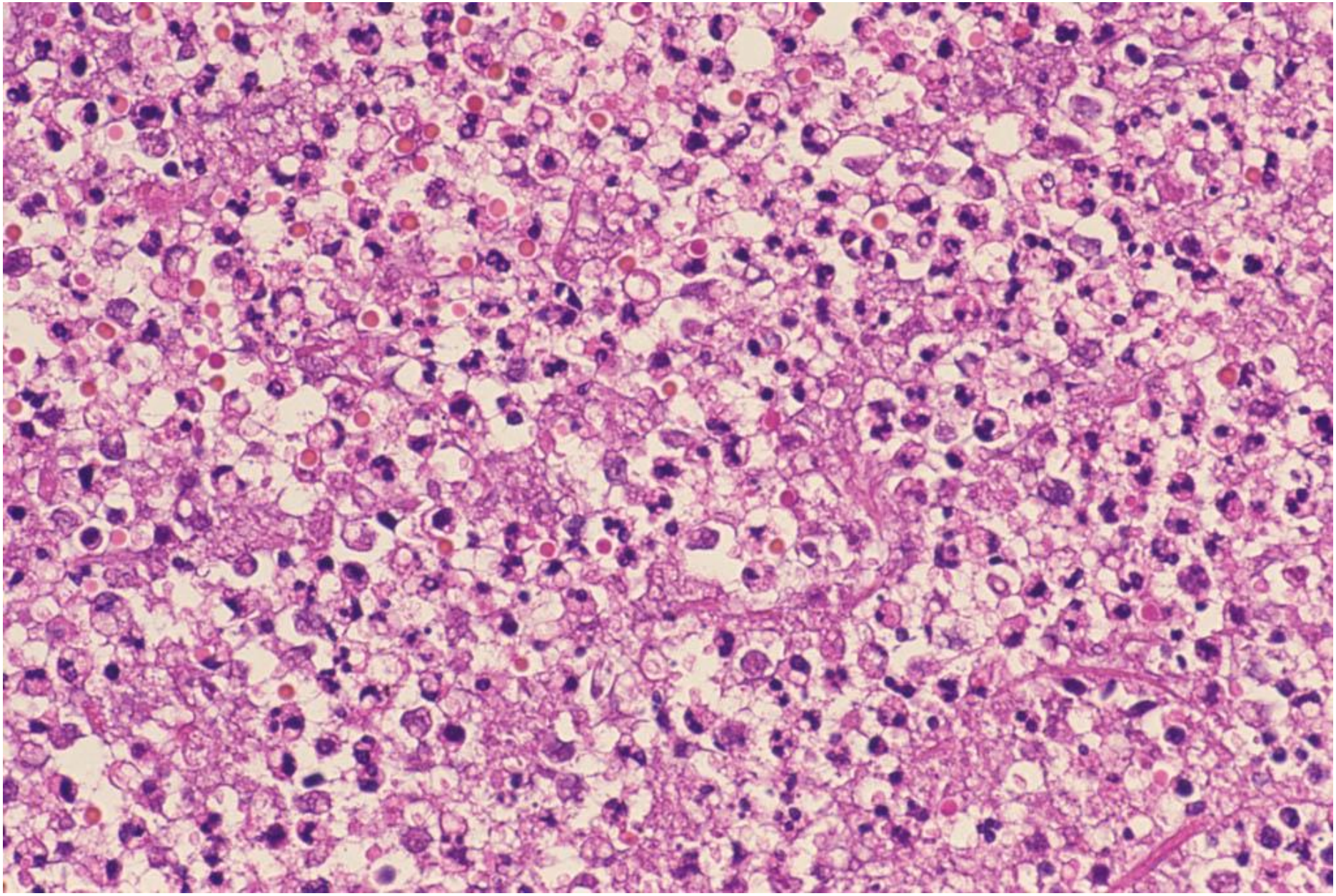

Abscess: localized accumulation of neutrophils (H&E)

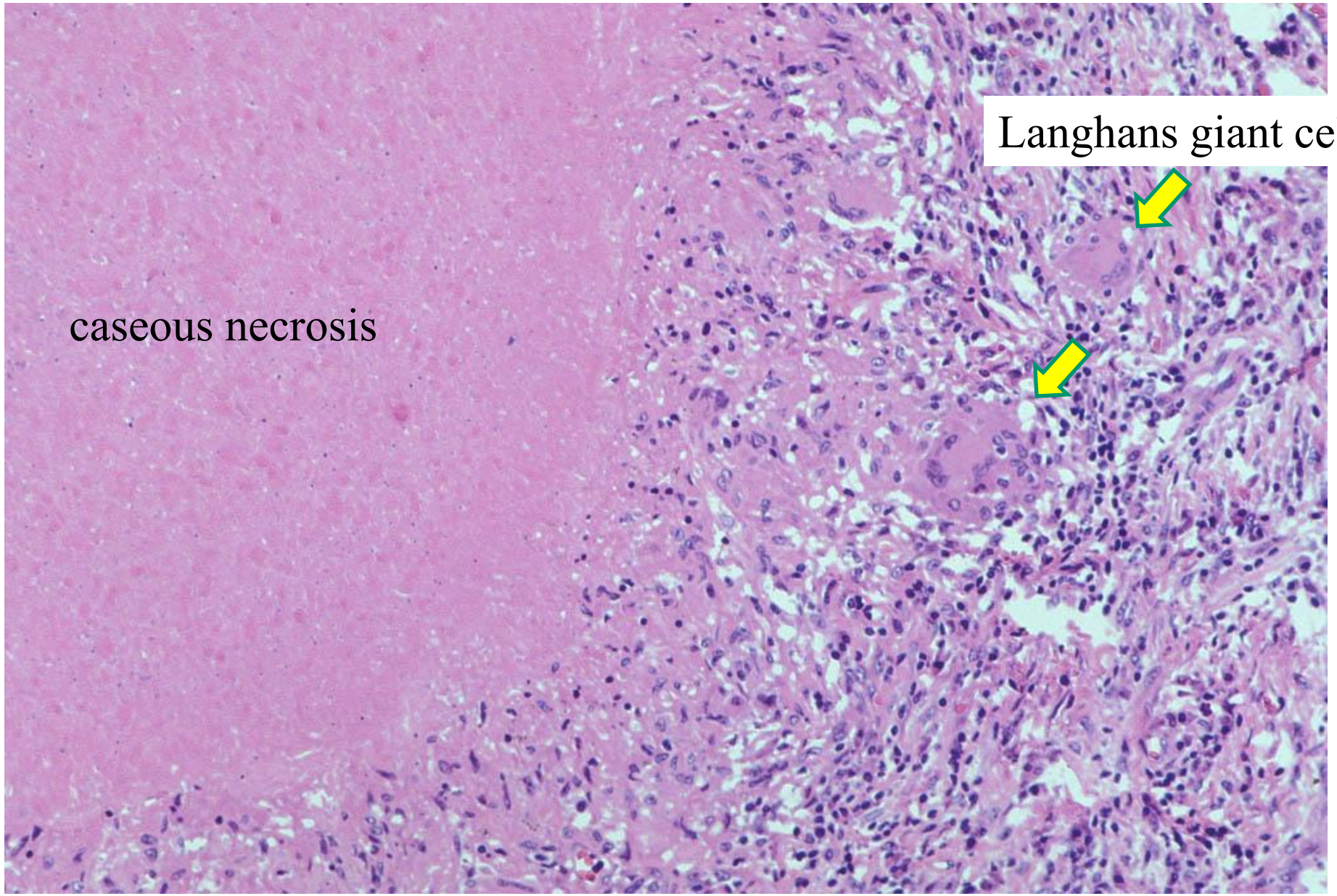

Caseous granuloma with caseous necrosis and Langhans' giant cells in **tuberculosis** (H&E)

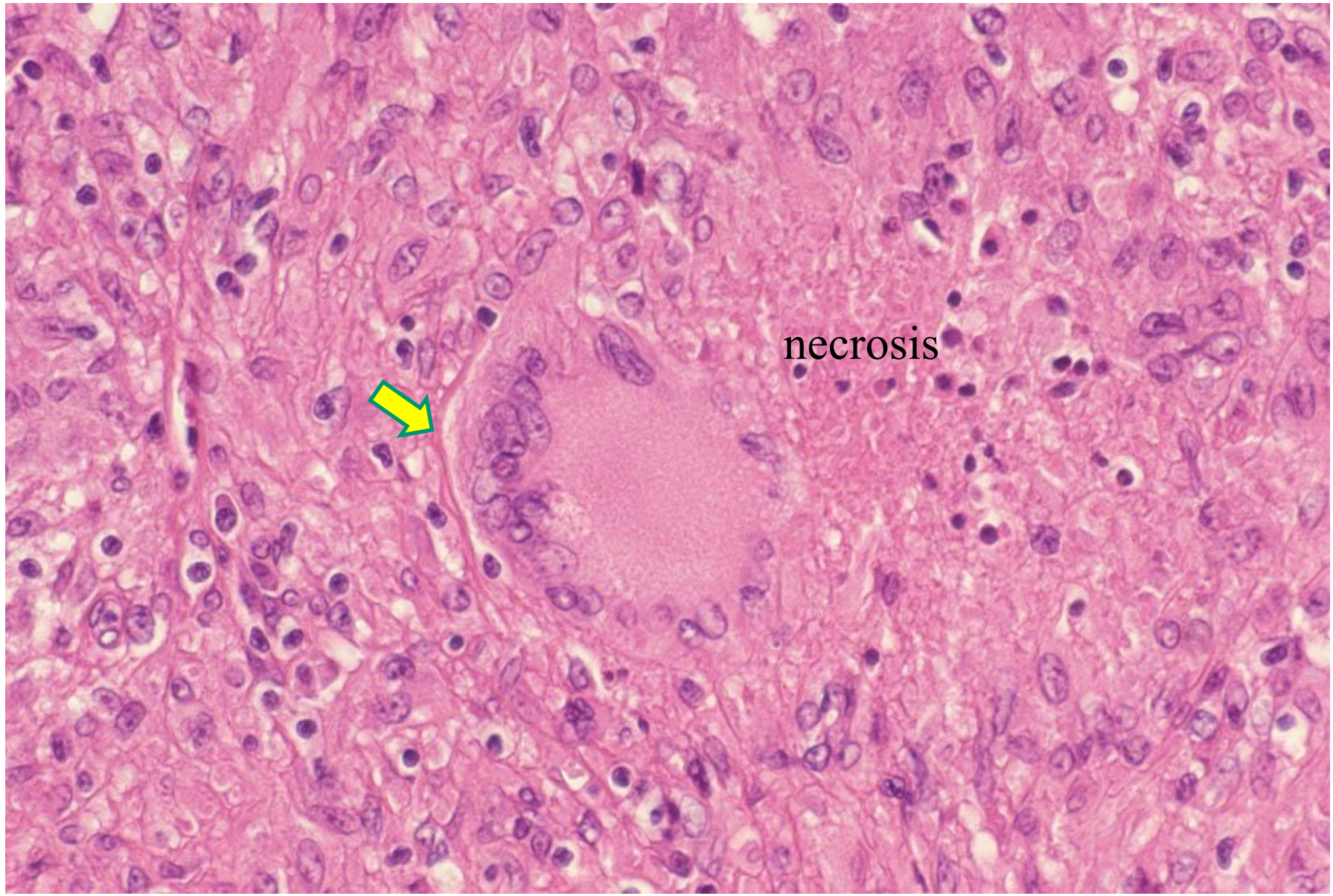

Langhans giant cell with a C-shaped nuclear arrangement in tuberculosis (arrow). The acellular zone of the giant cell faces onto the caseous necrosis (H&E)

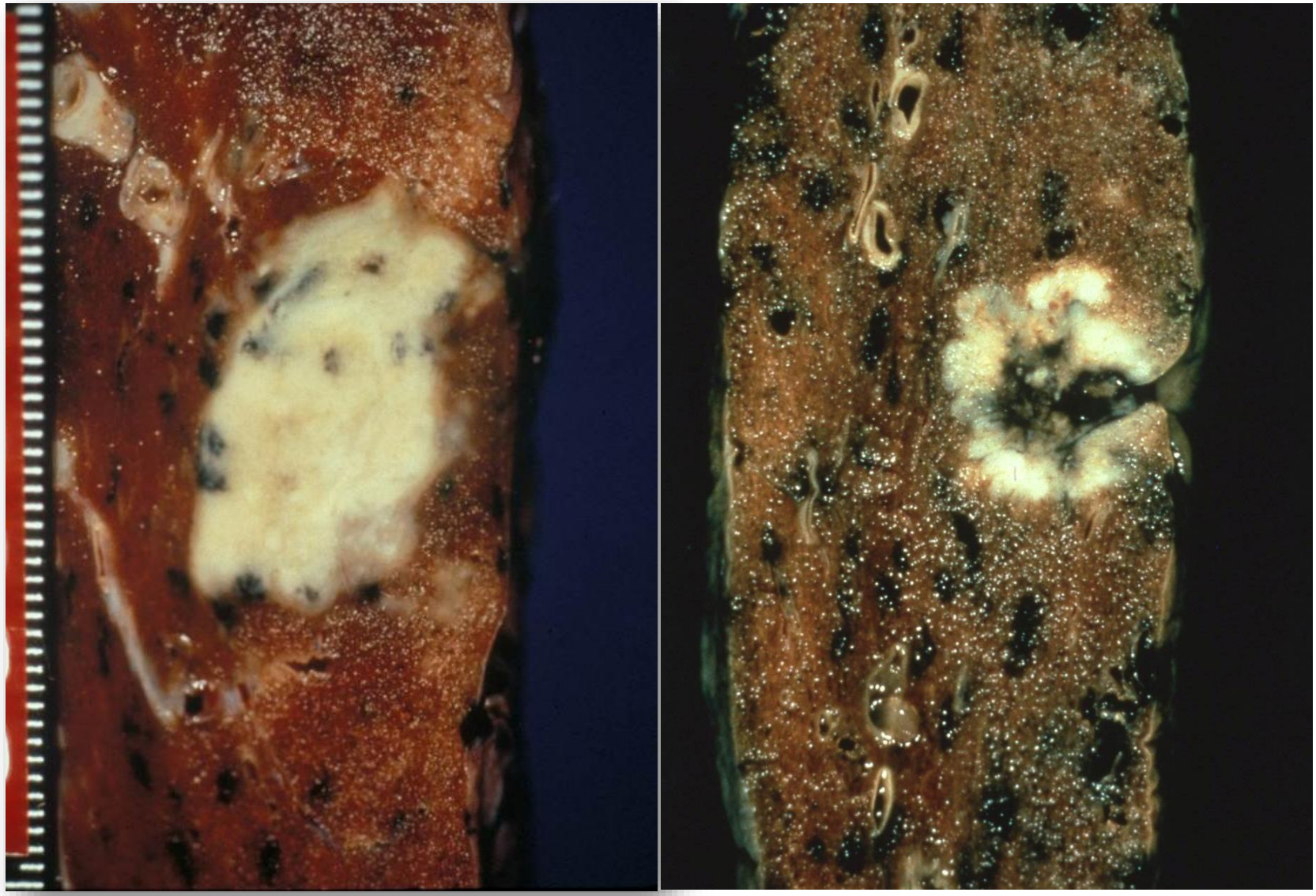

Gross appearance of lung **tuberculosis** (left) vs. lung **adenocarcinoma** (right). Caseous necrosis is a type of coagulation necrosis, and pre-existing lung structures such as anthracotic bronchioles are retained within the lesion. The lung cancer destroys the normal lung structure and forms central scarring and pleural indentation.

Eosinophilic infiltration : Helminth infection and allergy

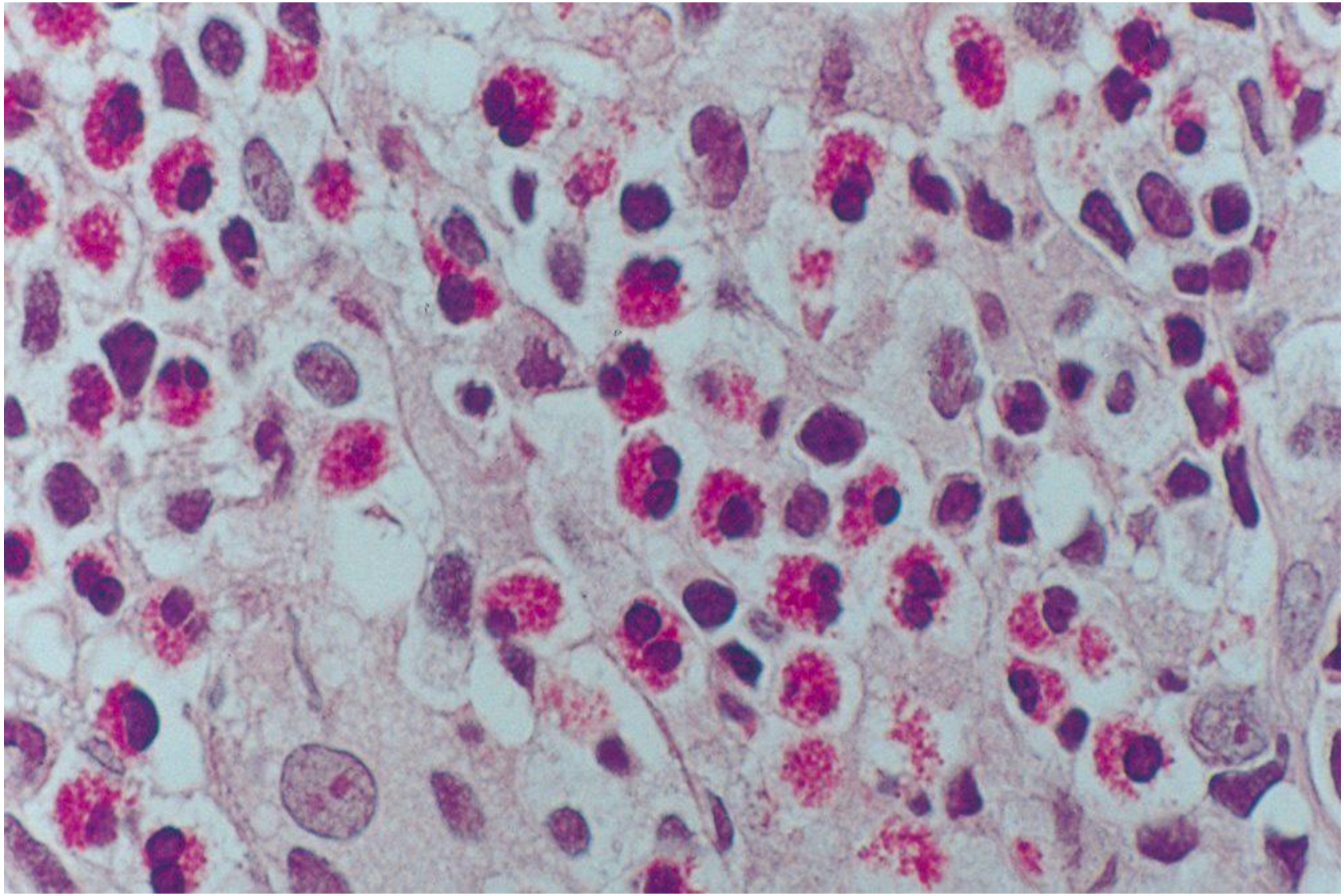

Eosinophilic infiltration in allergic rhinitis (H&E). Eosinophils are featured by bright red-stained coarse granules and bilobed (eye glasses-like) nuclei.

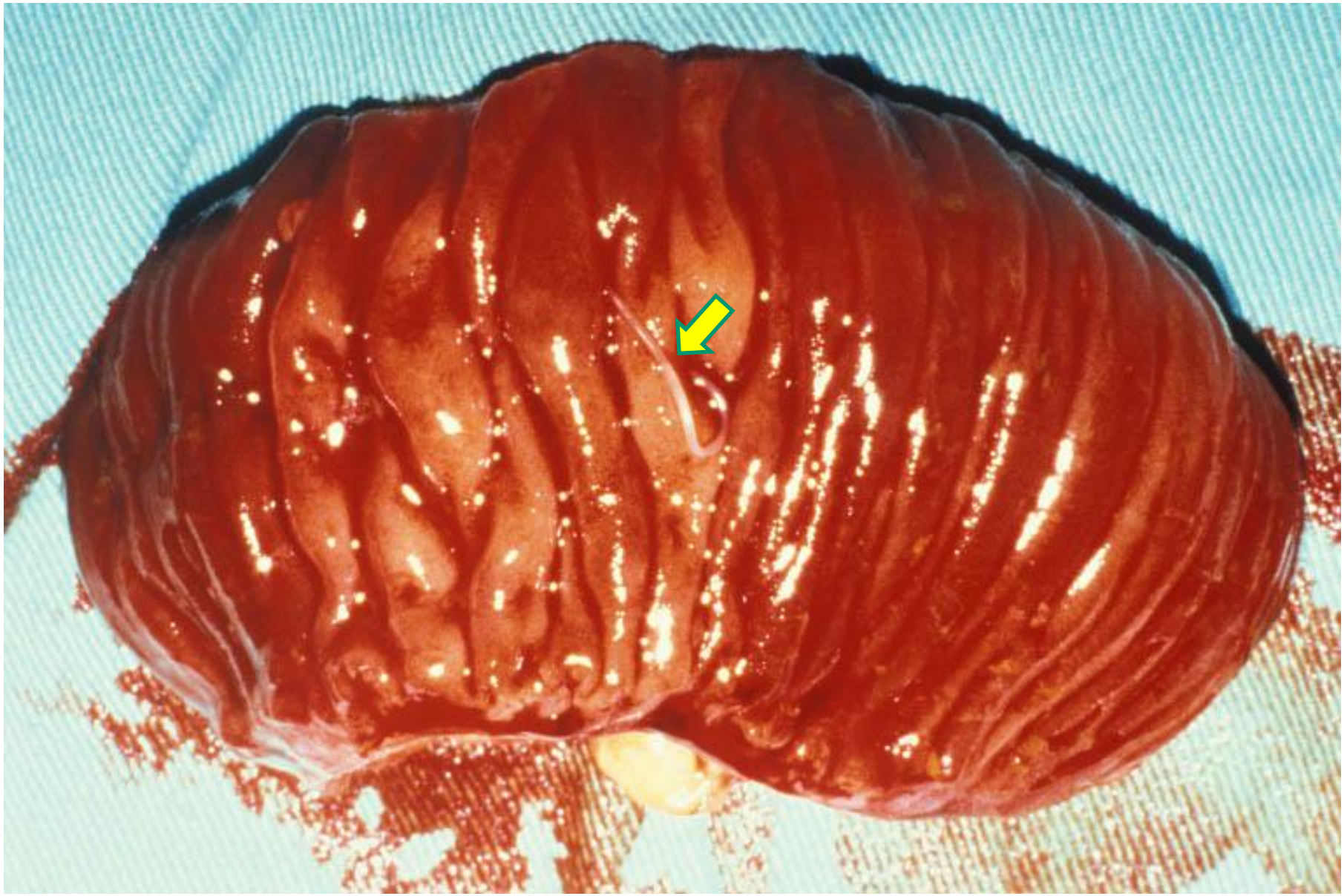

Intestinal anisakiasis presented by acute abdomen, and an emergency jejunal resection was performed. Note a thin and white nematode stuck into the jejunal mucosa (arrow).

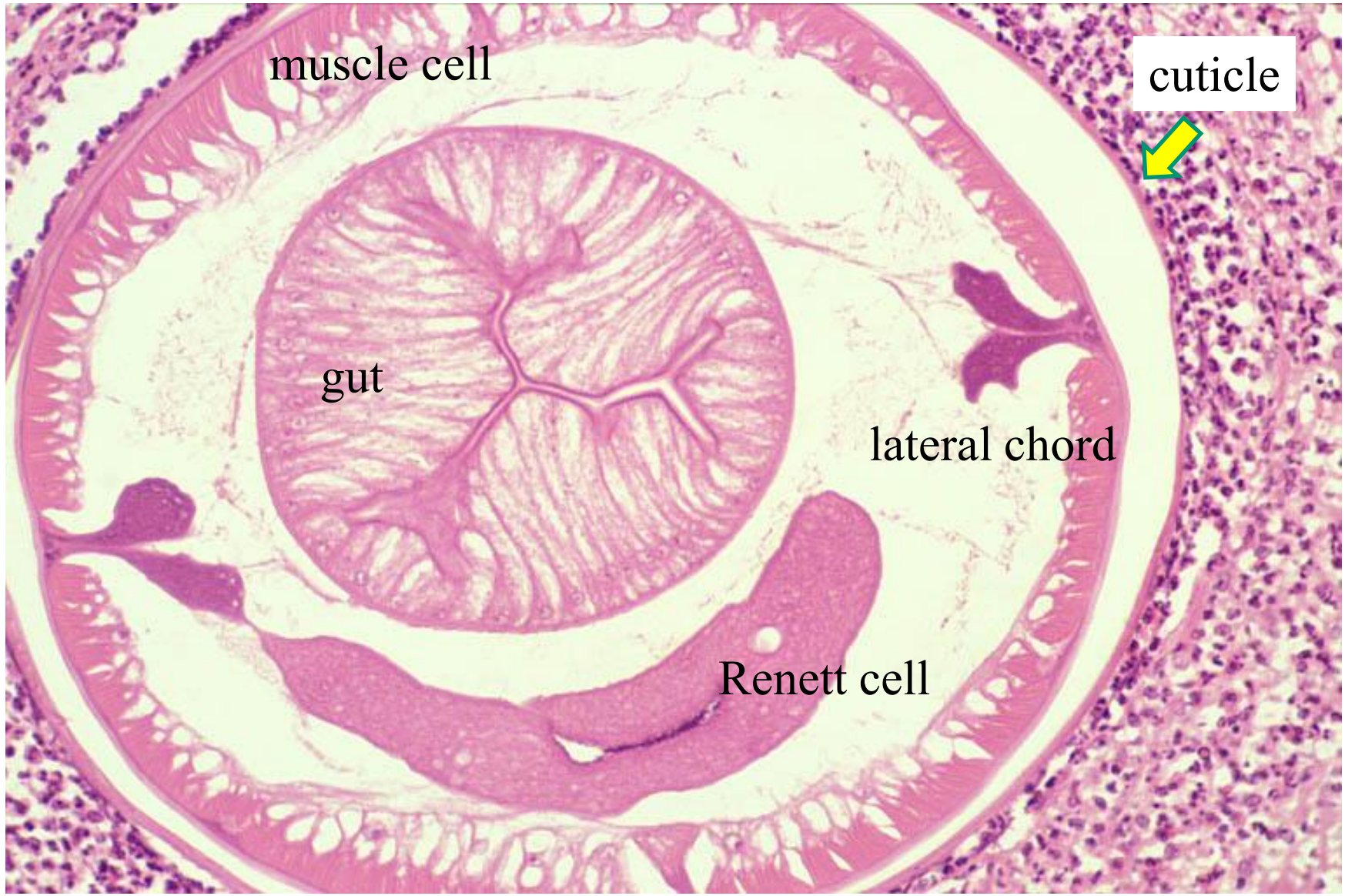

Intestinal anisakiasis. A cut surface of viable Anisakis simplex larva is shown (H&E). A pair of clover-shaped lateral chords, peripheral muscle layer inside the cuticle, gut, and Renett cell (an excretory organ) are observed. Eosinophilic phlegmonous inflammation is associated.

Infection of exotoxin-producing bacteria

Streptococcus (fulminant streptococcal infection)

Staphylococcus (food intoxication, epidermolysis)

Gas gangrene (hemolysin)

Enterohemorrhagic E. coli O-157 (hemolytic uremic syndrome)

Clostridium difficile (pseudomembranous colitis)

Diphtheria

Pertussis

Tetanus

(DPT vaccine is effectively preventive)

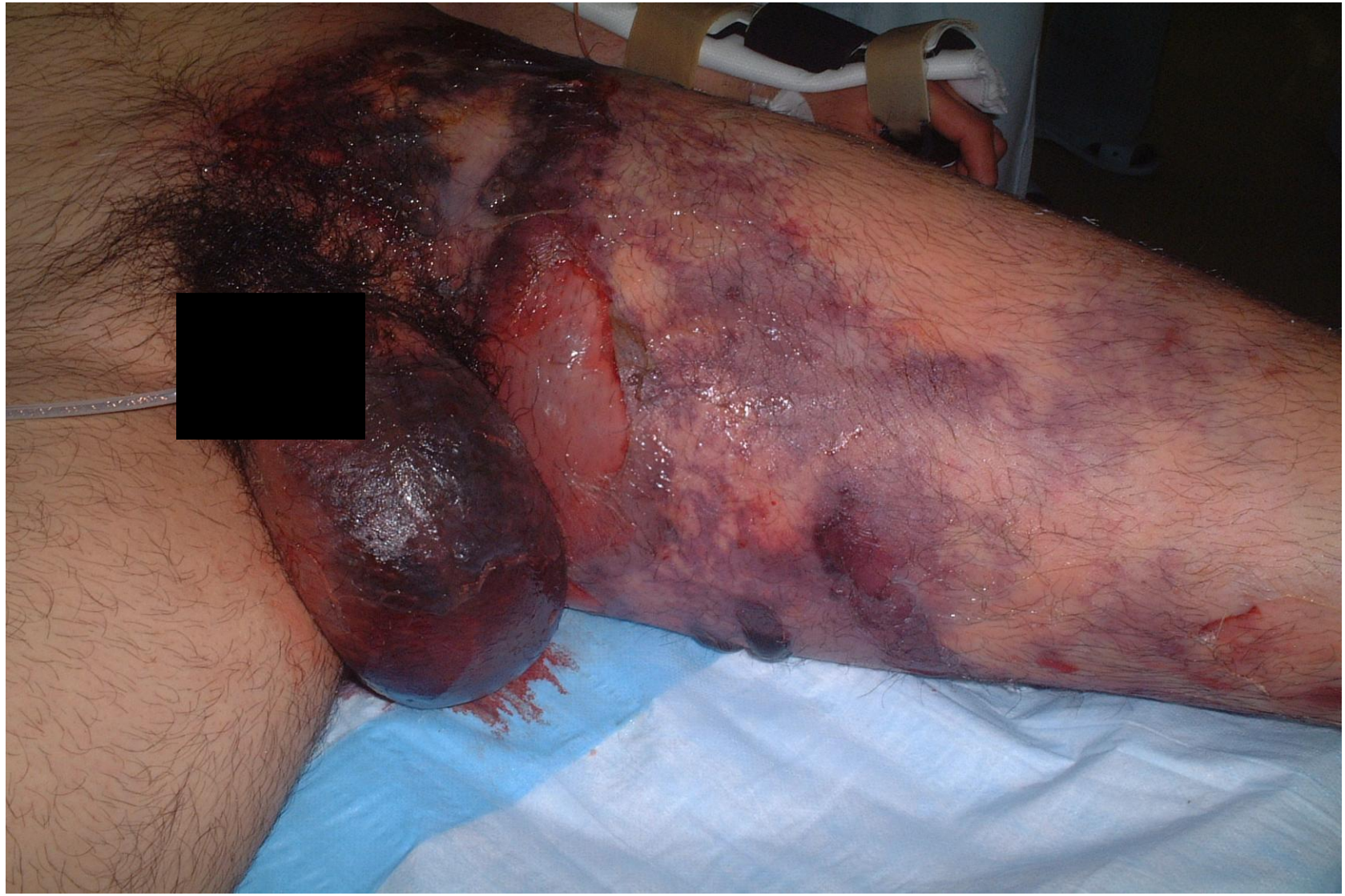

Fulminant streptococcal infection with the primary focus in the scrotum (Fournier's gangrene). Progressive gangrene in the left leg necessitated emergency amputation, but the patient died soon.

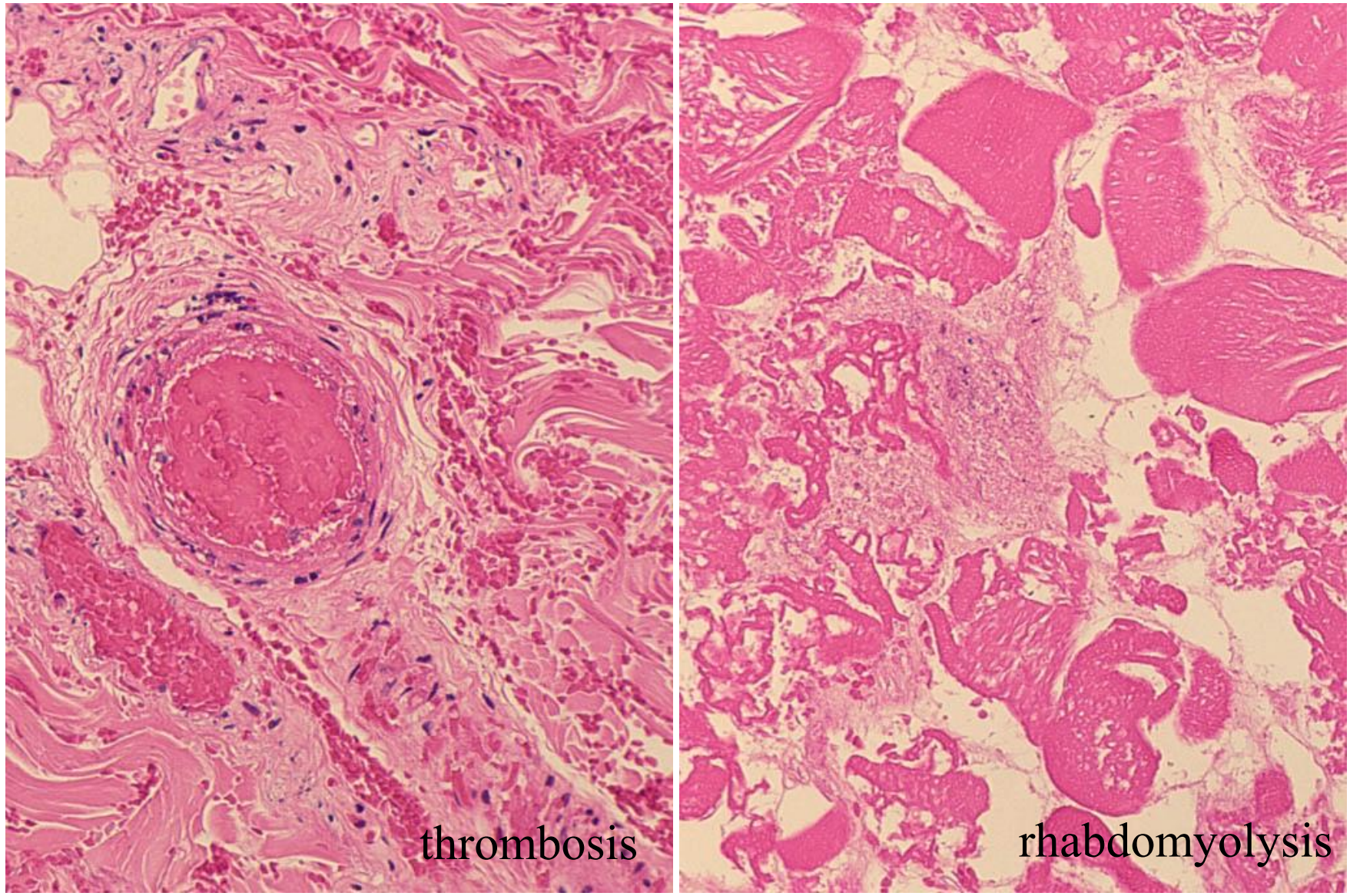

Fulminant streptococcal infection. The emergency amputated left leg shows massive ischemic changes: thrombosis (left) and myonecrosis (right) are observed (H&E).

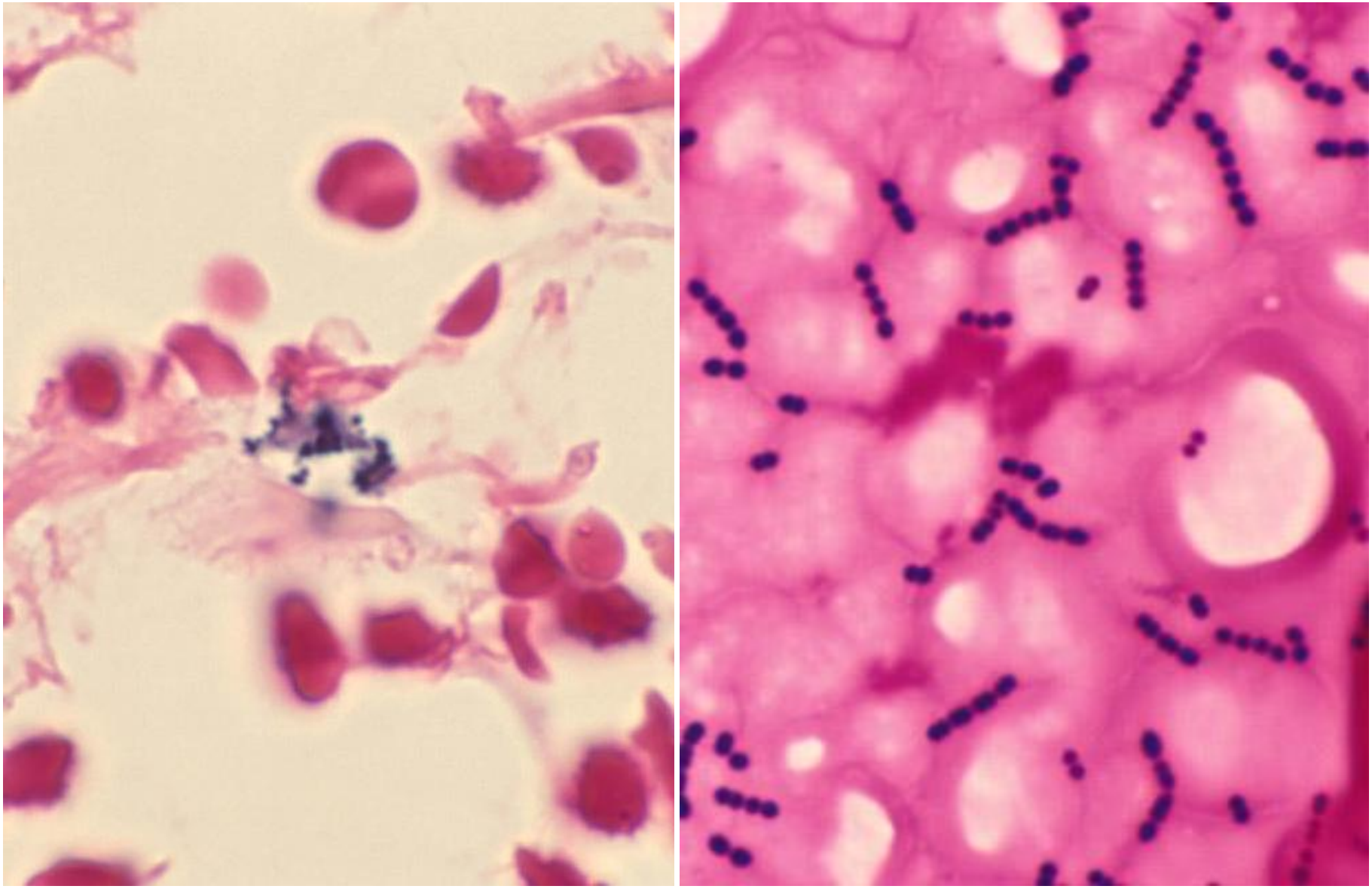

Fulminant streptococcal infection (Gram). Left: focal colonization of Gram-positive cocci in necrotic striated muscle tissue, right: the growth of chained Gram-positive cocci in the cultured peripheral blood.

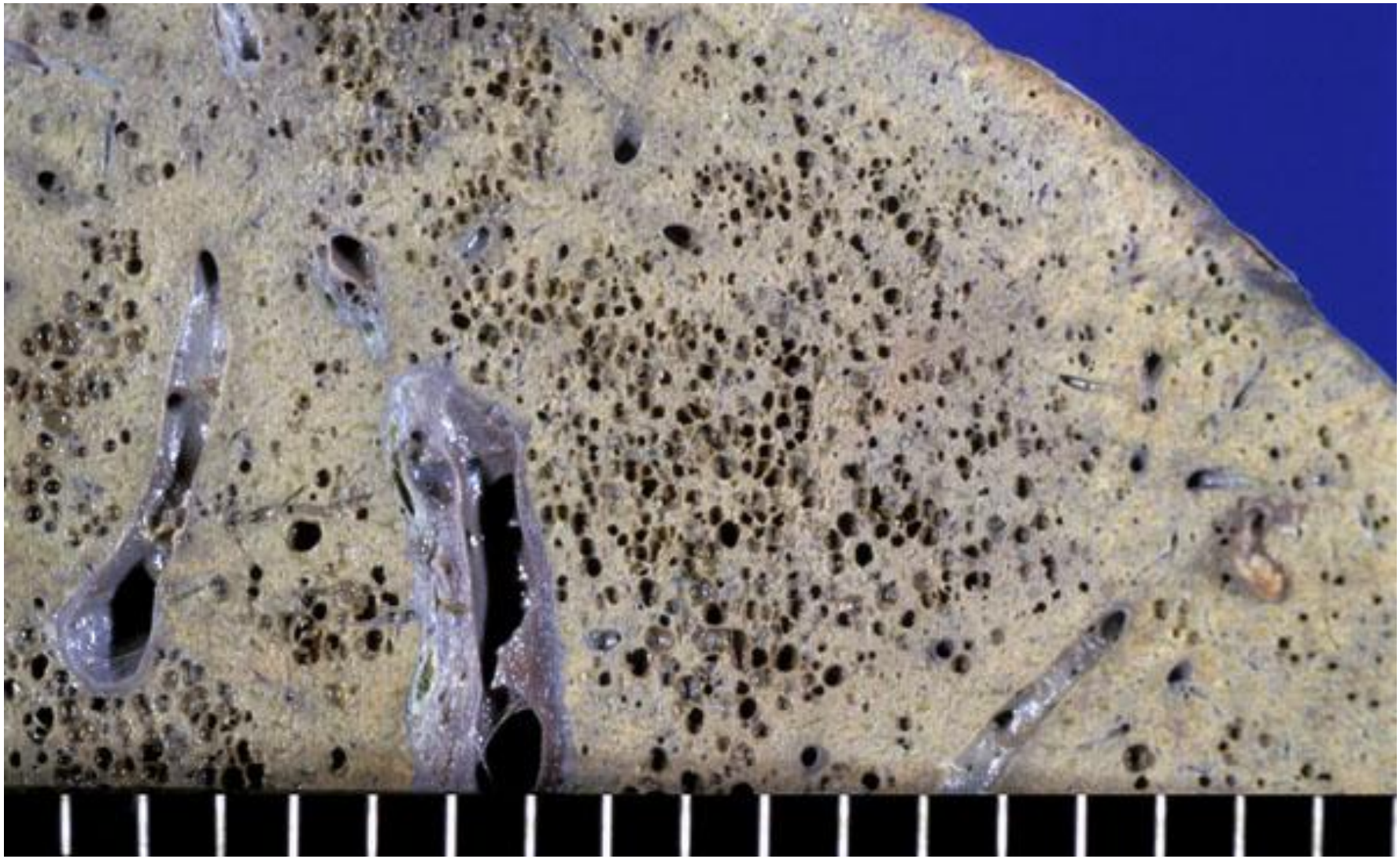

Gas gangrene. A cut surface of foamy liver after formalin fixation at autopsy.

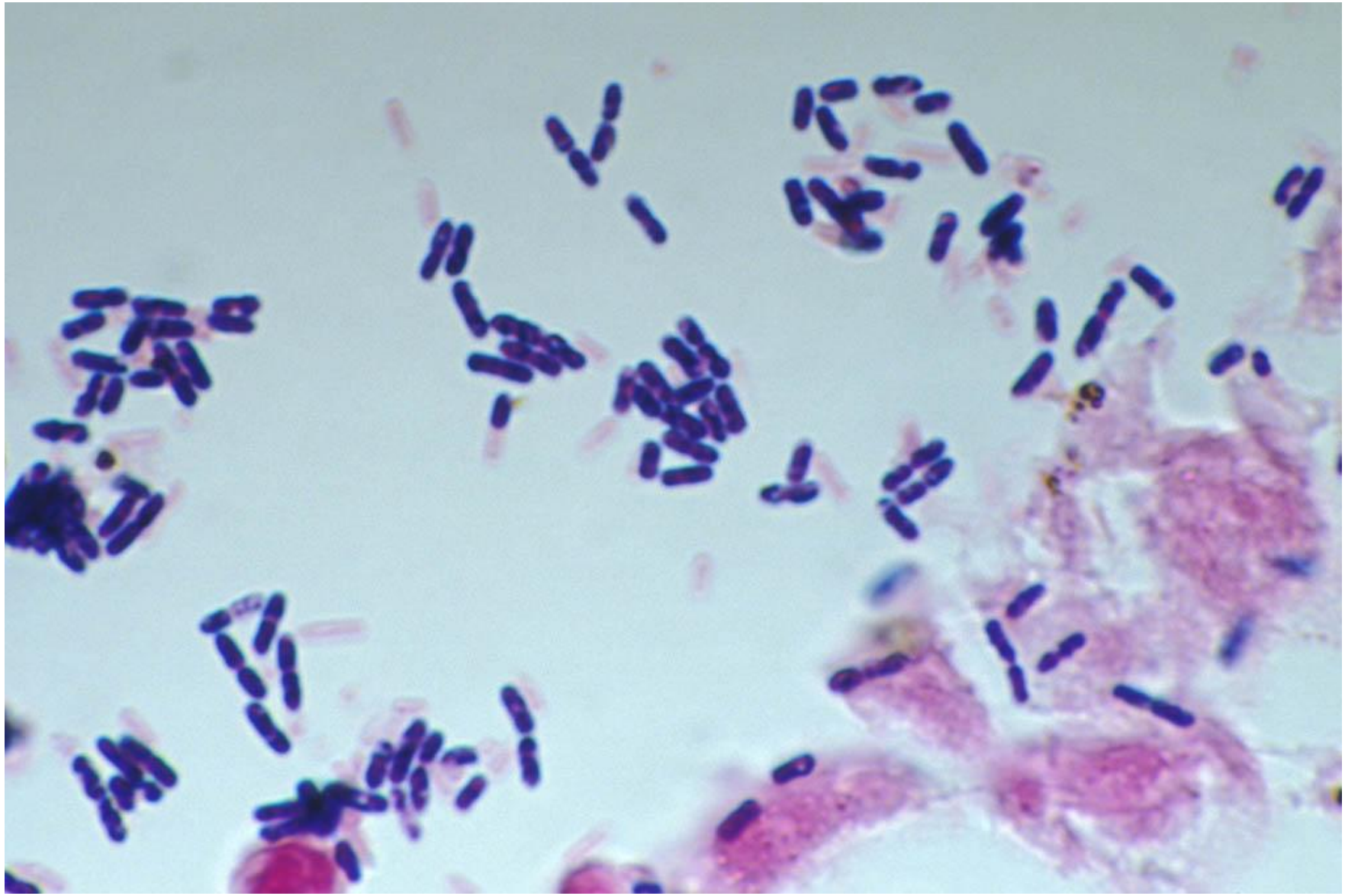

Gas gangrene: infection of *Clostridium perfringens* clustered around the gas bubble in the liver (Gram). Gram-positive rods occasionally form spores (endospores) recognized as small unstained globular structures within the bacterial cells.

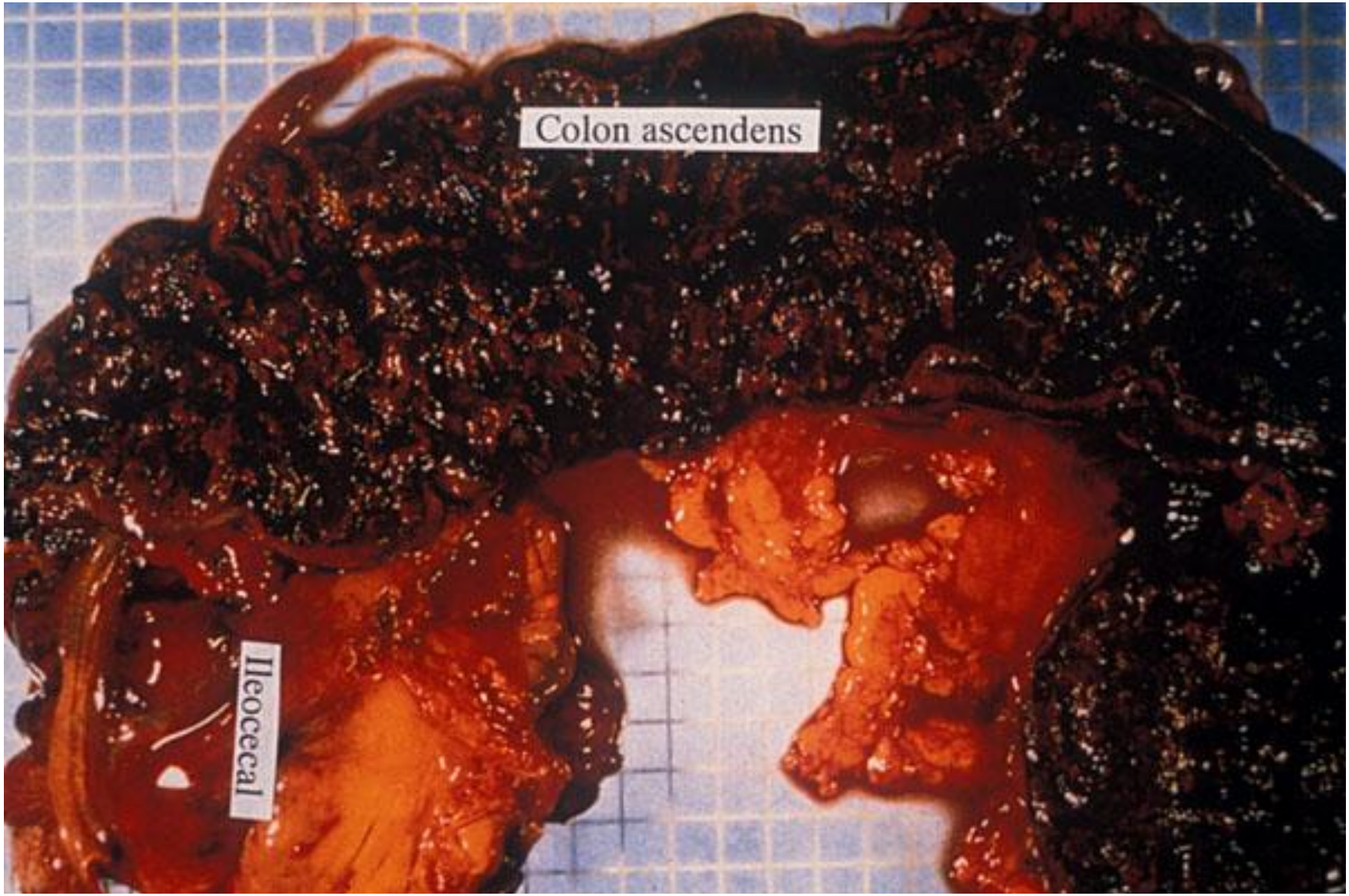

Enterohemorrhagic *E. coli* O-157 infection seen in a 4 y-o girl. The colon at autopsy grossly shows massive hemorrhage, indistinguishable from bacillary dysentery.

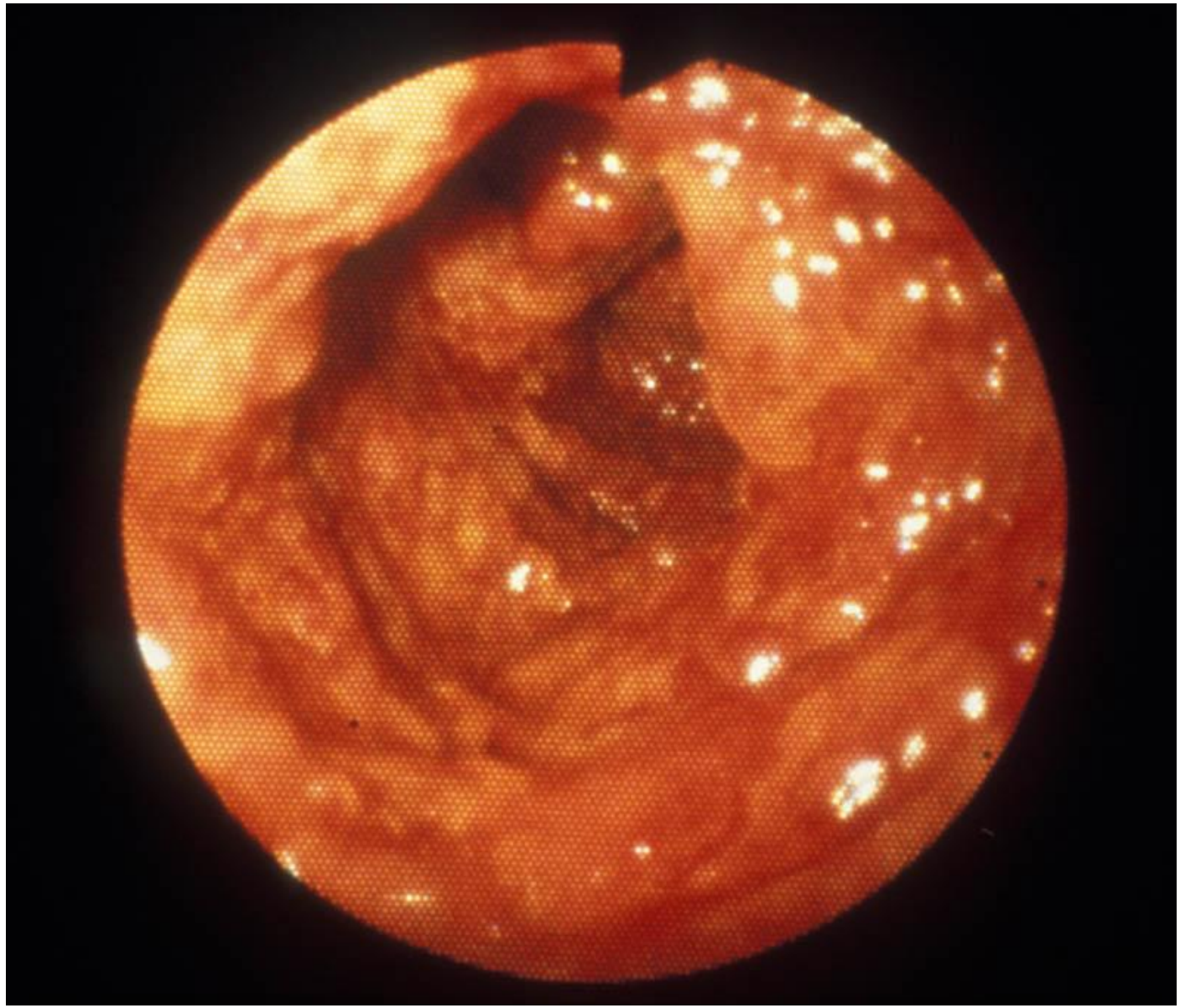

Pseudomembranous colitis: endoscopic findings of *Clostridium difficile* infection. The colonic mucosa is multifocally covered with fibrinous exudates (pseudomembranes).

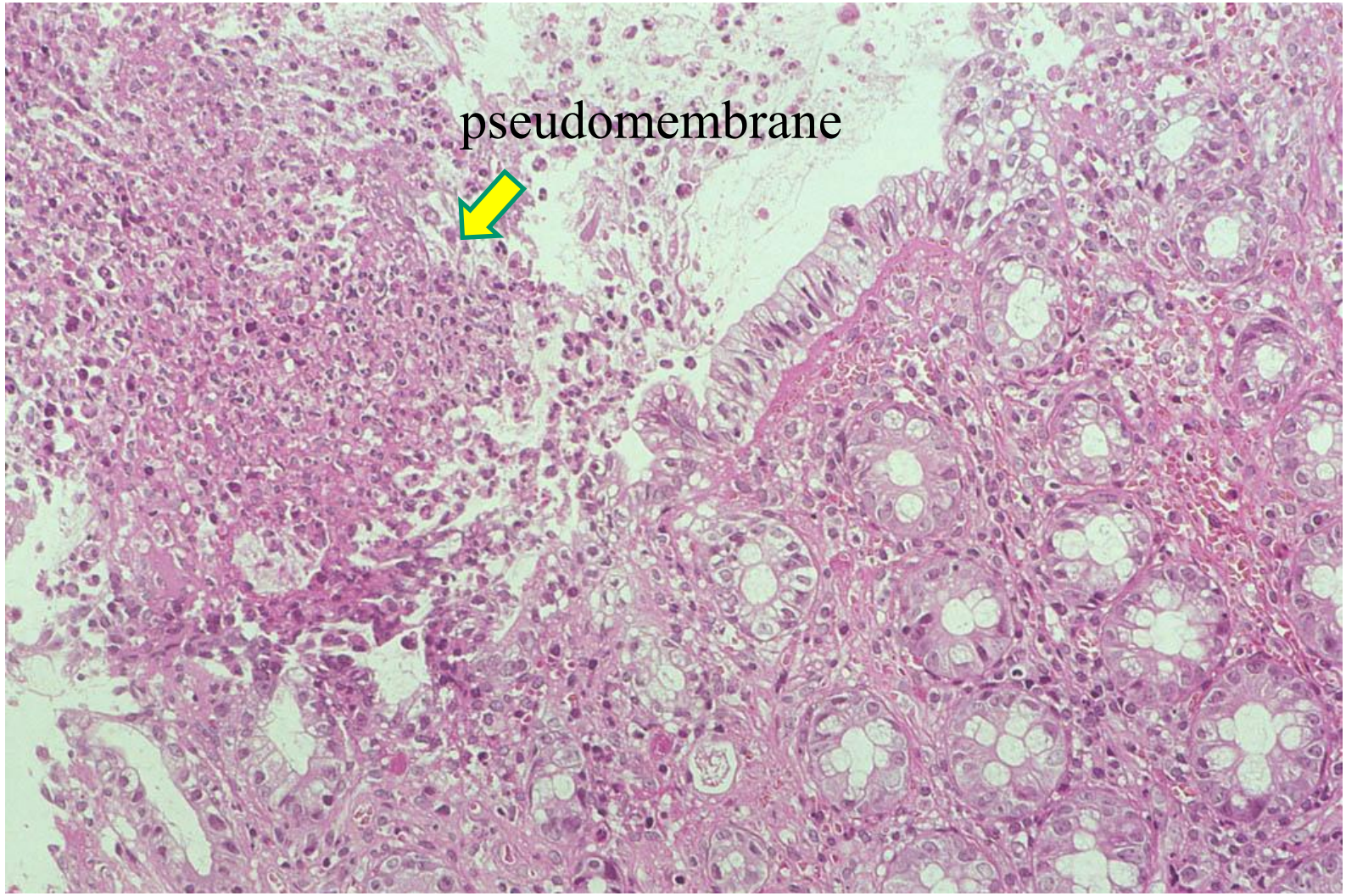

Pseudomembranous colitis: *Clostridium difficile* infection (H&E). Fibrinous and neutrophilic exudates (arrow) cover the eroded and inflamed colonic mucosa. Note that the endoscopic procedure and biopsy trial may accelerate contamination of spore-forming (disinfection-resistant) bacteria on the floor of the endoscopy room.

Facing biohazard: examples

1) Autopsy of active tuberculosis

2) Intraoperative diagnosis of tuberculous lung nodule

3) Cytology examination of the sputum or bronchial lavage of lung tuberculosis

4) Autopsy of meningococcal meningitis

5) Autopsy of Creutzfeldt-Jakob's disease (CJD)

6) Paraffin sectioning of the CJD brain

7) Cerebrospinal fluid cytology for CJD

8) Autopsy of SARS-CoV-2 infection

Autopsy of a plague patient (Manchu, China, 1911): Prof. Akira Fujinami, professor of pathology, Kyoto University, second from the left

Yersinia pestis: first isolated in 1894 in Hong Kong by Dr. Shibasaburo Kitasato and Dr. Alexandre Yersin (Swiss-French), respectively.

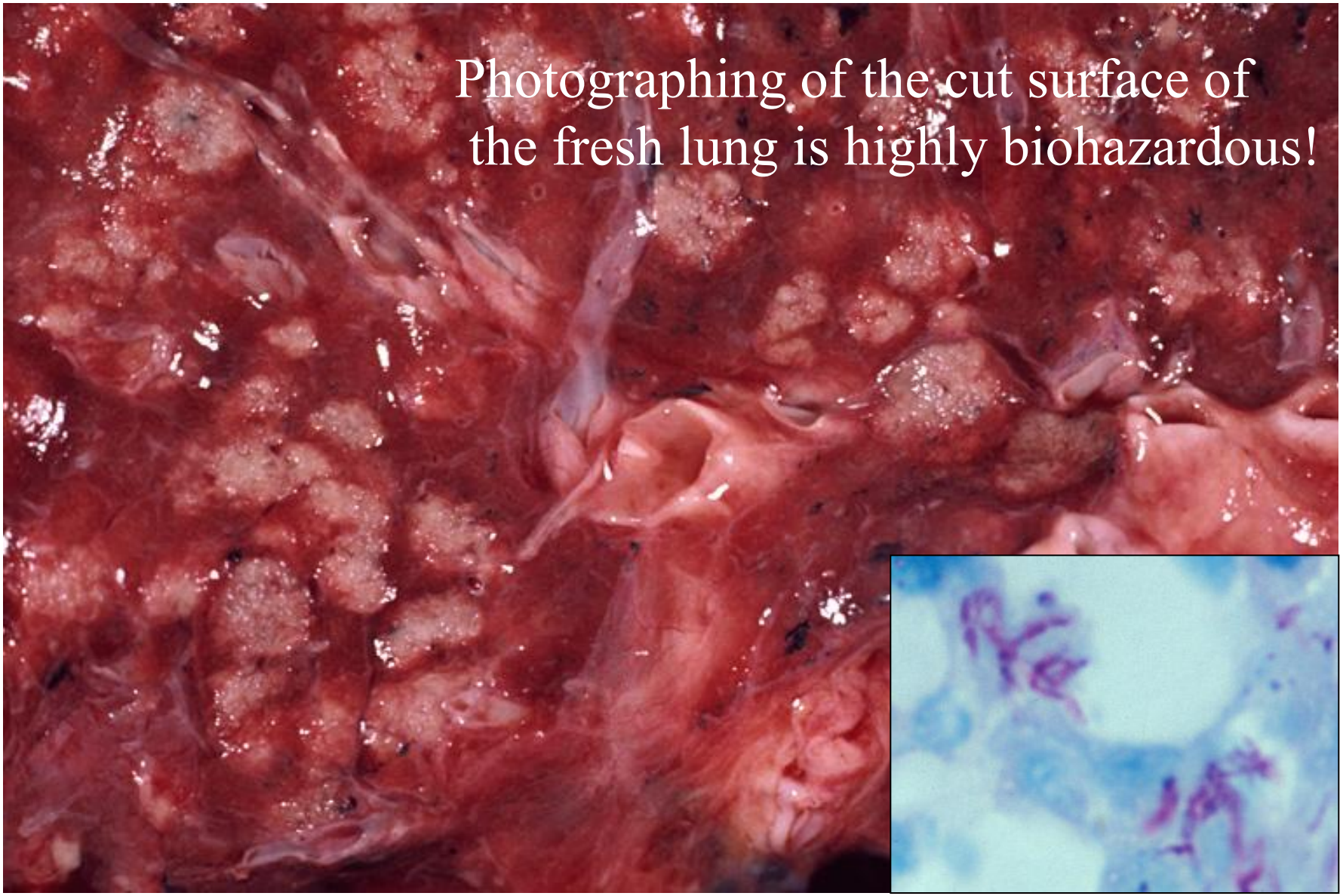

Exudative lung tuberculosis (S/P: chemotherapy for leukemia). Gross appearance (inset: Ziehl-Neelsen). The lesion with innumerable tuberculous mycobacteria is highly biohazardous.

Meningococcal meningitis accompanying Waterhouse-Friederichsen's syndrome

- A 25 years-old Japanese female staying abroad for trip
- Manifesting fever, headache and consciousness disturbance
- Death from disseminated intravascular coagulation and shock
- Clinical course: 3 days; autopsy was done next morning

  The dead body was kept overnight in a refrigerator.
- Culture of cerebrospinal fluid: negative. Why?

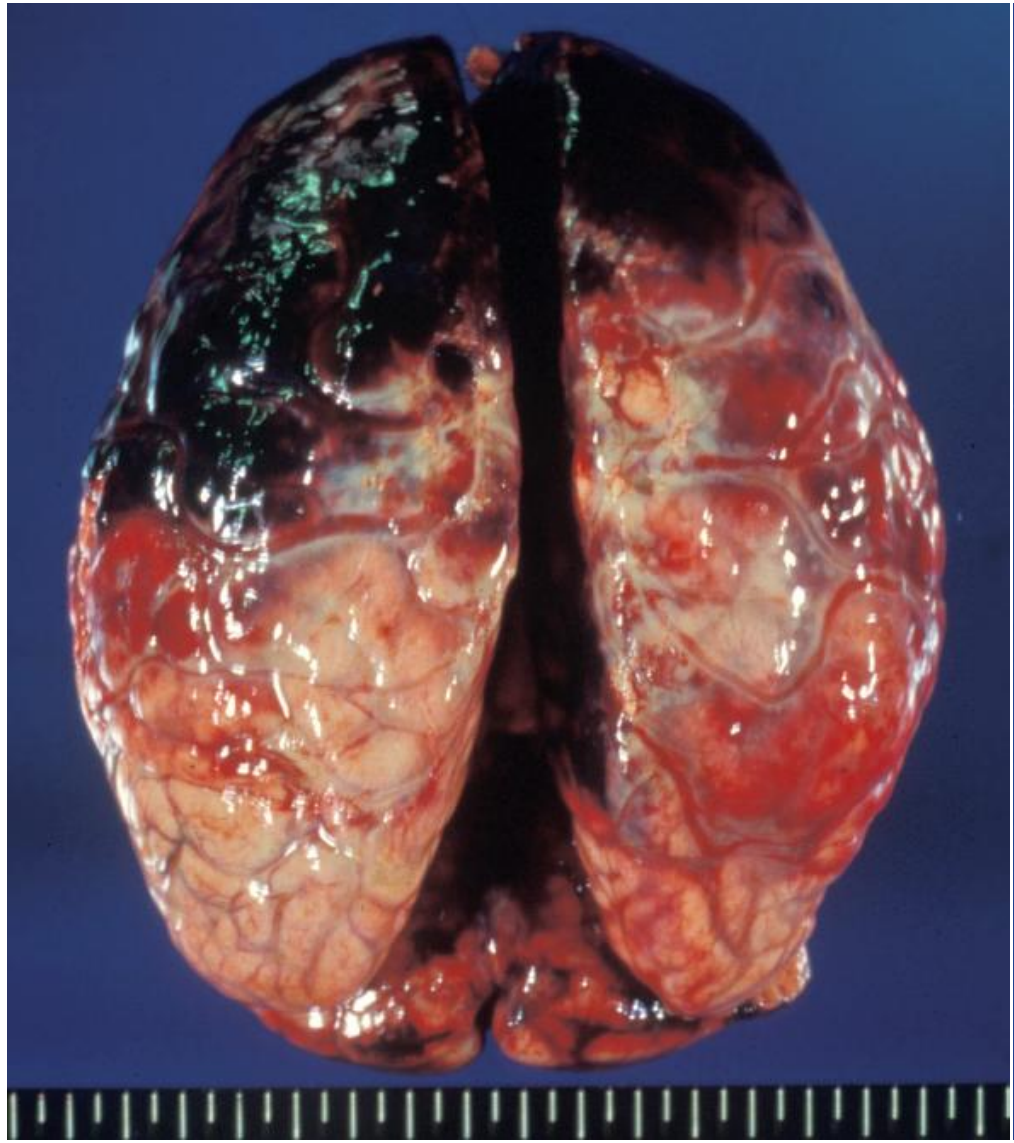

Autopsy of **acute hemorrhagic purulent meningitis** (a young lady case with 3-days clinical course). How is the biohazard against Meningococci? In the present case, the cadaver was kept in a refrigerator overnight, and this procedure greatly reduced the biohazard, since Neisseria meningitidis is highly susceptible to low temperature.

Lethal diphtheria

A 75-year-old Japanese male patient manifesting acute respiratory distress without fever. The intubation trial failed at the emergency unit, because of the stenosis by thick pseudomembranes on the upper respiratory mucosa. A piece of pharyngeal mucosa was submitted for pathology diagnosis. The patient died on the table. Autopsy was not performed. How about biohazard? Diphtheria is very infrequent in Japan, and the clinicians did not suspect the possibility of diphtheria at all. It was a lack that no secondary infections happened, probably because of DPT vaccination.

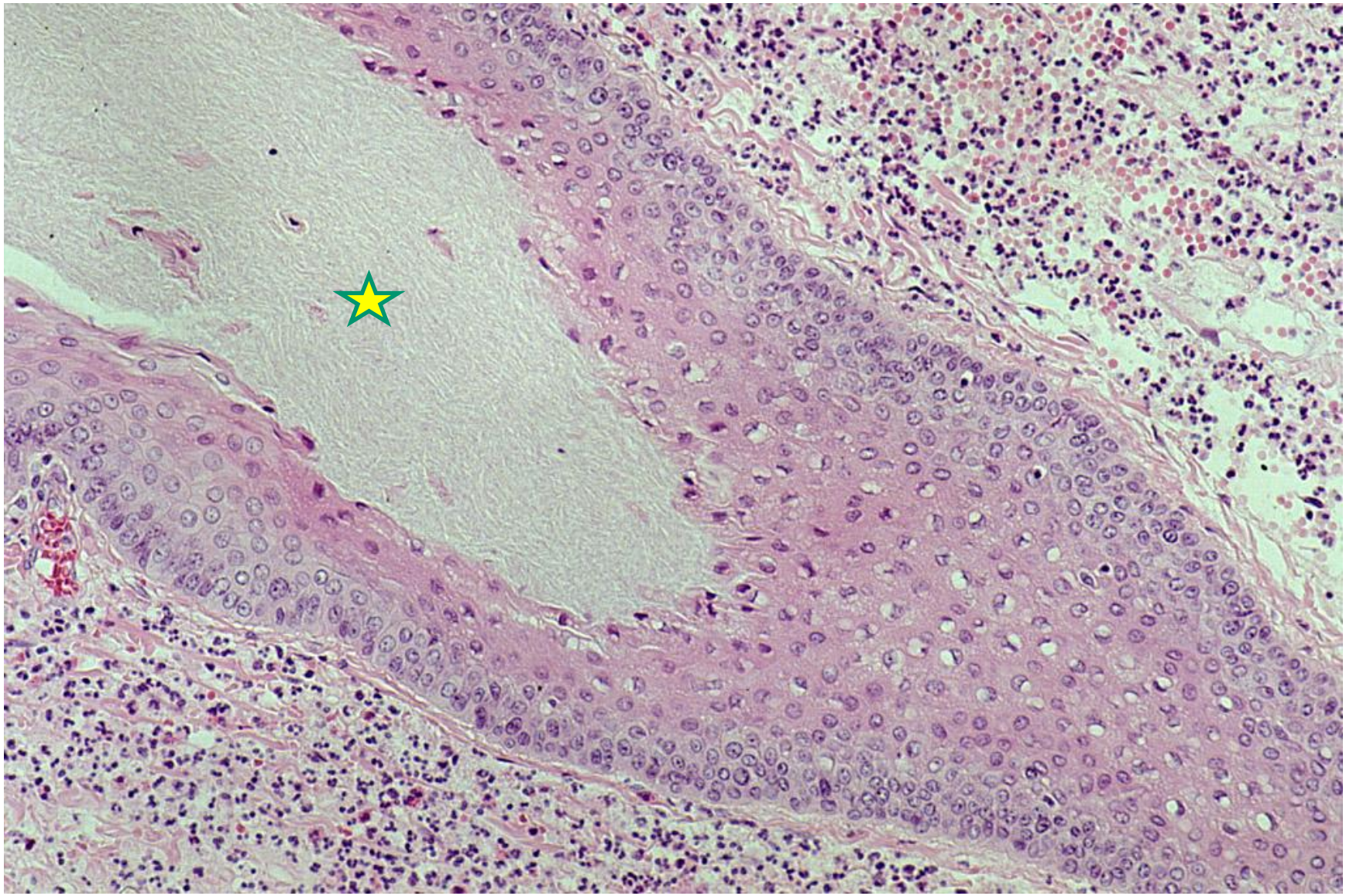

Biopsy-based diagnosis of **diphtheria** (H&E), showing pseudomembranous pharyngitis with finely basophilic pseudomembrane (asterisk). Neutrophilic reaction is seen subepithelially.

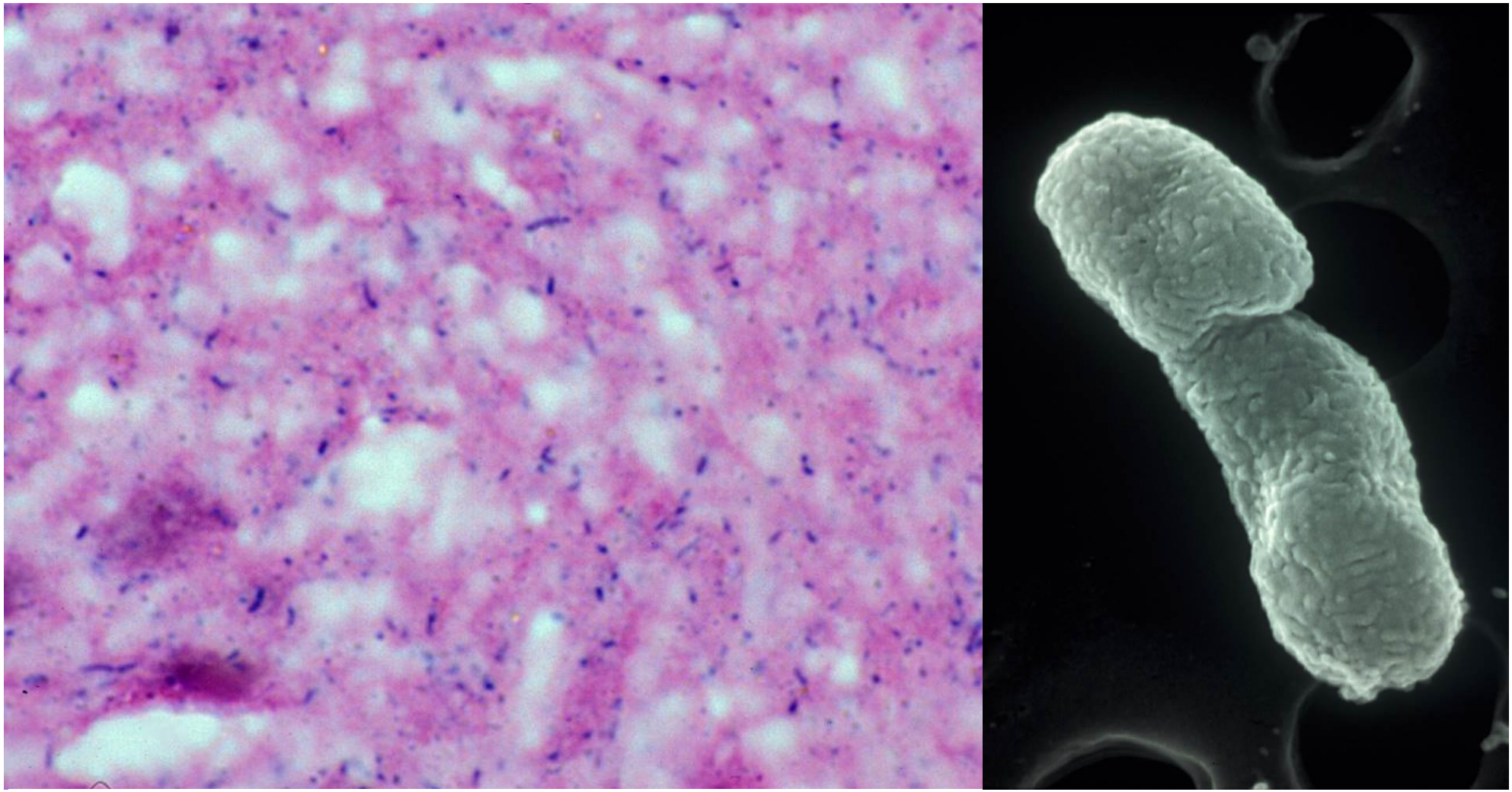

Diphtherial pharyngitis. Numerous Gram-positive rods are seen in the pseudomembrane. The scanning electron microscopic examination using a sediment of the formalin solution used for the fixation of the biopsy material demonstrates a non-flagellated club-shaped bacillus, consistent with *Corynebacterium* species.

Schema of viral inclusions

DNA virus forms intranuclear inclusions (smudge type or Cowdry type A), while RNA virus may form cytoplasmic inclusions. Most RNA viruses, however, do not form intracellular inclusion bodies. Exceptions include HBs antigen-positive cytoplasmic inclusions in ground-glass hepatocytes and intranuclear inclusions in measles virus infection.

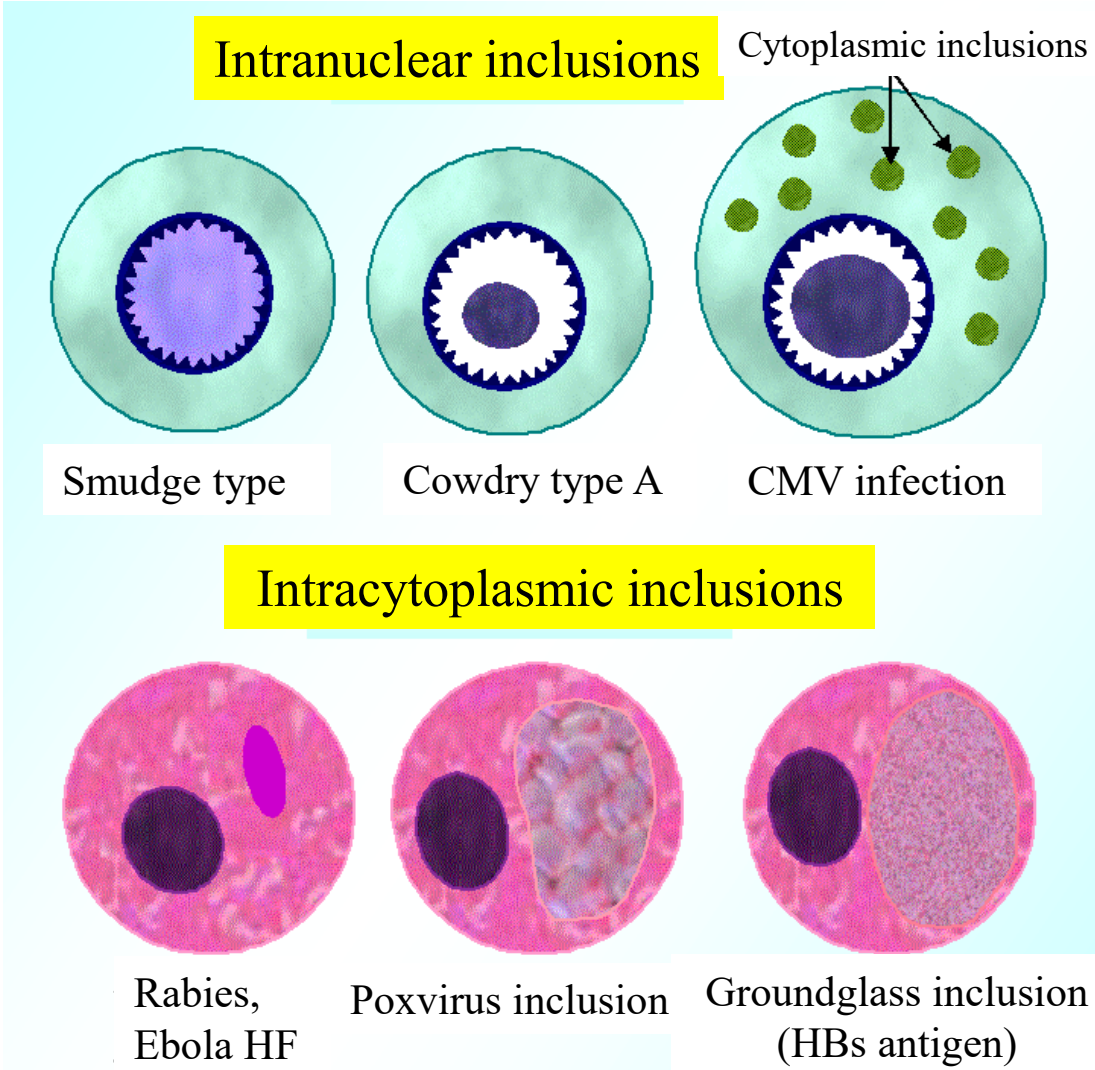

	Inclusions	Exceptions
DNA virus	Intranuclear inclusions	Poxvirus, CMV, hepatitis B virus (cytoplasmic)
RNA virus	Cytoplasmic inclusions/none	Measles virus (nucleus)

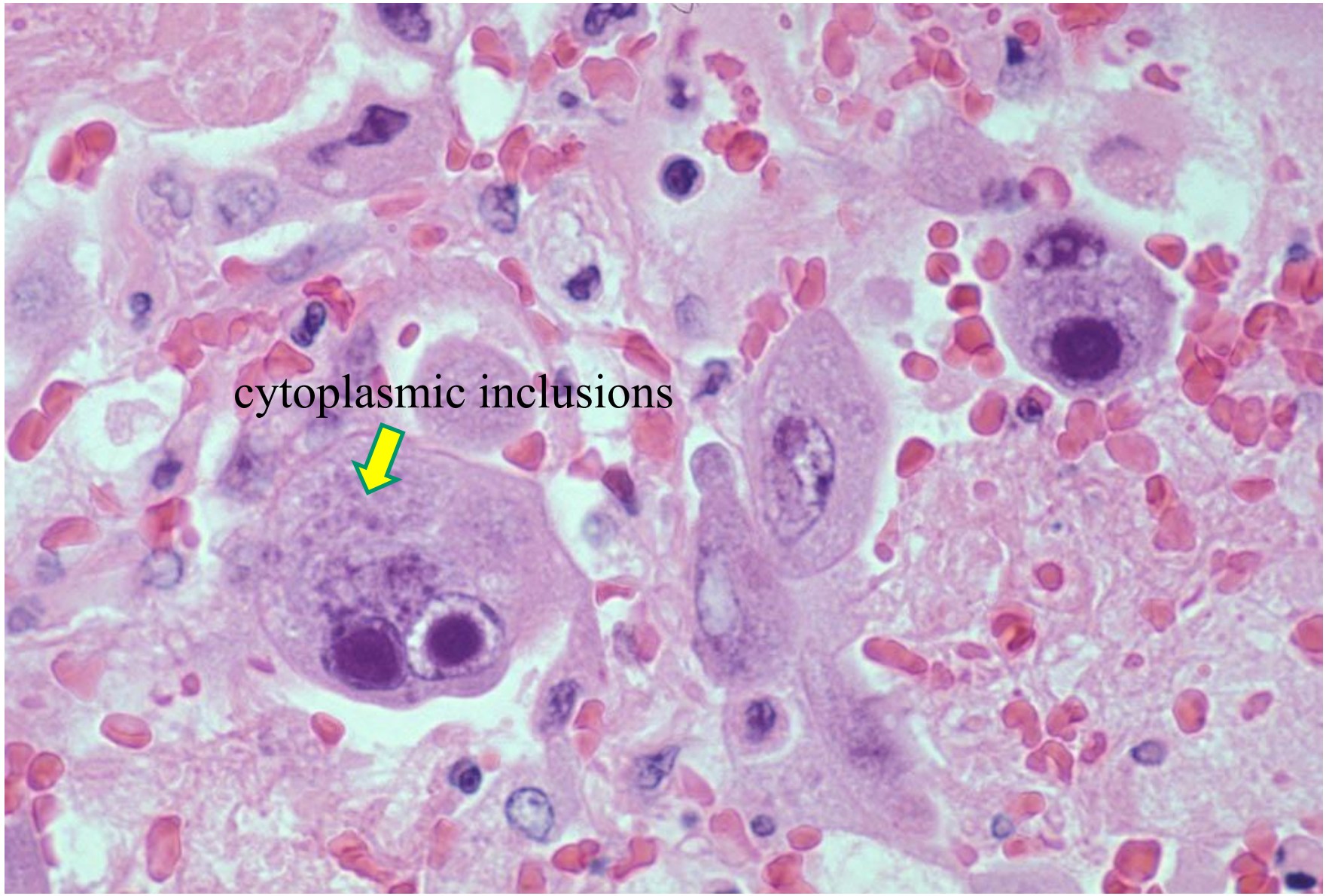

Cytomegalovirus (CMV) infection of the lung: owl-eye appearance with intracytoplasmic inclusions (H&E). Interstitial lung reaction is associated.

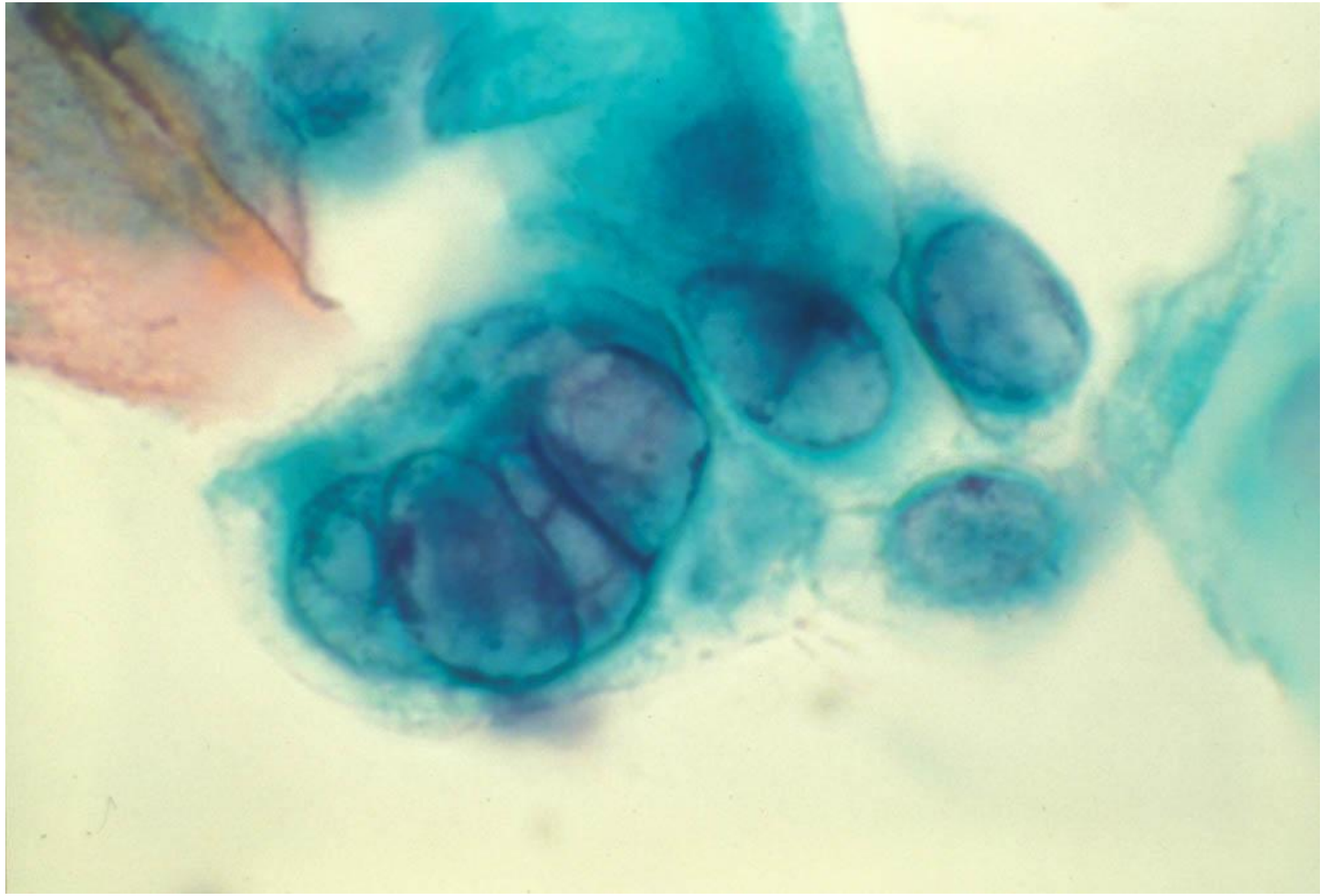

Herpes simplex virus infection of the vulva. Smear cytology reveals intranuclear inclusions of smudge type (Pap). Multinucleation of the infected keratinocytes is characteristic.

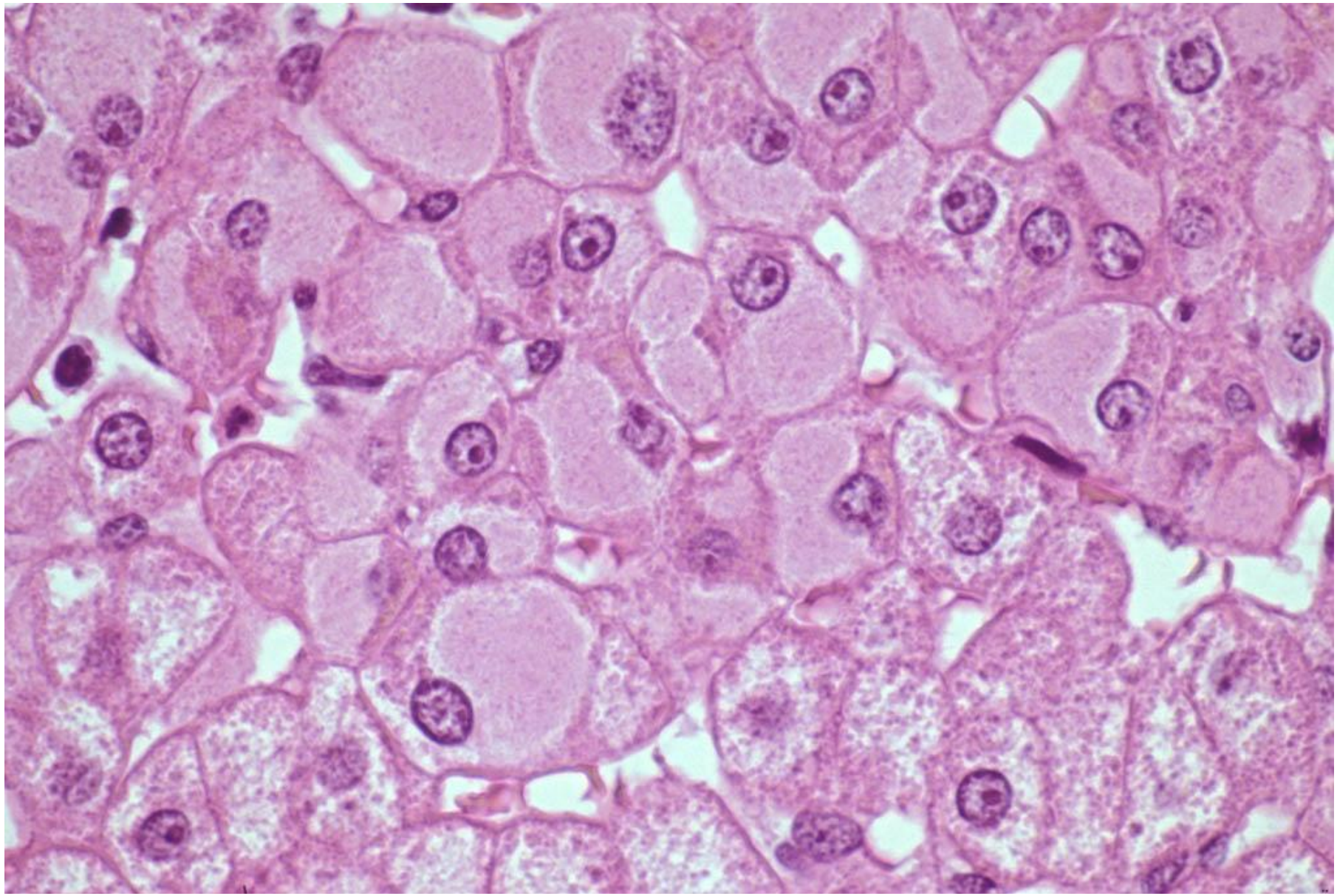

Healthy carrier of hepatitis B virus (HBV) in the biopsied liver (H&E). Ground-glass hepatocytes with large cytoplasmic inclusion bodies is characteristic.

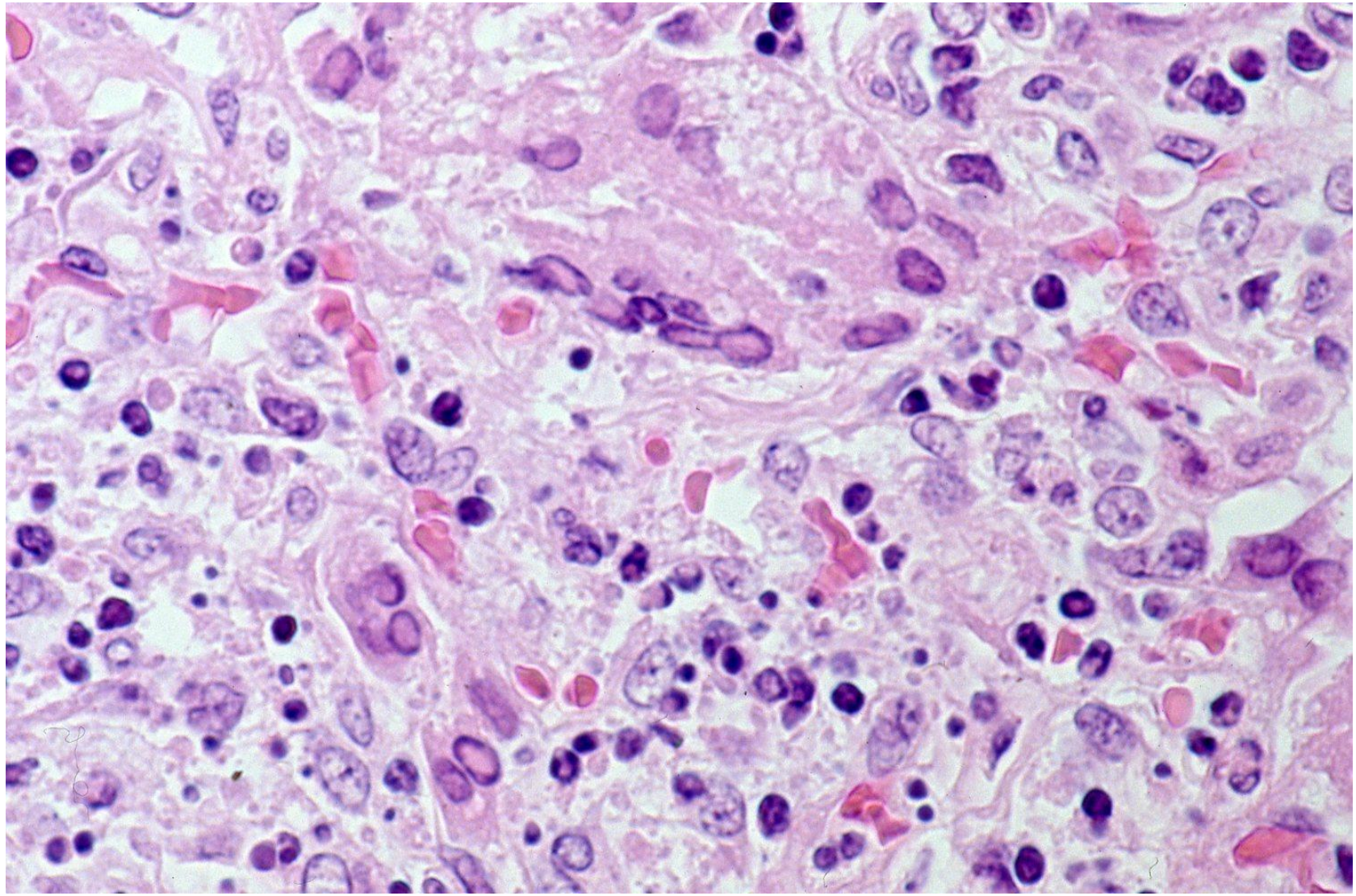

Measles pneumonia (H&E). Multinucleated giant cells contain intranuclear inclusion of smudge type. Measles virus is an exceptional RNA virus forming intranuclear inclusions.

Importance of Gram stain on sputum for the diagnosis of pneumonia

Gram stain is quick.

Causative bacteria can be suspected.

- Gram-positive cocci
- Gram-negative rods

Mycobacteria and Legionella are undetectable.

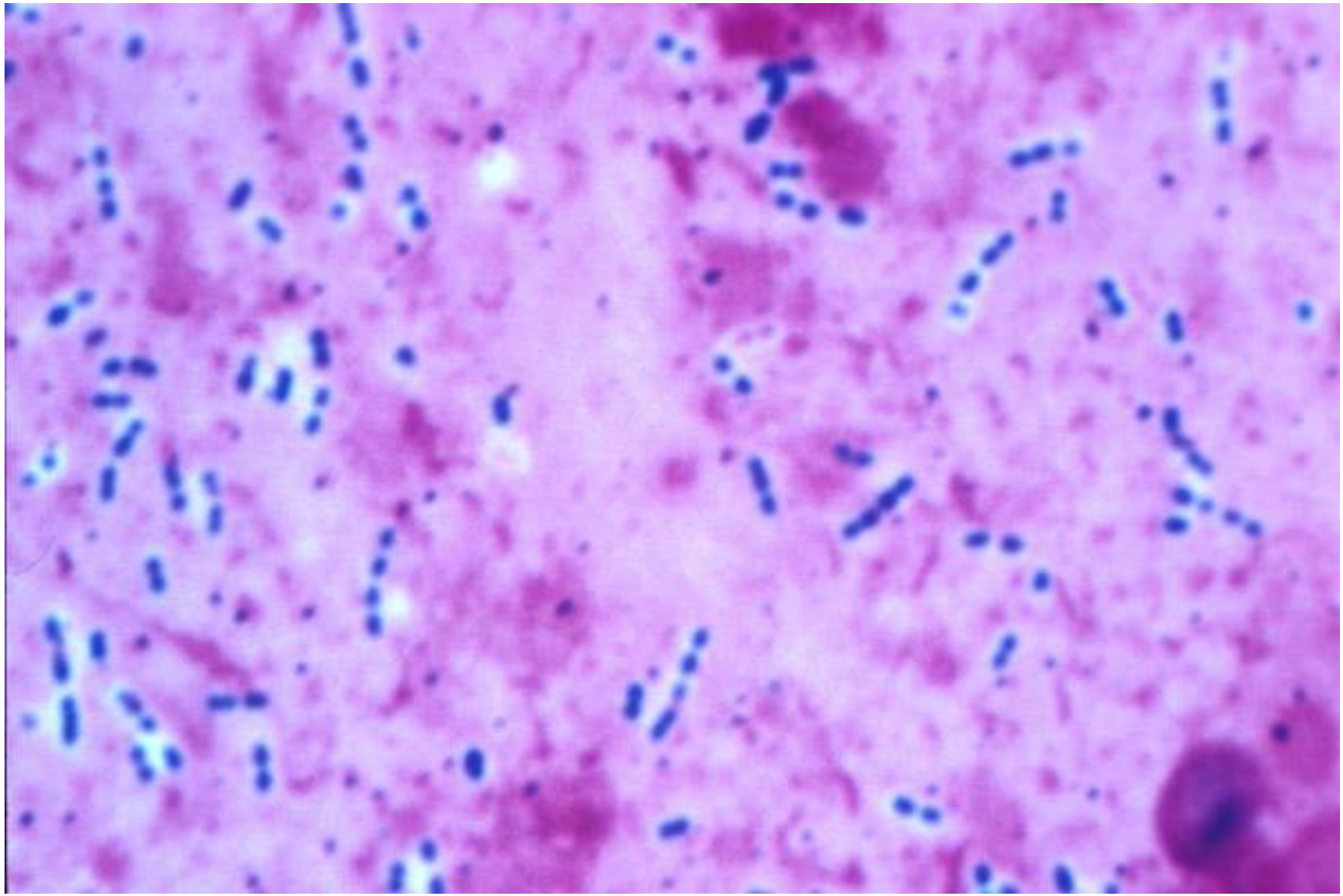

Pneumococcal pneumonia (Gram). Sputum smear demonstrates chained Gram-positive cocci with capsule formation. Diplococci are scattered. The capsule-forming cocci are not phagocytized by neutrophils.

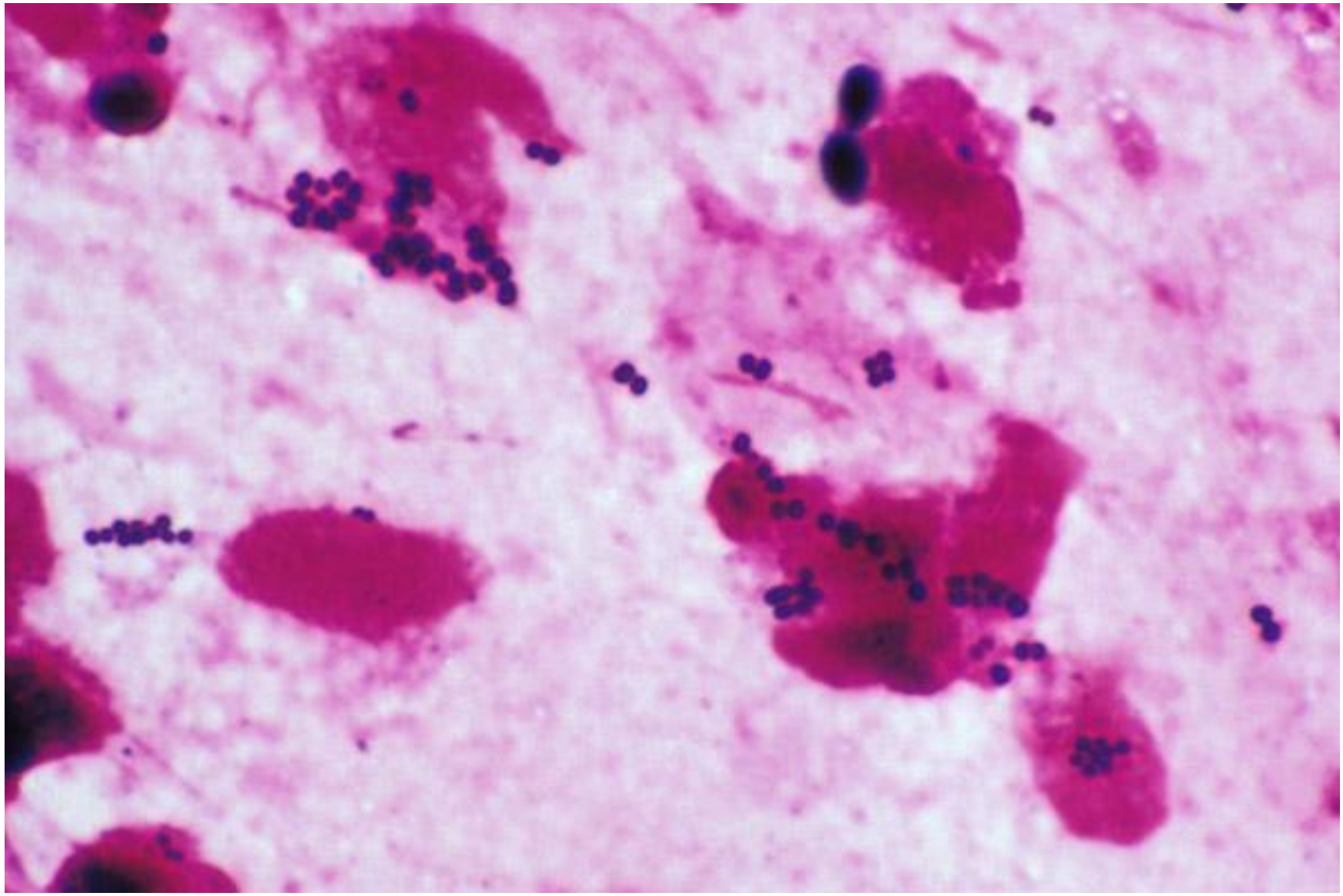

***Staphylococcus aureus* (MRSA) pneumonia** (Gram). Irregularly clustered Gram-positive cocci are phagocytized by neutrophils. MRSA and MSSA are not distinguishable.

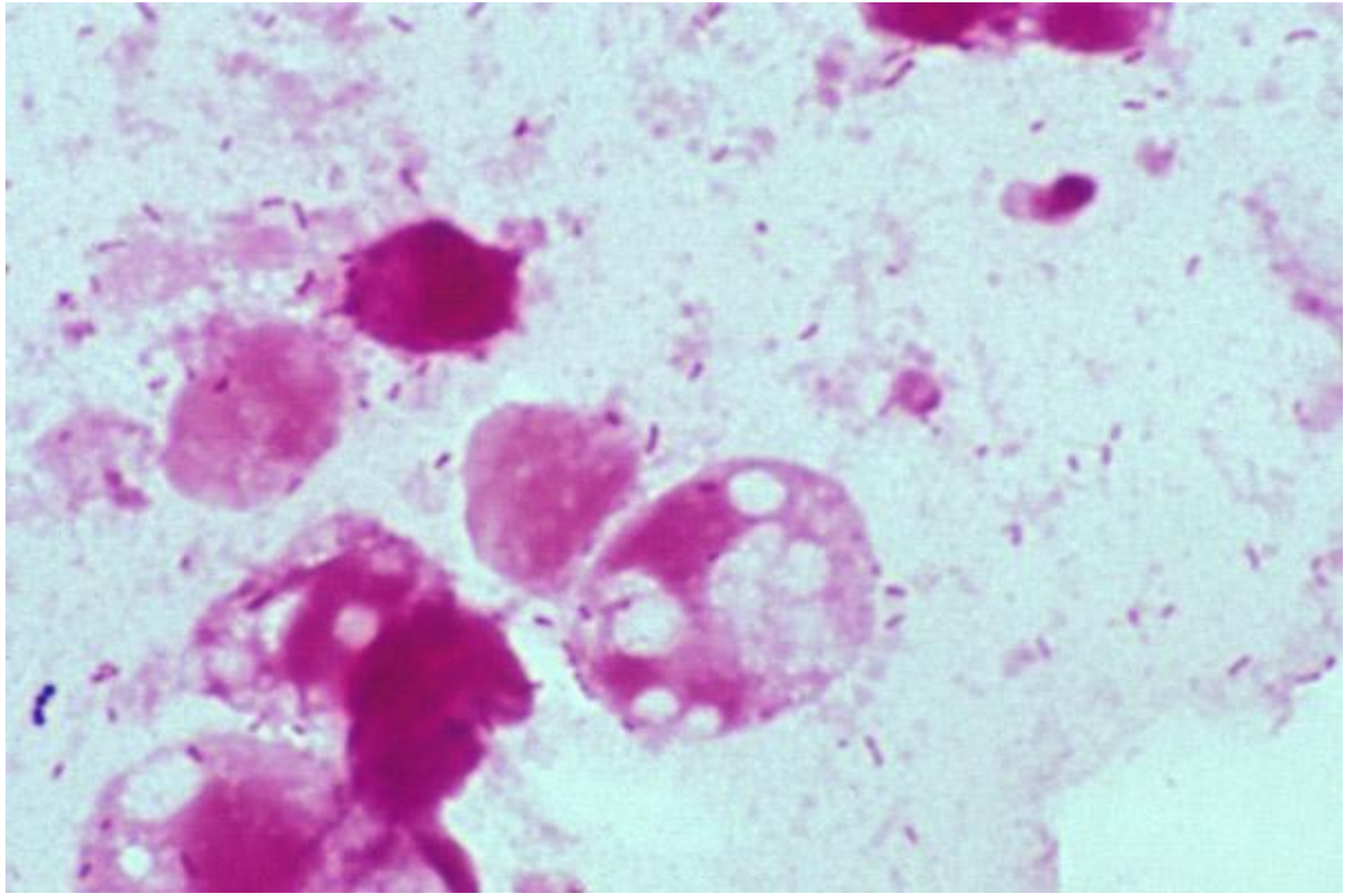

Haemophilus influenzae **pneumonia** in childhood (Gram). Small-sized rods are not phagocytized by neutrophils. Capsule formation is visible around the rods.

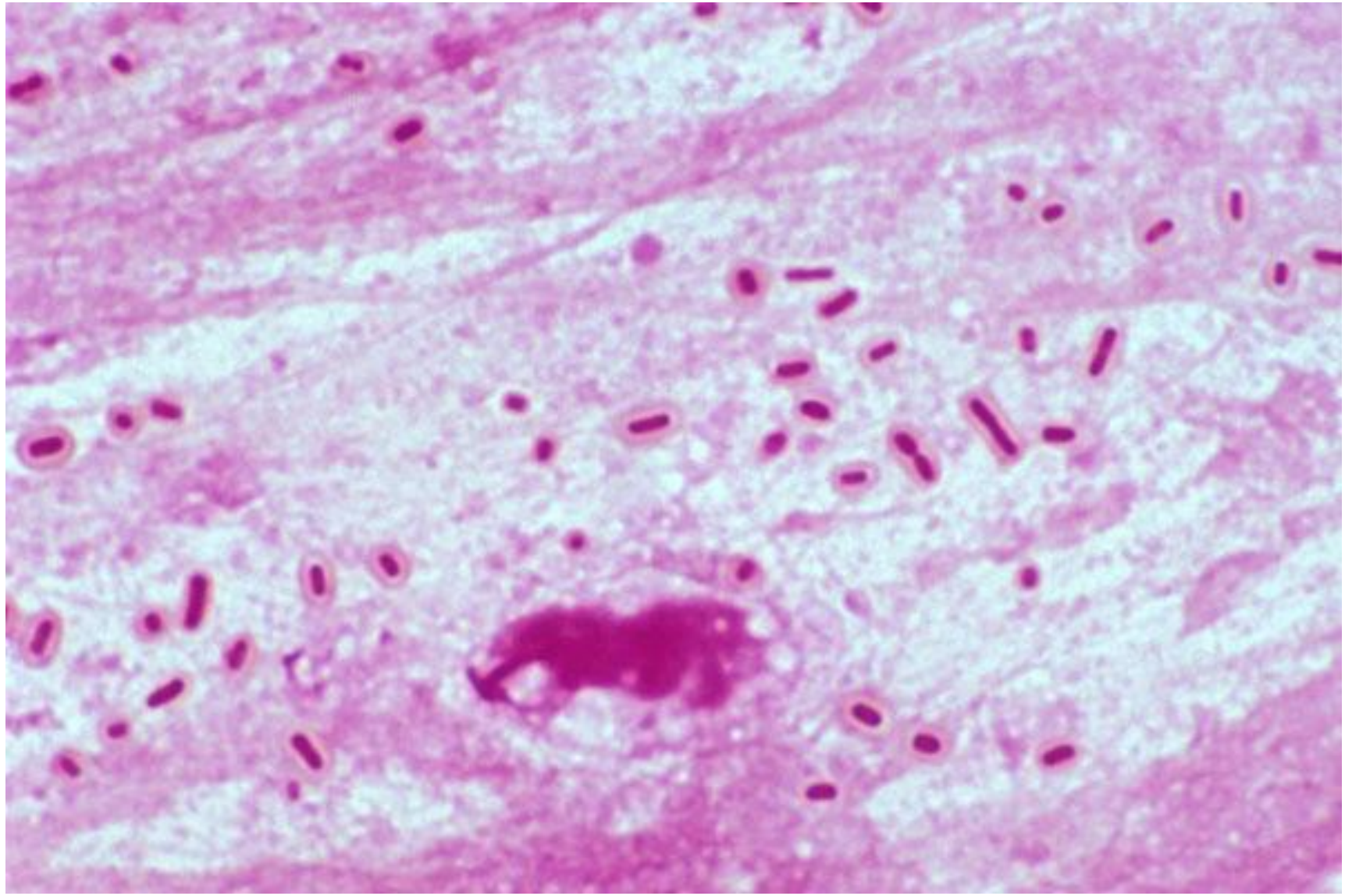

Klebsiella pneumonia (Gram). *Klebsiella pneumopniae*, large-sized bacillus, forms a thick capsule. The bacteria are not phagocytized by neutrophils.

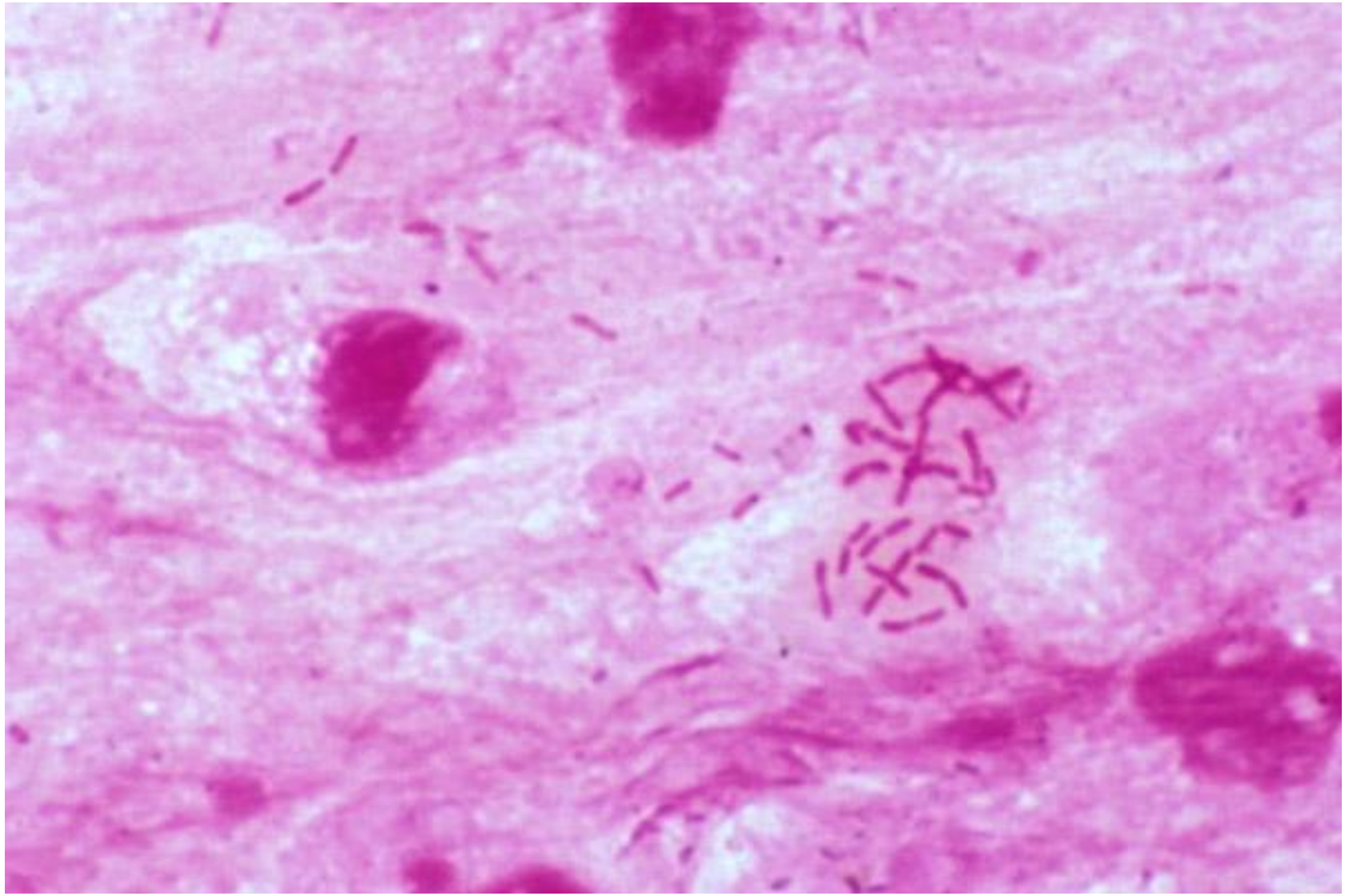

Pseudomonas pneumonia (mucoid type, Gram). Large-sized Gram-negative rods are clustered within mucoid-like capsule-derived material. Drug-resistant persistent airway infection of *Pseudomonas aeruginosa* is indicated.

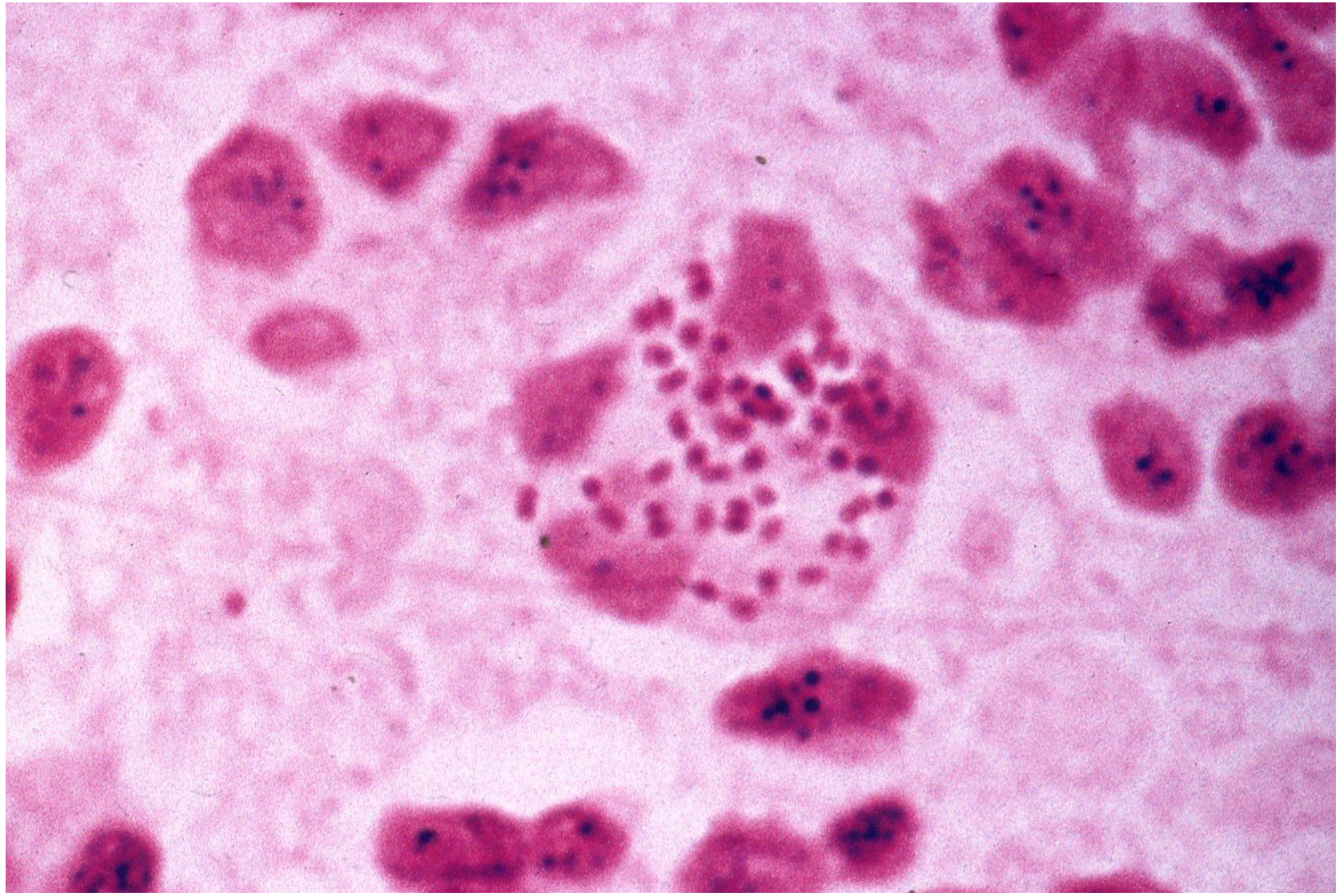

***Moraxella catarrhalis* (*Branhamella catarrharis*)** (Gram). Gram-negative diplococci (paired Gram-negative cocci) are phagocytized by neutrophils. It causes sinusitis, otitis media and pneumonia.

Summary of capsule-forming pathogens

Streptococcus pneumoniae (Pneumococcus)

Neisseria meningitides (Meningococcus)

Haemophilus influenzae (Hib)

(Vaccine prevention is effective particularly for meningitis)

Pseudomonas aeruginosa

Klebsiella pneumoniae

Cryptococcus neoformans

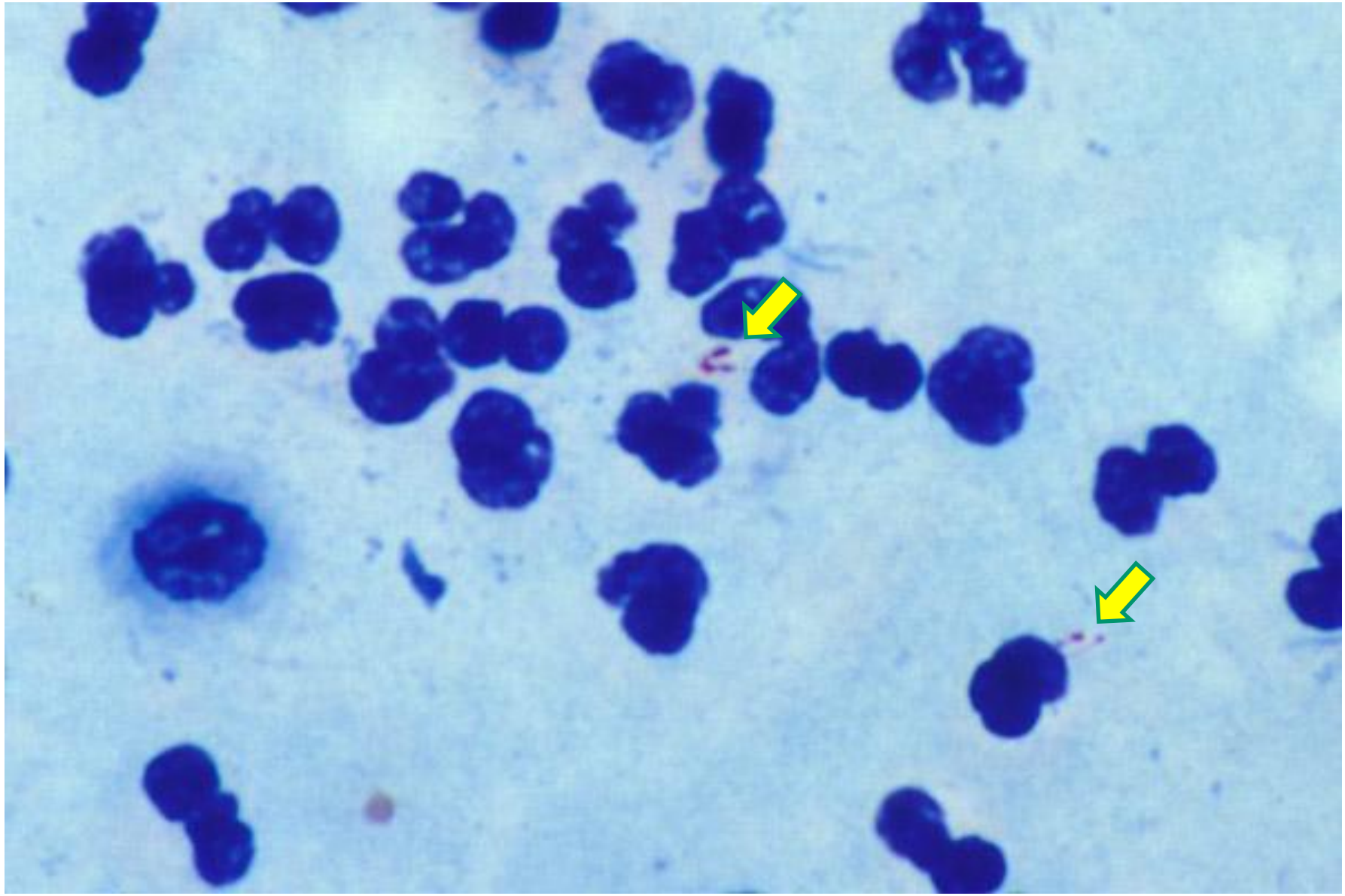

Mycobacterium tuberculosis in the sputum smear (Ziehl-Neelsen). *M. tuberculosis* is an intracellular pathogen, and grows within the cytoplasm of macrophages.

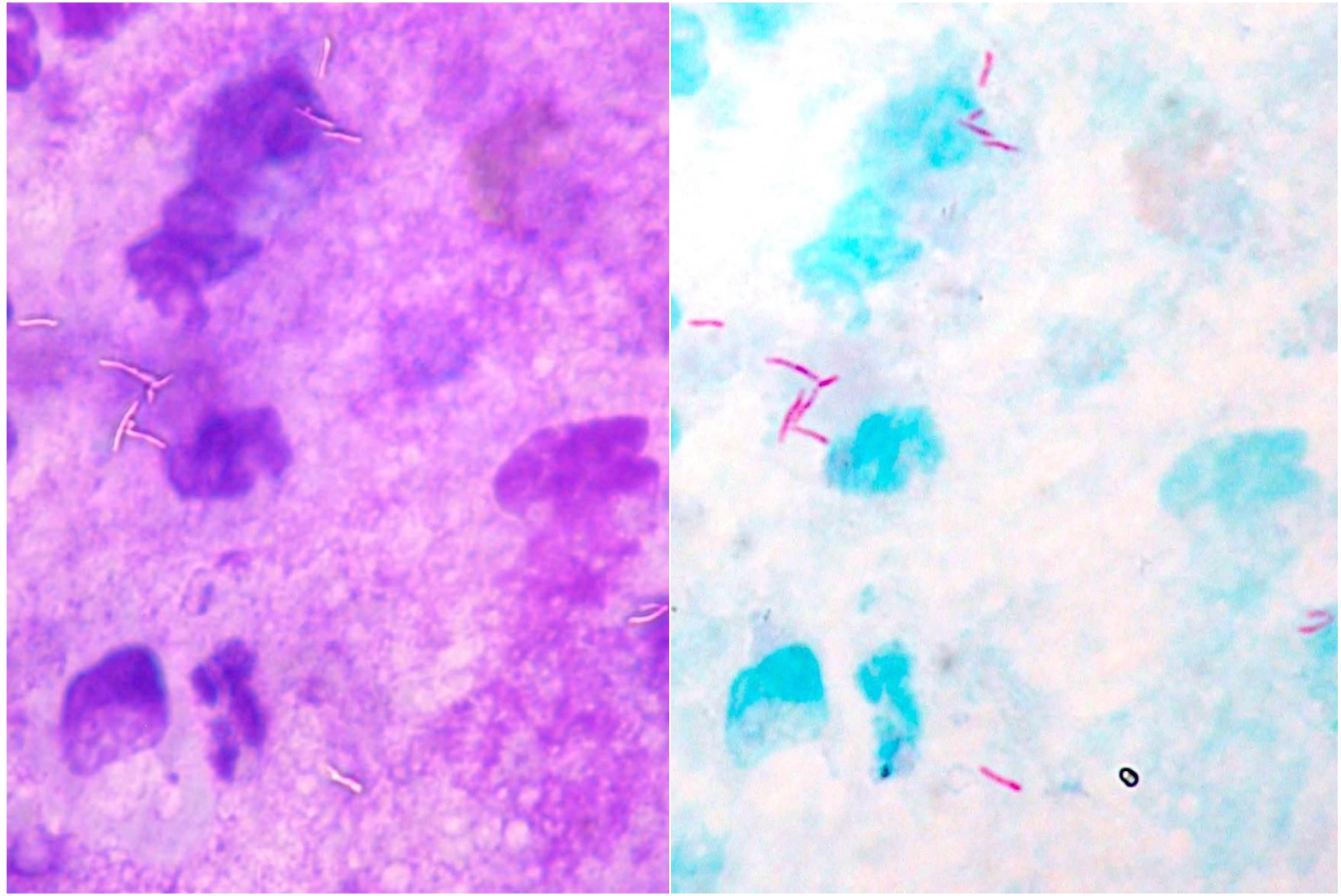

***Mycobacterium avium* infection** (sputum cytology). Left: Giemsa, right: restained with Ziehl-Neelsen. *Mycobacteria* are seen as "**negative images**" in Giemsa-stained preparations. Restaining on the same preparation reveals acid-fastness of the large bacteria. *M. tuberculosis* and non-tuberculous mycobacteria are indistinguishable microscopically. Ref.: Watanabe T, et al. *Mycobacterium avium* infection detected as a negative image in Giemsa-stained sputum cytology preparations. Ann Infect Dis Ther 2021; 2(1): 1-5.

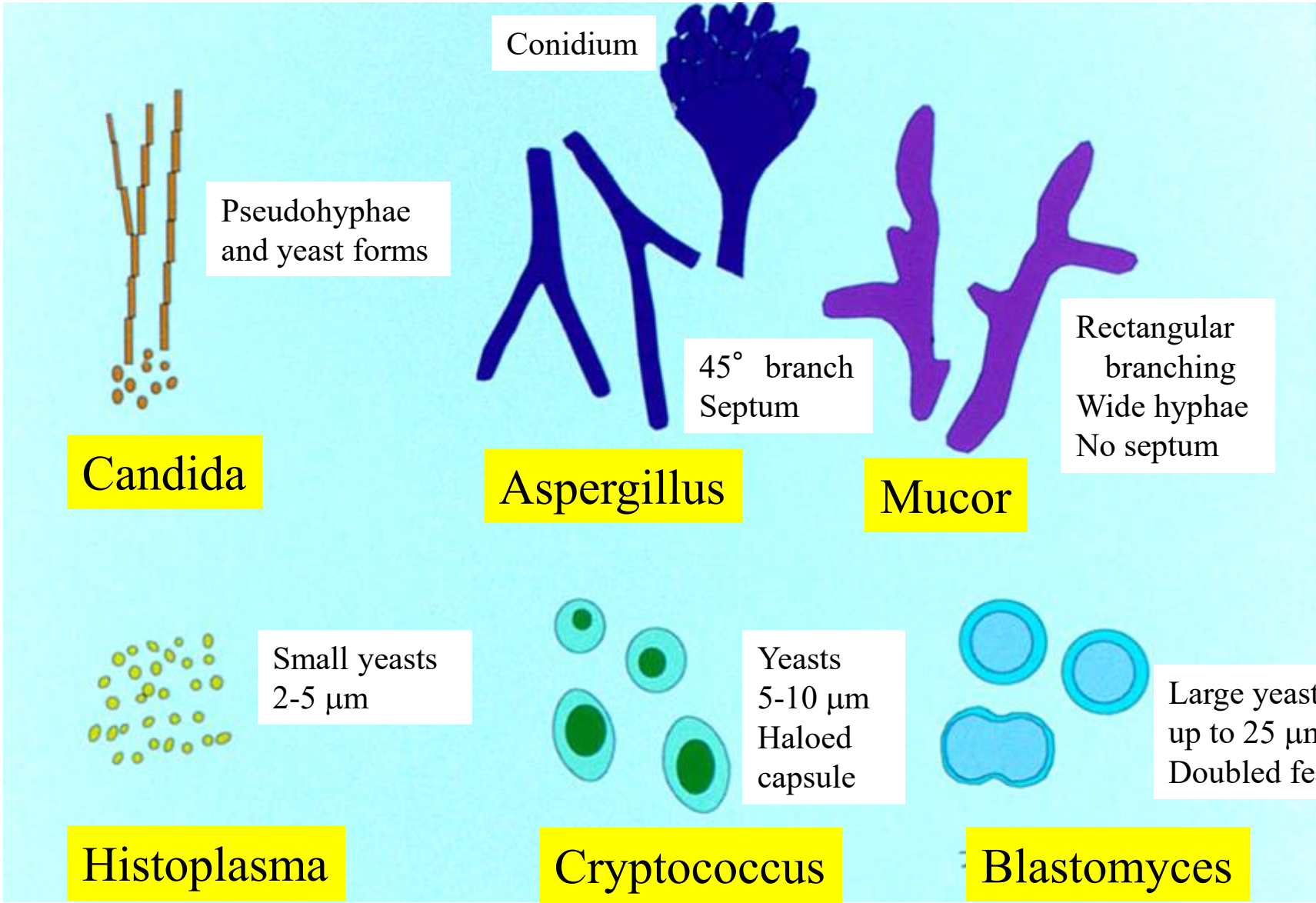

Schematic morphology of fungi (hypha-forming vs. yeast form)

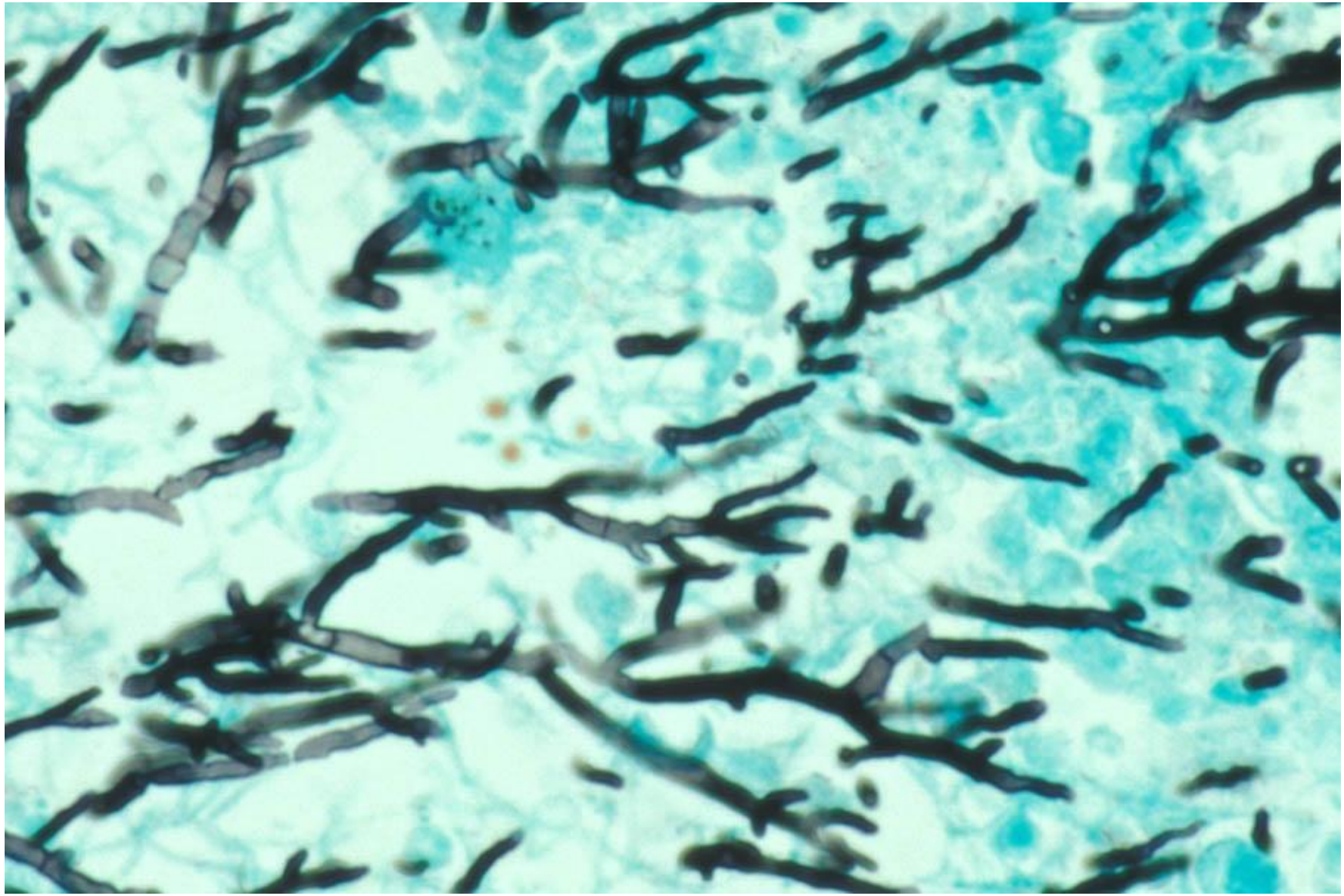

Aspergillosis of the lung (Grocott). Y-shaped lamifying hyphae with septum formation are noted.

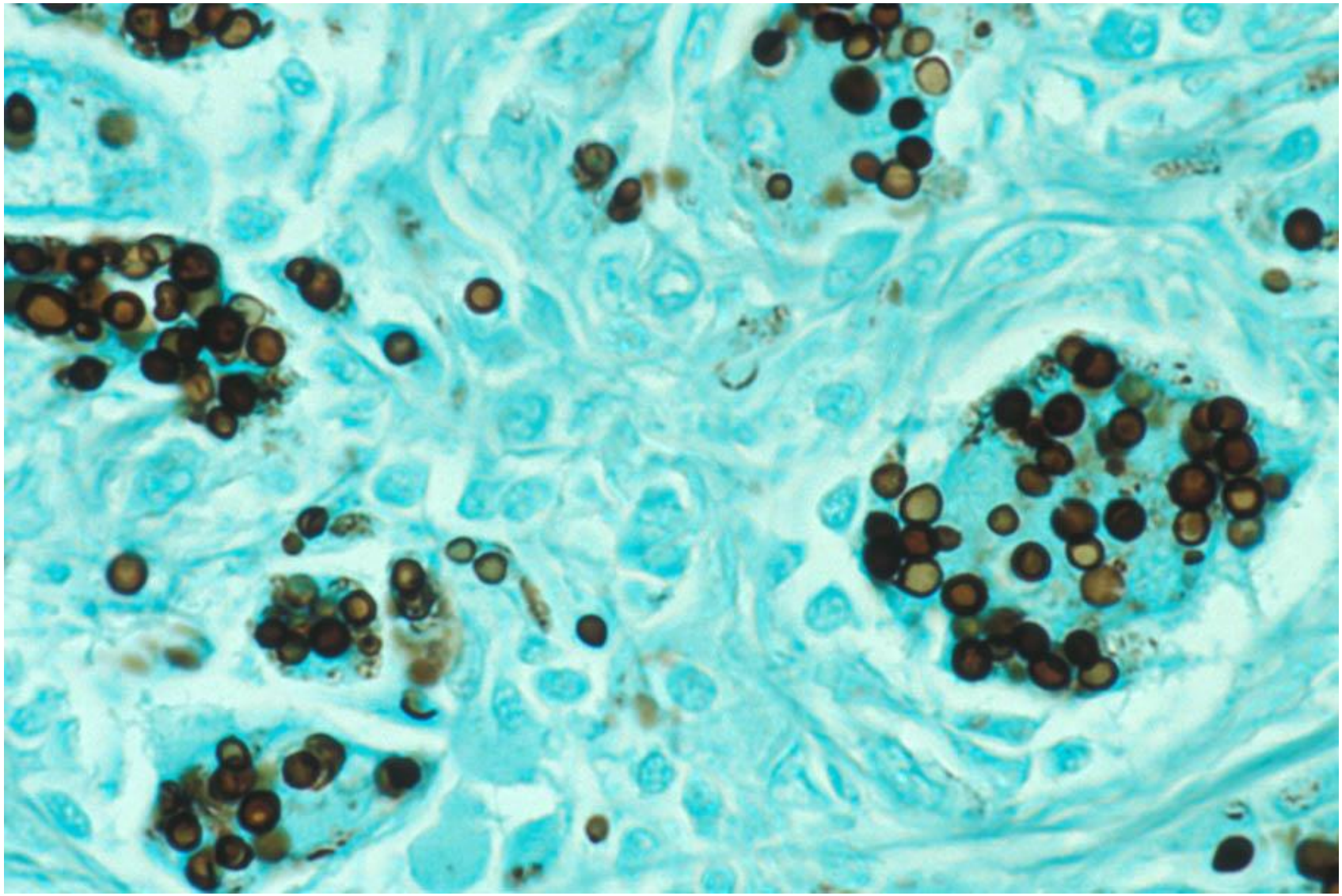

Cryptococcal granuloma of the lung (Grocott). Yeast forms are phagocytized by multinucleated giant cells.

Cellular reactions against fungal infection

1）Hypha-forming fungi = extracellular pathogen
　　－Neutrophilic reaction to form abscess
2）Yeast-type fungi = intracellular pathogen
　　－T-cells and macrophages to form granuloma
3）Candida reveals two phases
　　（Deep-seated＝1, superficial mucosal＝2）
4）Cutaneous mycosis = intermediate reaction
　　(sporotrichosis, chromomycosis, paracoccidioidomycosis)
　　－Suppurative granuloma
　　(granuloma with central abscess formation)

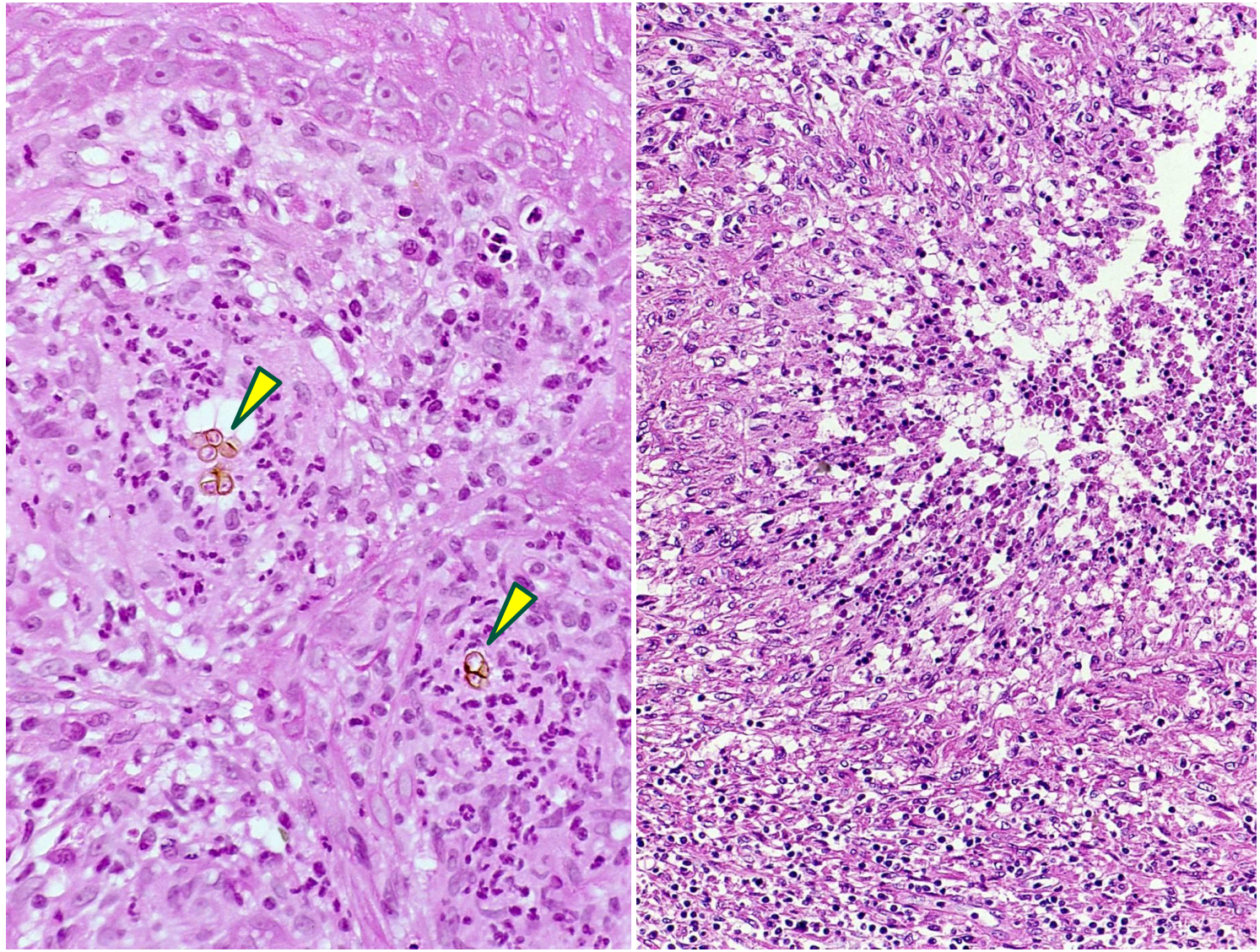

Suppurative granulomas in cutaneous chromomycosis (left) and melioidosis of the spleen (right). Neutrophilic clusters are surrounded by epithelioid granulomas. Melanin-producing yest-type fungi of *Fonsecaea pedrosoi* are seen in the centrally located abscess cavity (arrowheads).

Case presentation: accurate pathological diagnosis of infectious diseases directly leads patients to appropriate treatment !

1) Syphilis in the second stage

2) Chlamydial salpingitis

3) Chlamydial epididymitis

The 2nd stage syphilide (neck skin)

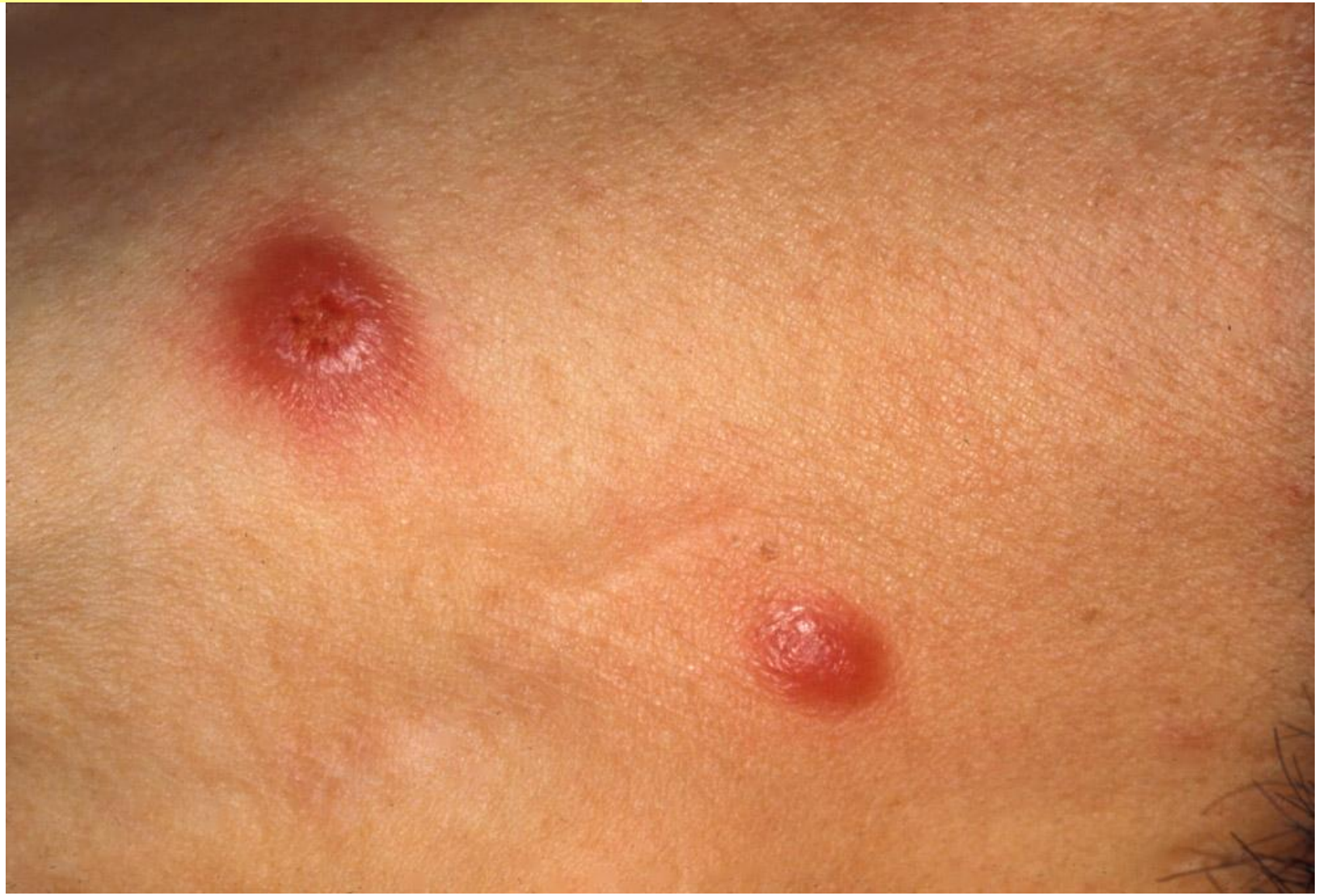

A 50 y-o male with a history of chemotherapy for malignant lymphoma presented skin rash and fever. Clinically, skin recurrence was suspected, and biopsy was taken from the neck papule.

The 2nd stage syphilide (neck skin)

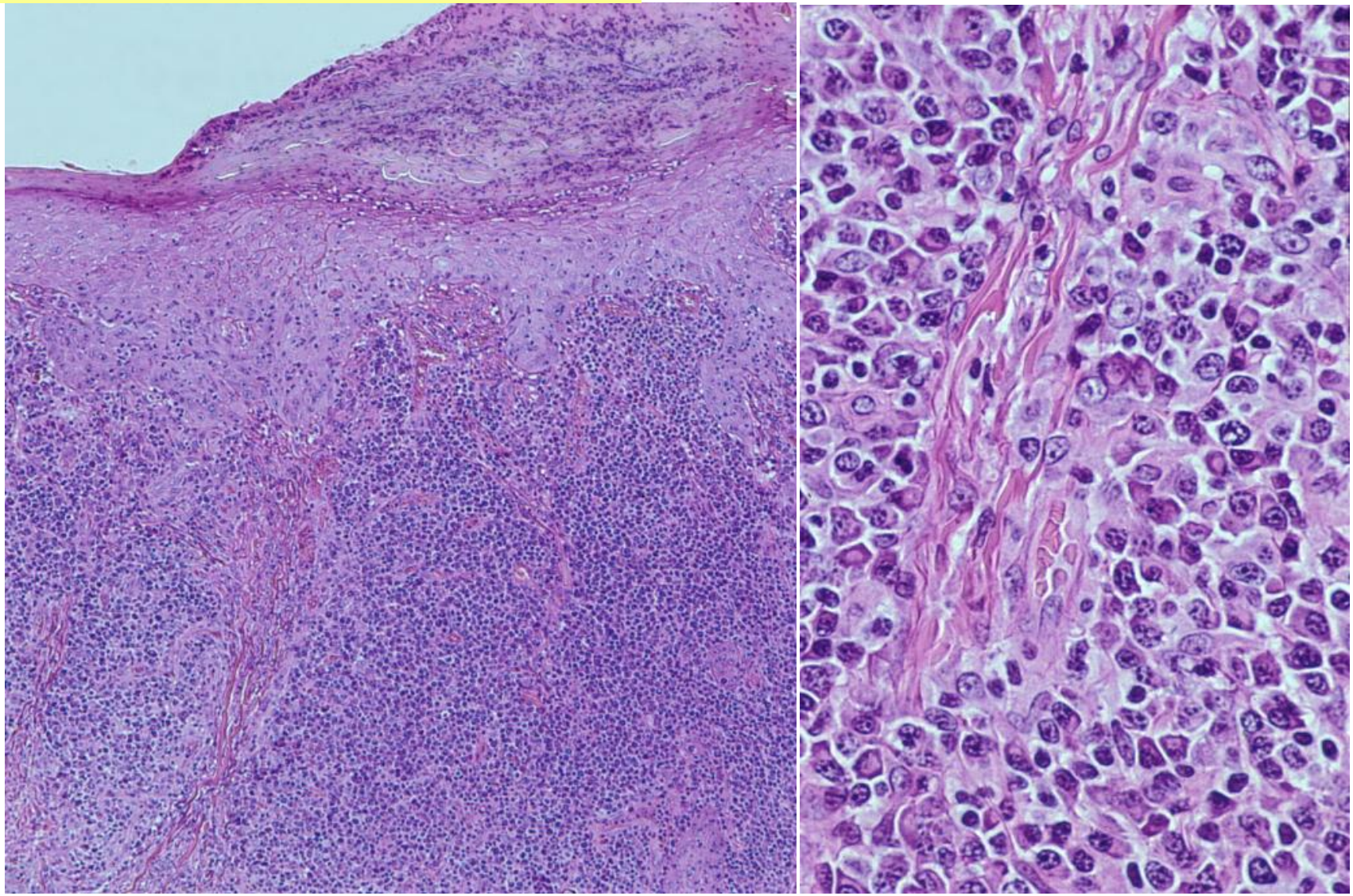

The biopsy from the neck papule reveals dense mononuclear infiltration in the dermis, mostly consisting of mature plasma cells. Swelling of the endothelial cells are associated. The possibility of syphilis was suspected microscopically.

The 2nd stage syphilide (neck skin)

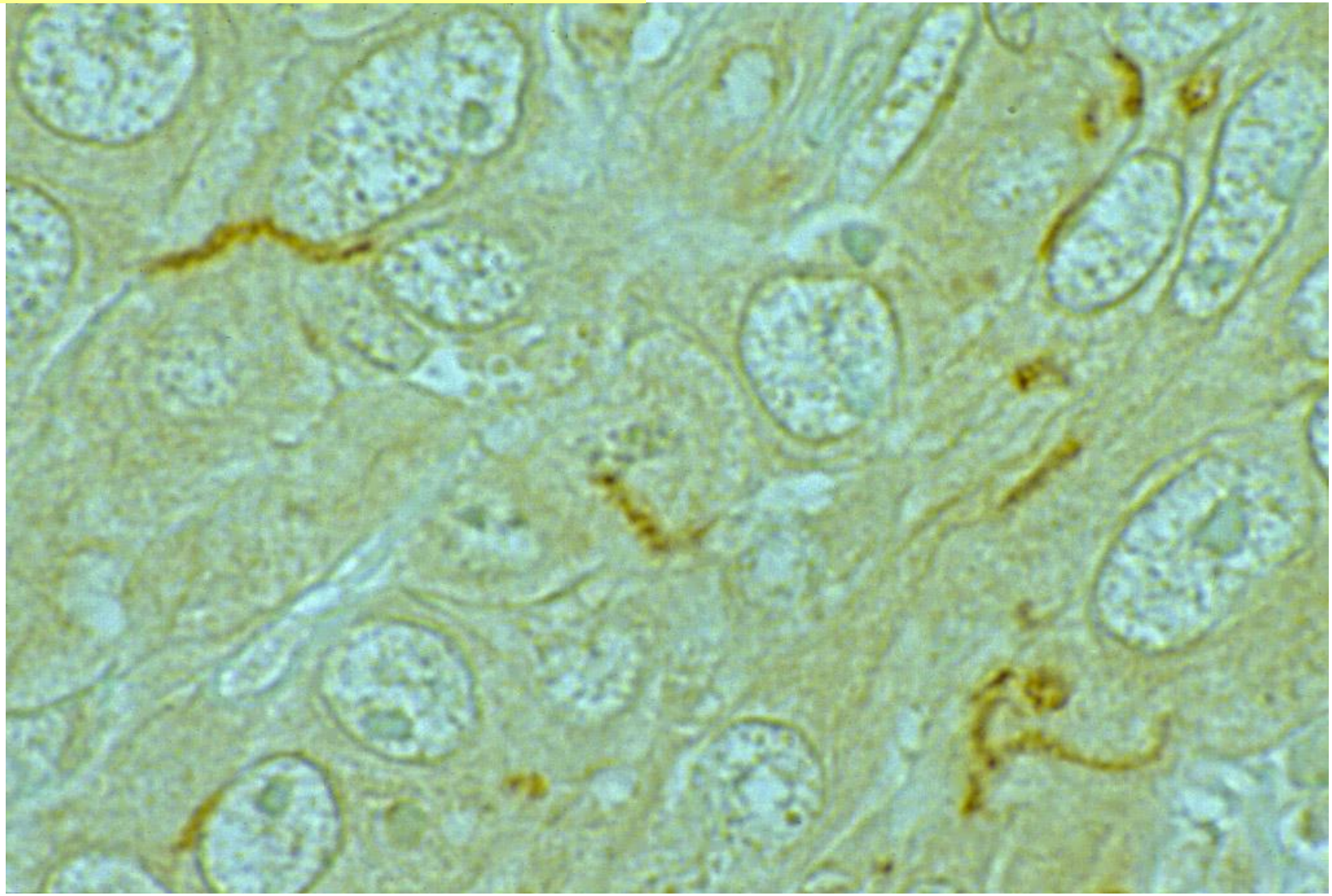

Immunostaining for *Treponema pallidum* identified spiral pathogens among keratinocytes, confirming the diagnosis of **second stage syphilis**.

Chlamydial salpingitis

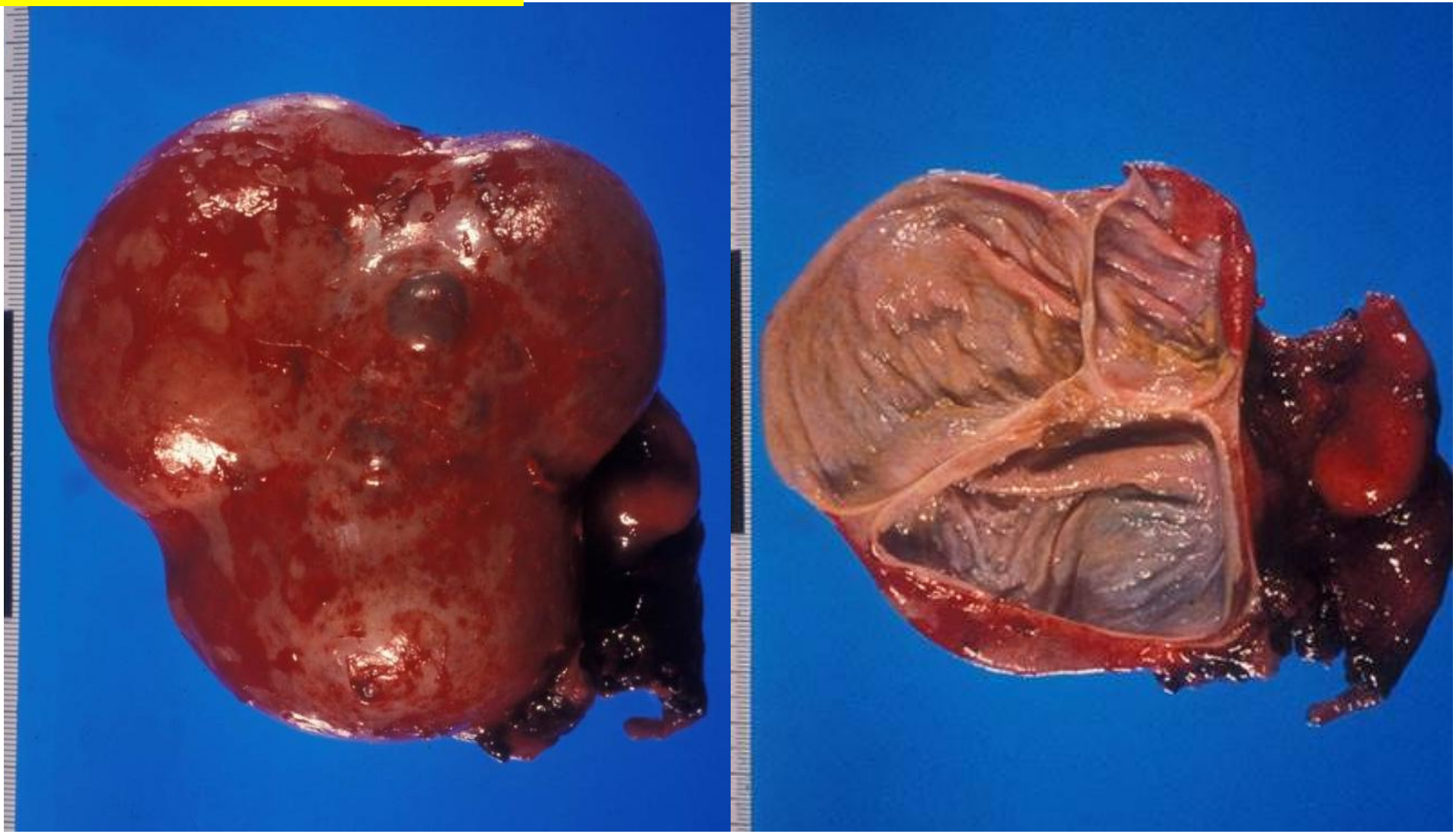

A 30 y-o female patient presented with abdominal pain. The enlarged left oviduct was resected. Sausage-like swelling is evident.

Chlamydial salpingitis

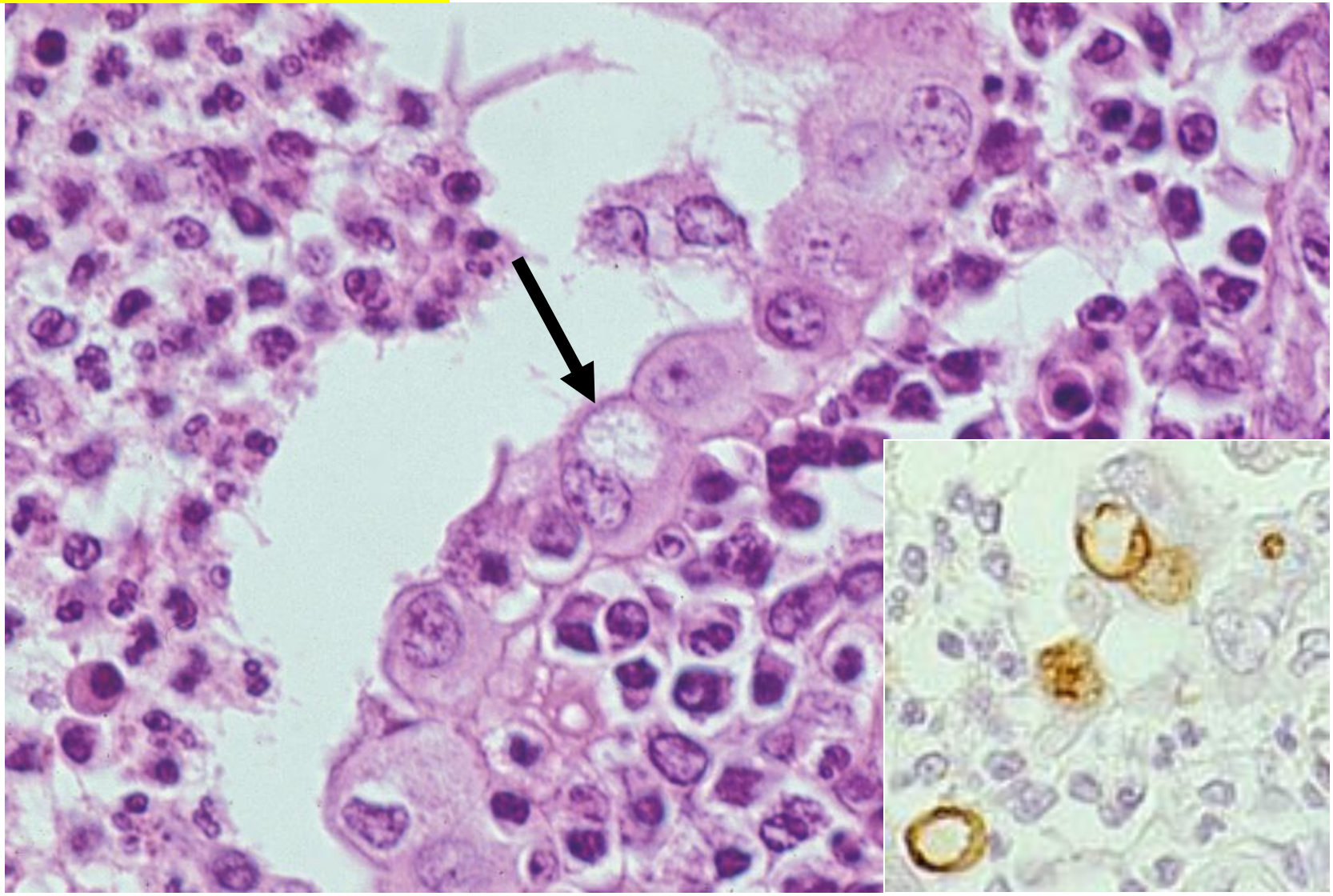

Chlamydial salpingitis (H&E). Intracytoplasmic inclusions are seen in the epithelial cells (arrow). Neutrophilic exudation is seen in the lumen, and lymphoplasmacytic infiltration is noted in the submucosal layer. Immunostaining for Chlamydia trachomatis antigen is positive in the cytoplasmic inclusions, confirming the diagnosis of chlamydial salpingitis.

Chlamydial epididymitis

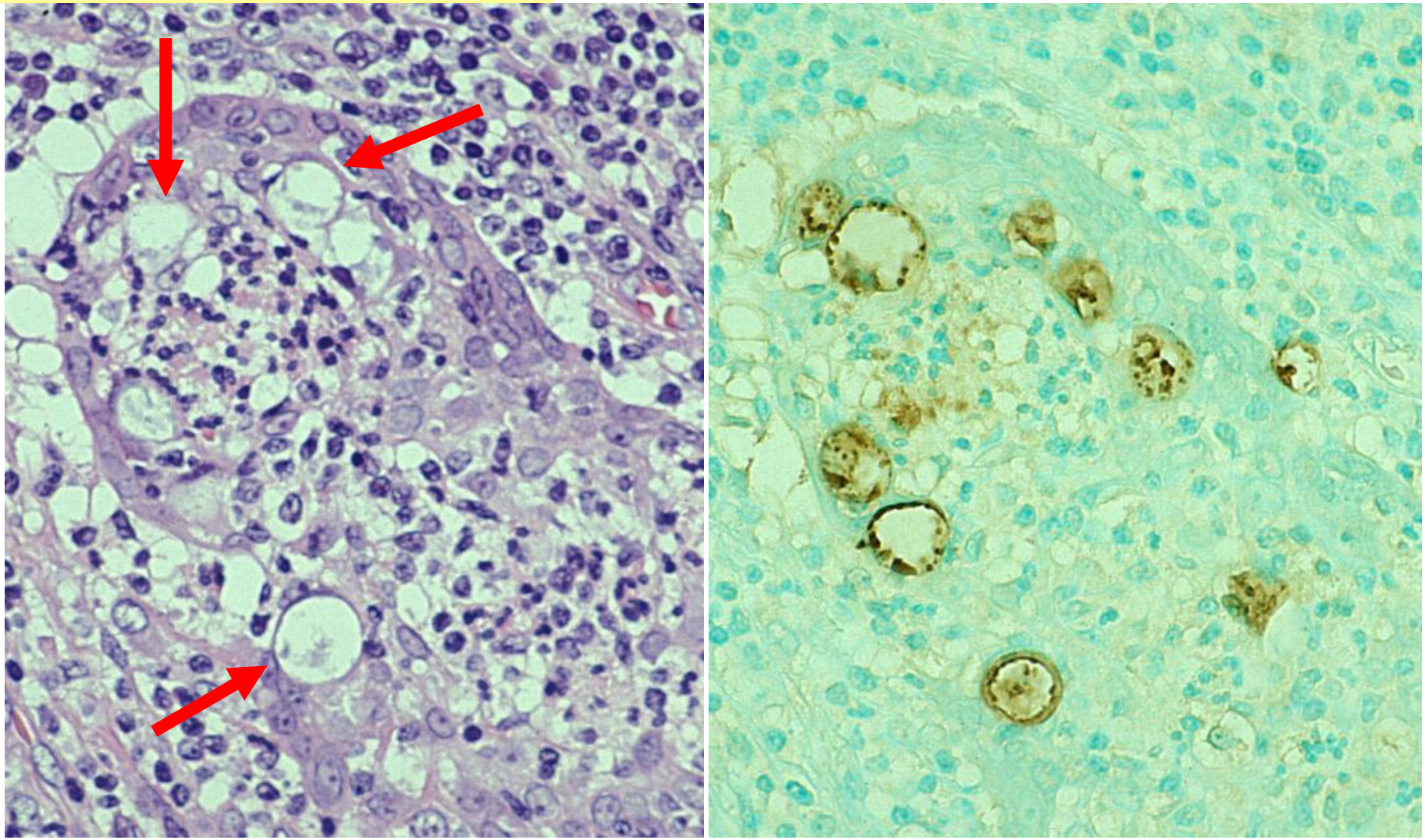

A 40 y-o male presented with scrotal swelling. Under the clinical diagnosis of epididymal tumor, surgical resection was performed. Under the features of chronic epididymitis, intracytoplasmic inclusions are observed in the epithelial cells (arrows). Serial sections disclosed positivity of *Chlamydia trachomatis* antigen in the inclusion bodies, confirming the diagnosis of **chlamydial epididymitis**.

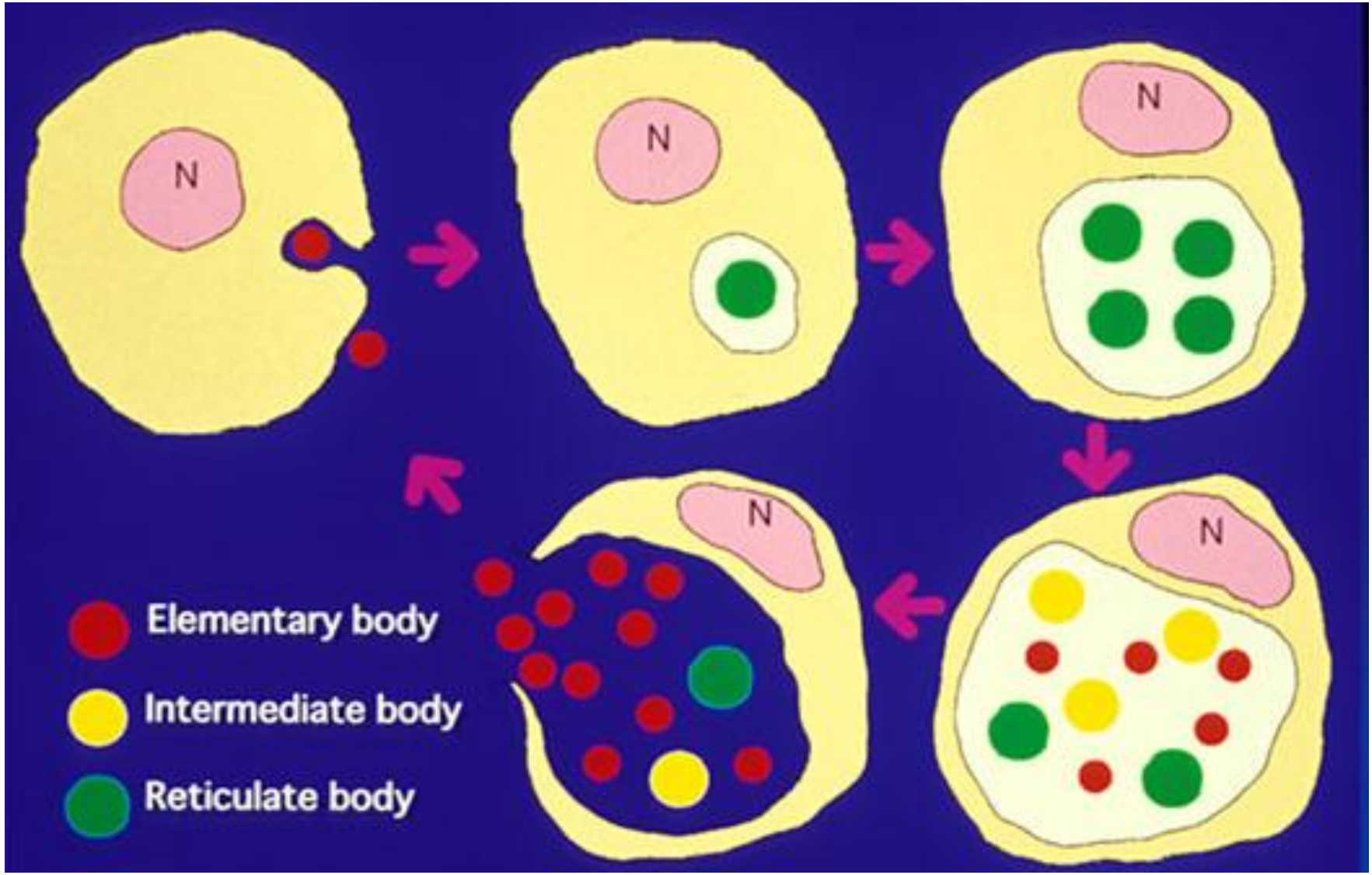

Schema of the growth cycle of *Chlamydia trachomatis*

Key techniques

Use of a single glass slide for plural kinds of staining

a) **Restaining method**
b) **Cell transfer technique**

Chlamydial cervicitis

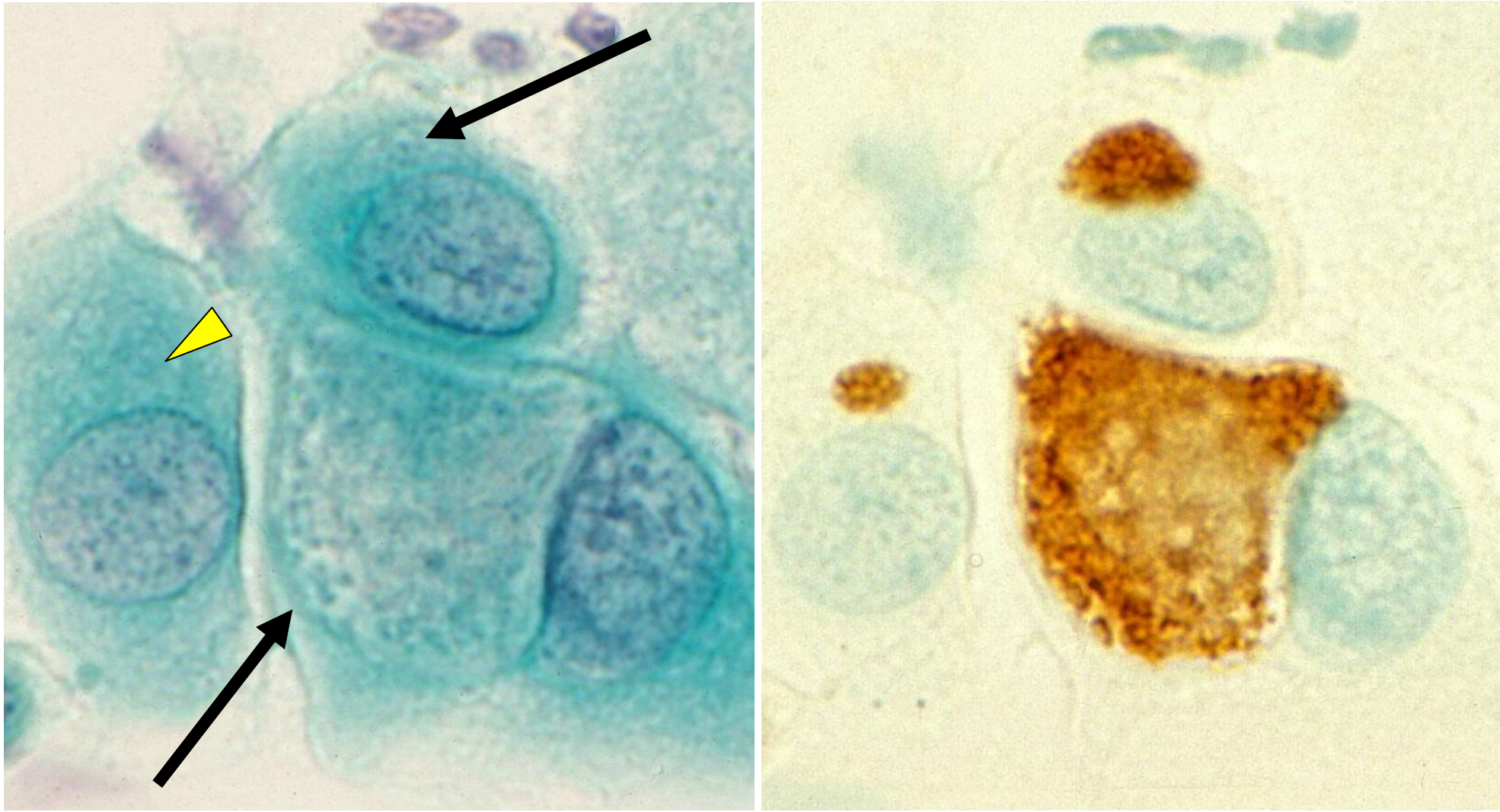

Chlamydial cervicitis. A 20 y-o female complained of increased fluor. Uterine cervical smear was evaluated. Nevular cytoplasmic inclusion bodies are seen (arrows). Re-immunostaining after the "cell transfer" to the Silane-coated glass slide, *Chlamydia trachomatis* antigen is visualized in the same cells. A small inclusion (arrowhead) is scarcely visible in the Pap-stained preparation.

How to use a single cytology specimen for immunocytochemistry (”cell transfer” technique)

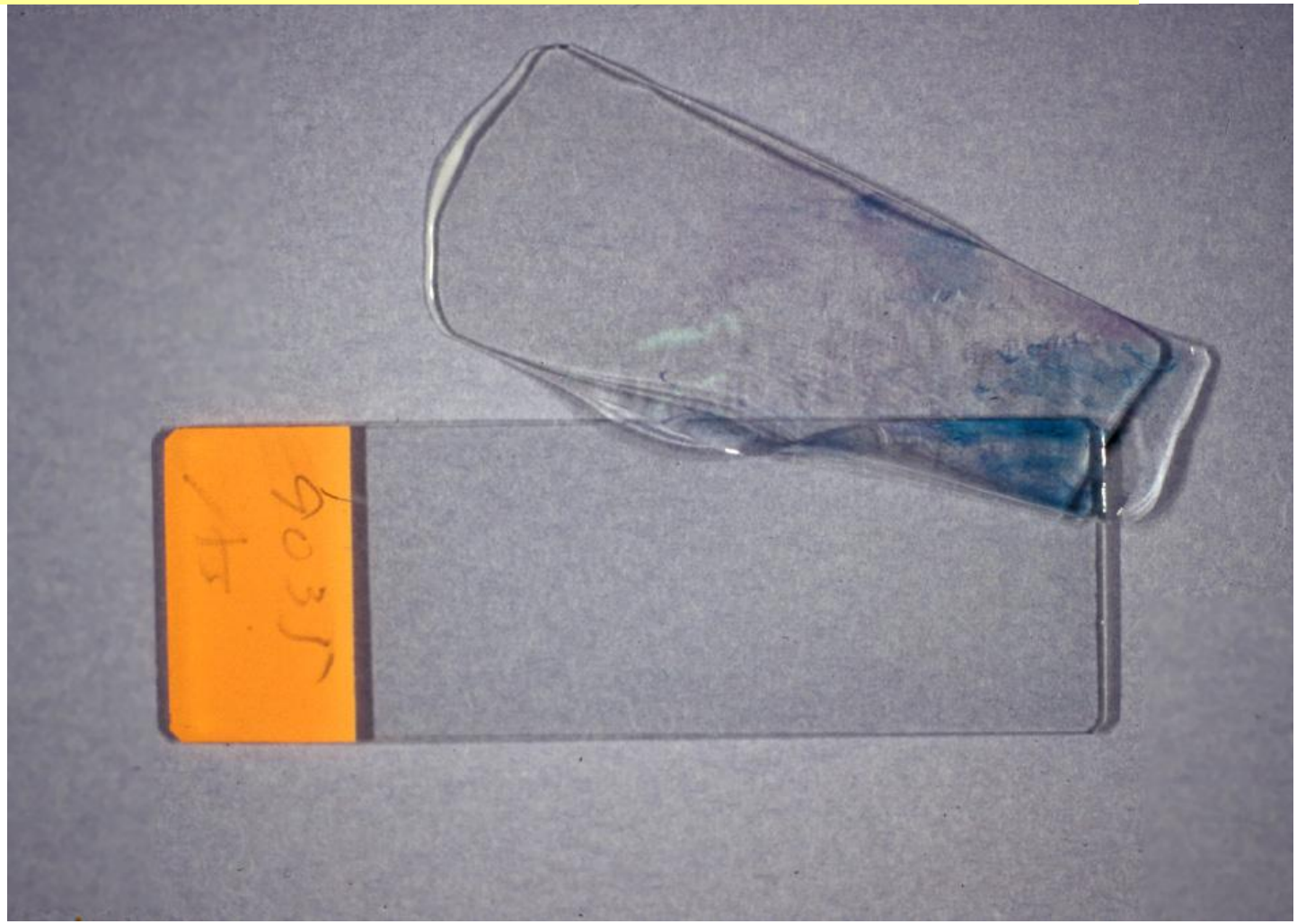

Pap-stained cells can be transferred to silane-coated glass slides by solidifying Malinol membrane. All the cells are included in the membrane side.

Cell transfer followed by cutting into pieces

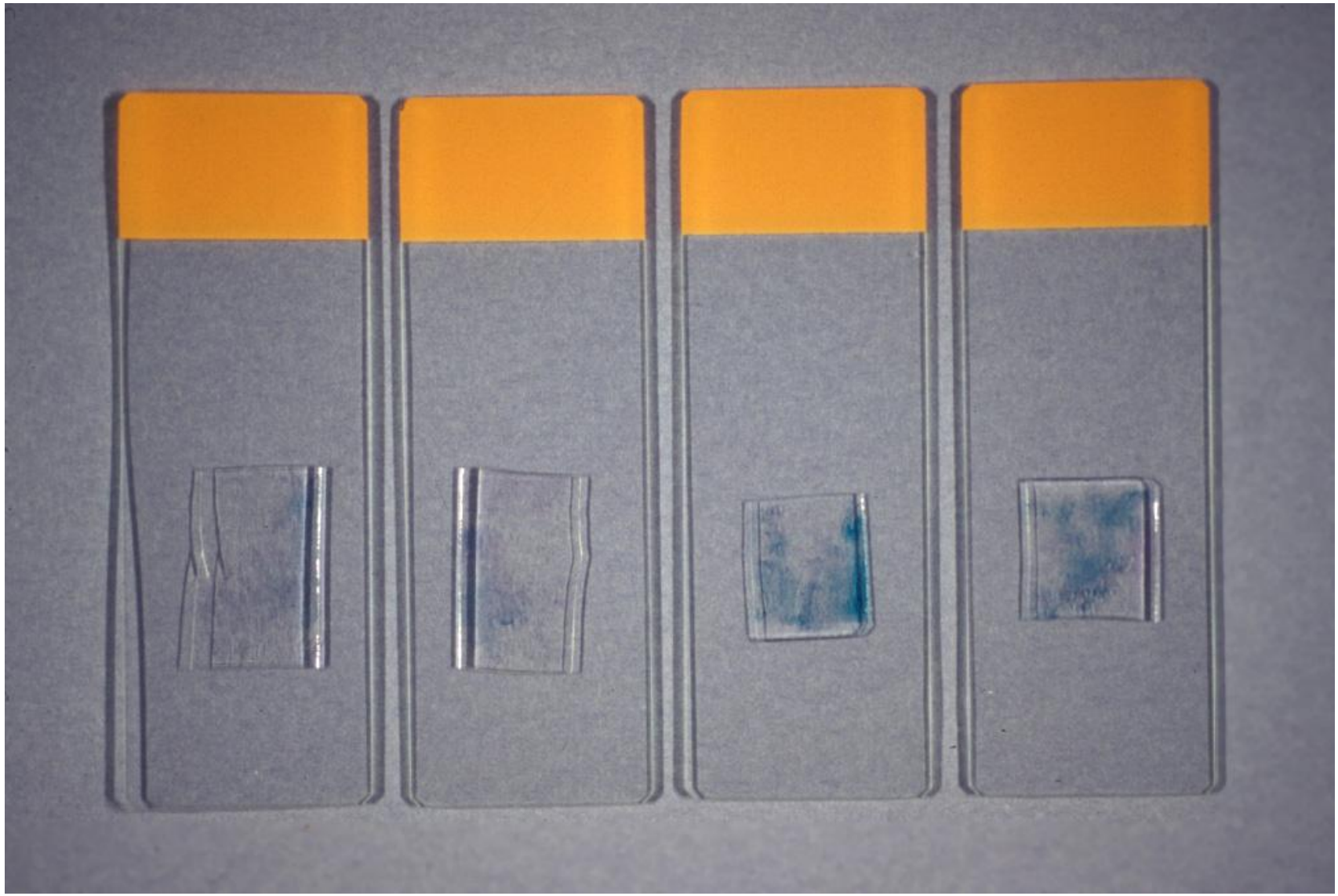

Several Silane-coated glass slides are ready for histochemistry by cutting the solidified Malinol membrane into several pieces.

HPV16-ISH in severe dysplasia

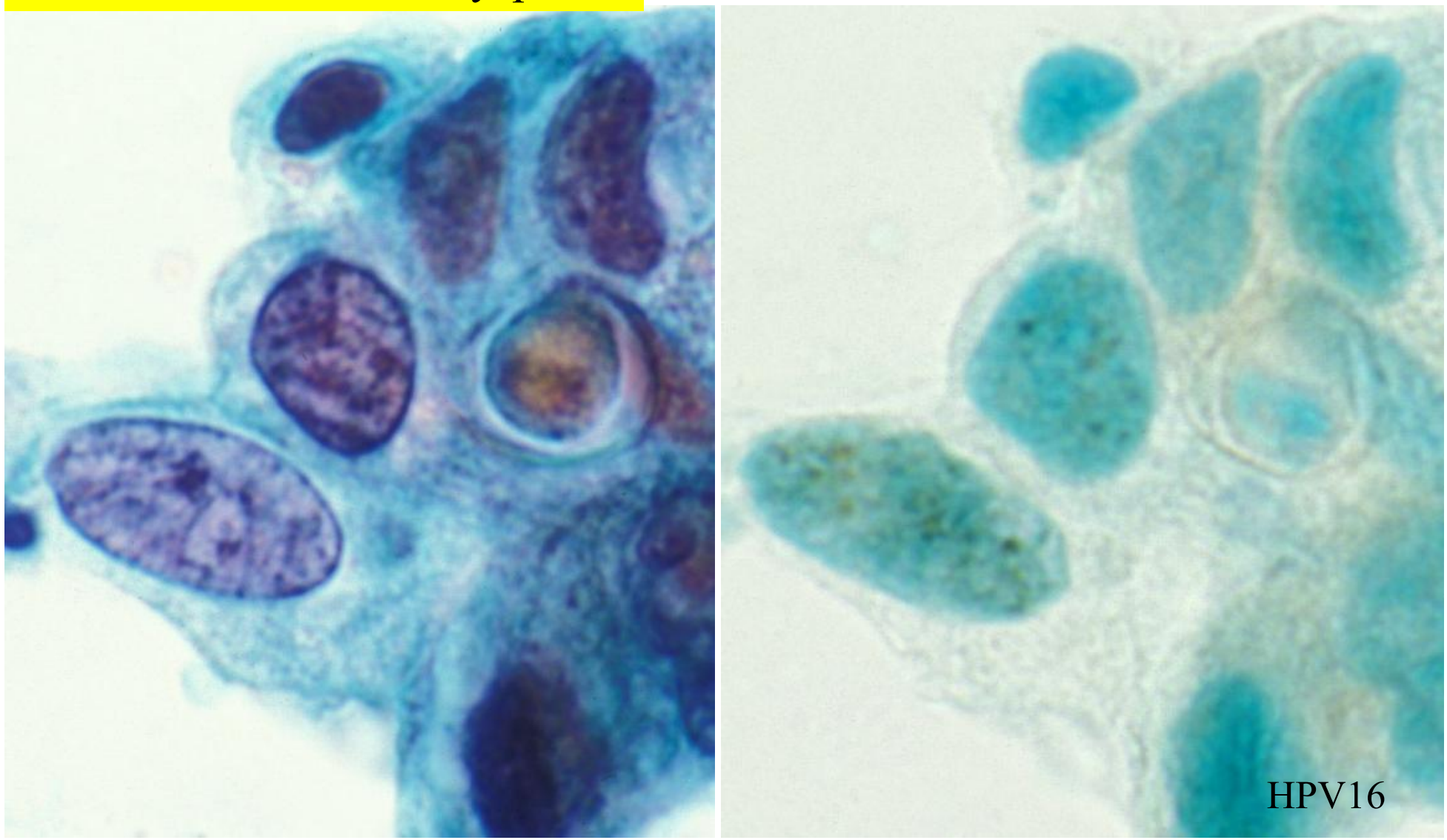

Severe dysplasia in cervical smear (left : pap, right : *in situ* hybridization). The smear was cell-transferred to Silane-coated glass slide to detect HPV16 genome with ISH. ISH requires heating to dissociated double-stranded DNA into single-stranded, the cell transfer technique is indispensable.

Entamoeba gingivalis colonization in the uterine cavity inserted with IUD

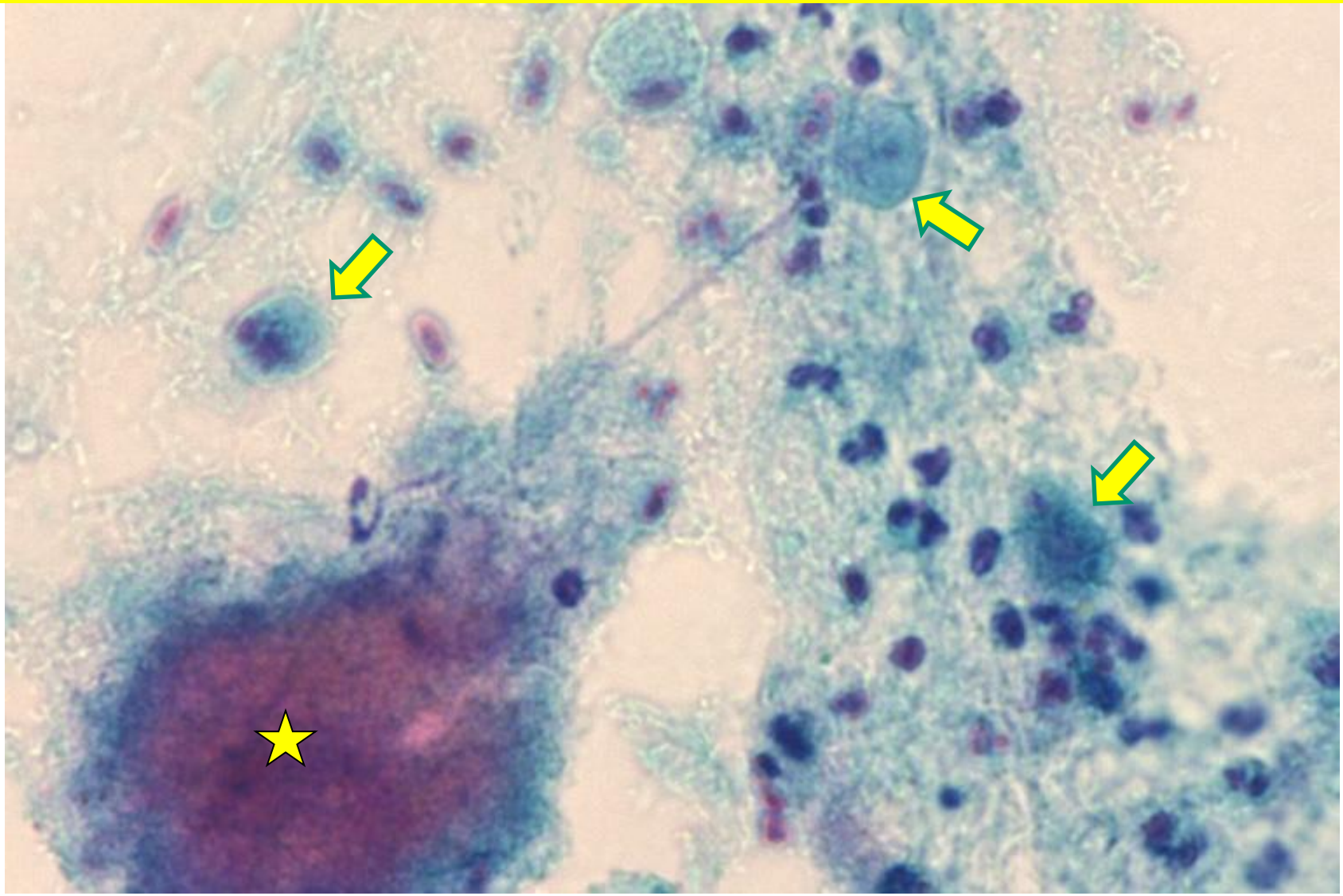

A 50 y-o female with prolonged insertion of intrauterine contraceptive device. Cytology specimen of the exudates around the device is shown (Pap). Adjacent to an actinomycotic grain (asterisk), amebic trophozoites phagocytizing neutrophils are scattered (arrows).

Entamoeba gingivalis colonization in the uterine cavity inserted with IUD

PCR for *Entamoeba* species

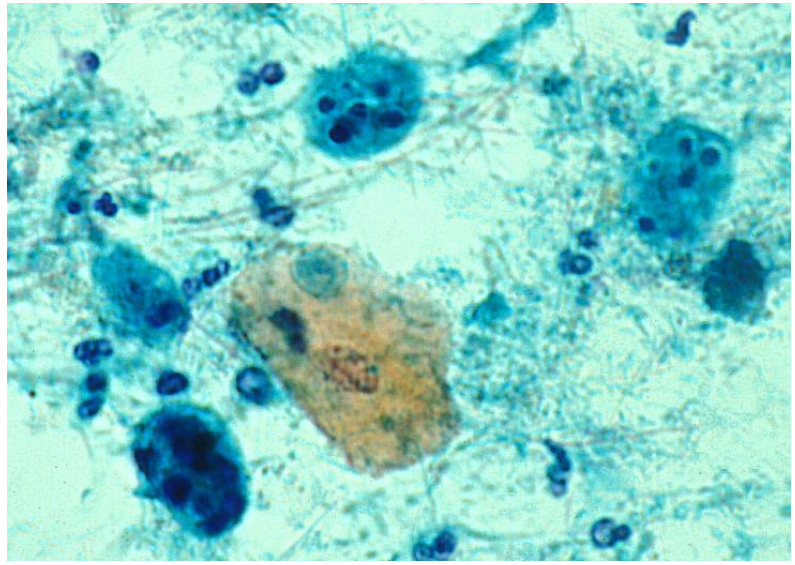

Entamoeba gingivalis is a commensal microbe in the oral cavity. Smear from the dental plaque discloses neutrophil-phagocytizing amebic trophozoites.

Primers sense 5'– tcagataccgtcgtagtcct – 3'
antisense 5'– cctggtgtgcccttccgt – 3'

PCR conditions: 94°C15 sec, 55°C30 sec, 72°C30 sec: 35 cycles

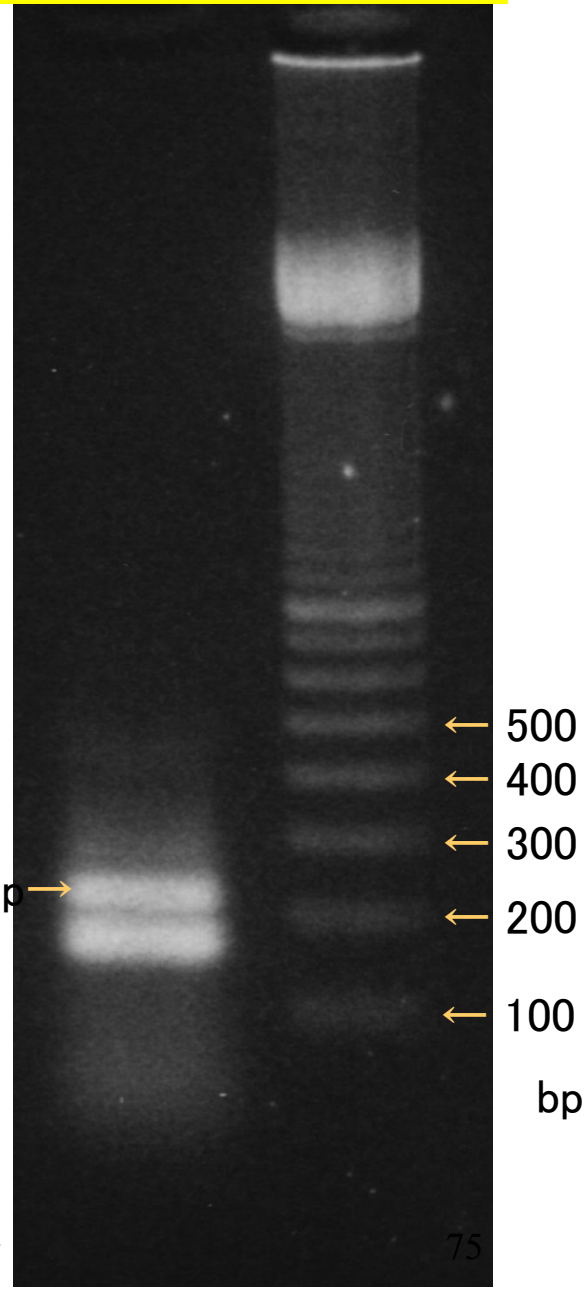

The 221bp PCR-amplified fragment shows a high homology with *E. gingivalis* genome.

E. gingivalis lacking mitochondria is an anaerobic microbe. The co-colonization with anaerobic *Actinomyces israelii* is essential for the protozoa to survive in the uterine cavity. The transmission is mediated by oral sex.

Use of patients' sera for histopathological diagnosis

1) High antibody titers (at 1: 1,000 dilution) are expected, when abscess or granulomas confirmed.

2) Indirect immunoperoxidase staining should be employed using formalin-fixed paraffin-embedded sections. The detection method with high sensitivity demonstrates endogenous human IgG in the background tissue fluid.

3) The technique is especially useful when commercial-based antibodies are hardly available.

4) High specificity is expected particularly for the protozoa and helminth.

5) Sera from carriers of hepatitis viruses and HIV should not be used to avoid biohazard.

Use of the patient serum for indirect immunoperoxidase staining

1) Check the viral markers of the patient
2) Make a phone call to keep the patient serum
3) Dilute the serum with PBS at 1:500 or 1:1,000
4) Incubate deparaffinized sections with diluted serum
5) Incubate then with HRP-labeled anti-human IgG (1:50)
6) Color reaction in diaminobenzidine-H_2O_2 solution
7) Nuclear counterstaining with Mayer's hematoxylin

Use of patients' sera for immunohistochemical diagnosis of infectious diseases

1) Bilharziasis
2) Visceral leishmaniasis
3) Cutaneous leishmaniasis
4) Acanthoamebic encephalitis

Ref.: Tsutsumi Y. Low-specificity and high-sensitivity immunostaining for demonstrating pathogens in formalin-fixed and paraffin-embedded sections. IntechOpen 2019; #66392) doi: 10.5772/intechopen.85055

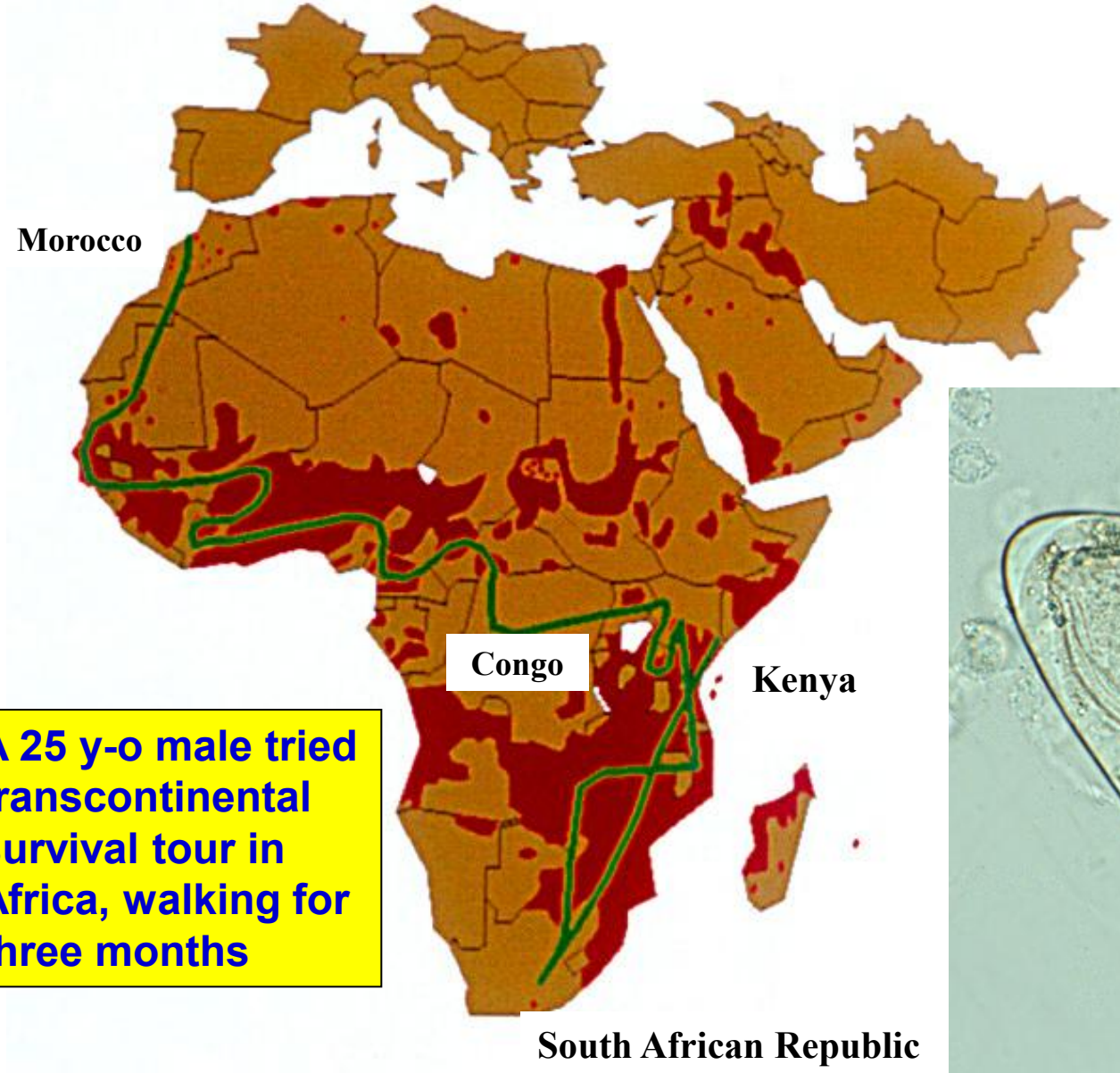

A 25 y-o male tried transcontinental survival tour in Africa, walking for three months

Distribution of bilharziasis

Route of survival tour

Three years later, the patient complained of hematuria

Ova of *Schistosoma hematobium* in urine ～movile miracidium seen under the microscope～

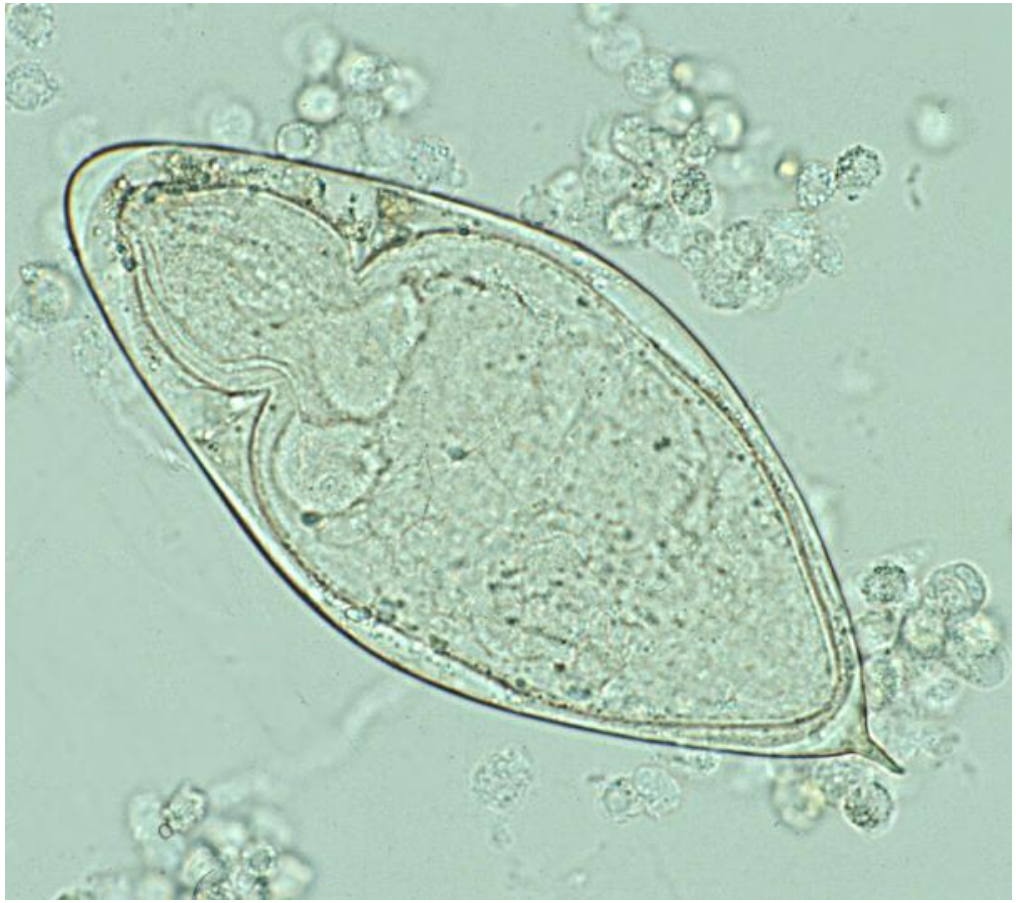

Bilharziasis of the colon

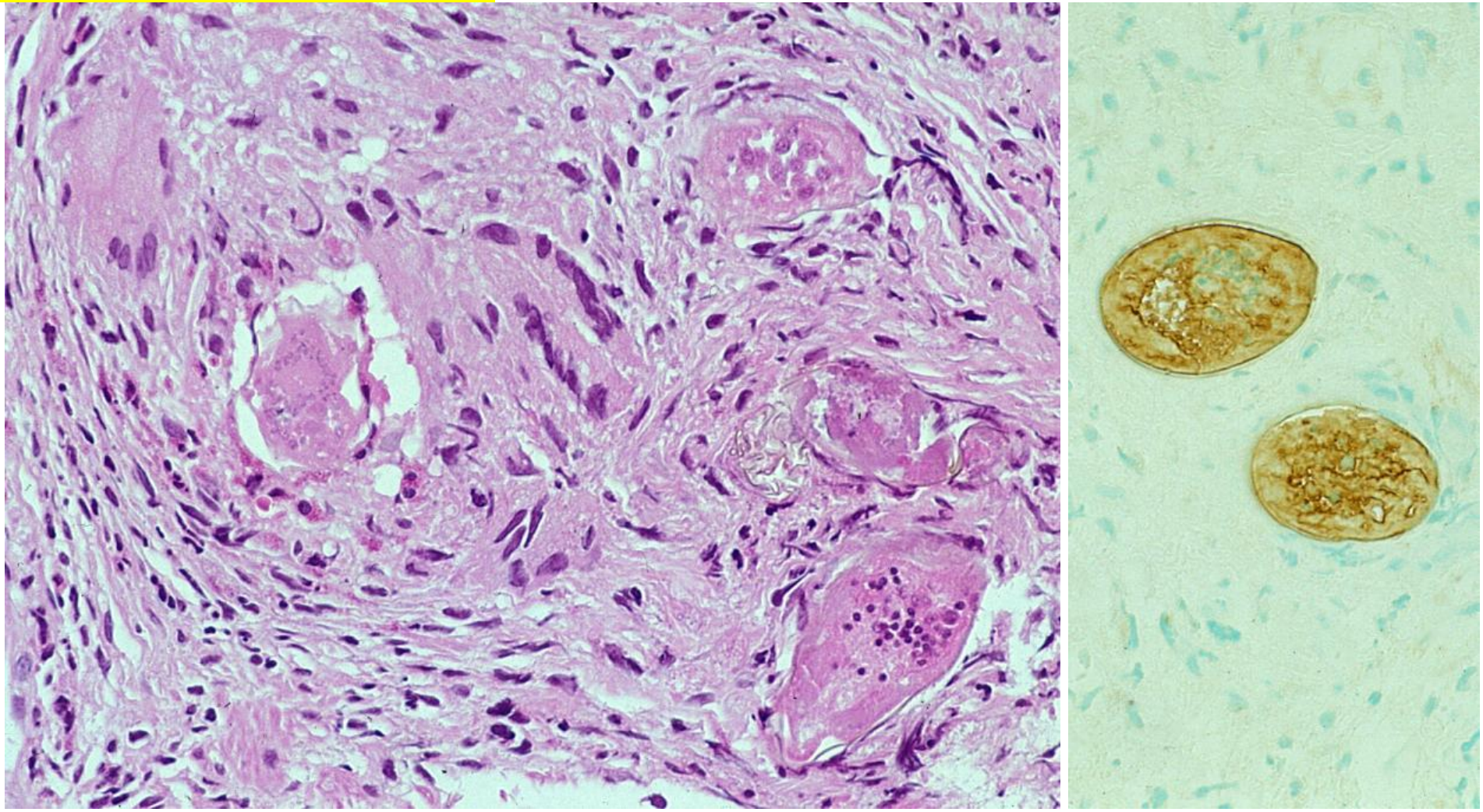

Bilharziasis of the colon. Colonofiberscopy demonstrated a whitish nodular lesion in the sigmoid colon. Biopsy revealed foreign body reaction against ova to form the egg tubercle (H&E). The 1:500 diluted patient's own serum reacts with the ova (indirect immunoperoxidase method).

Visceral leishmaniasis

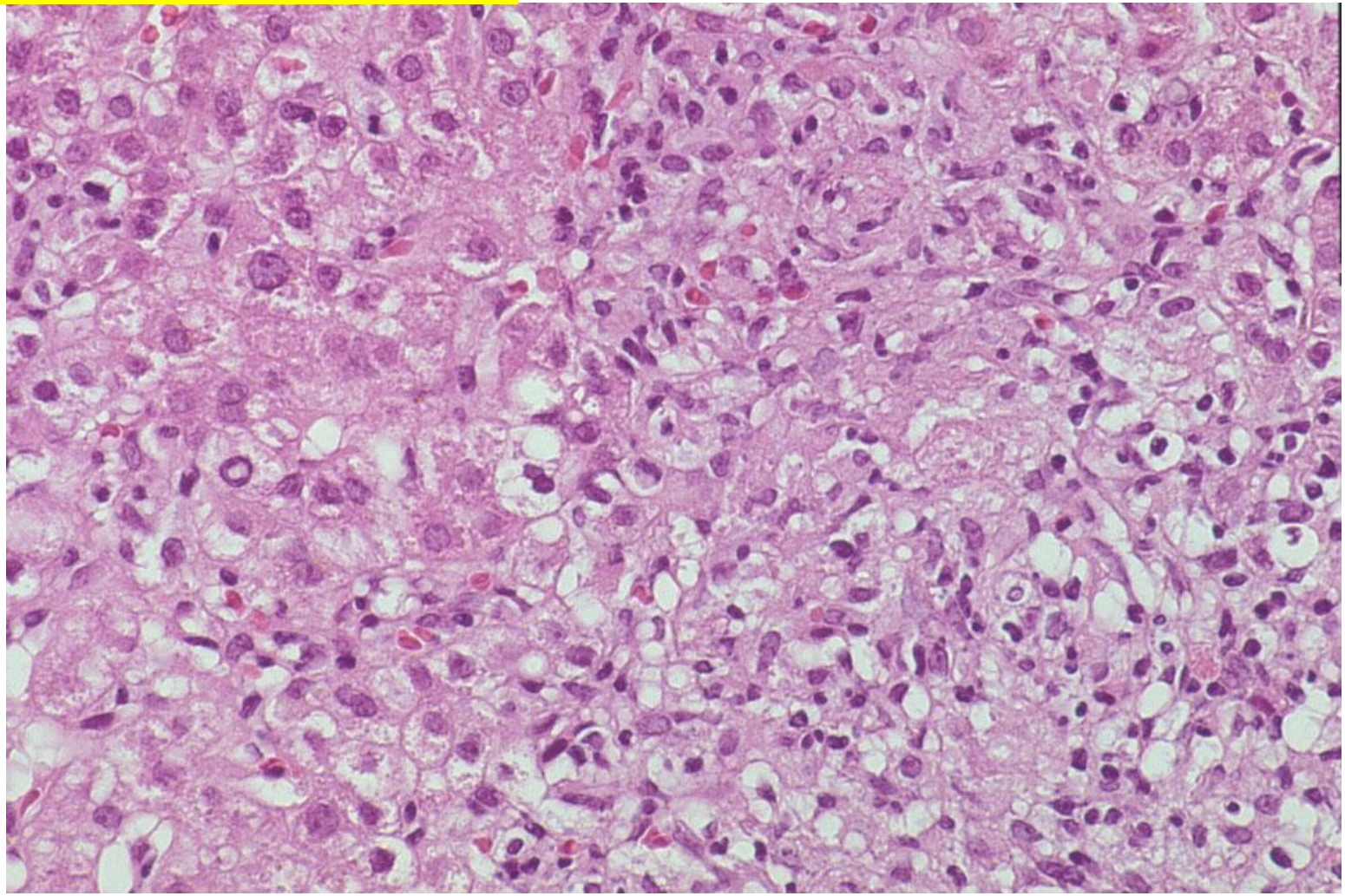

A 60 y-o businessman working in India manifested fever of unknown origin, liver dysfunction and DIC. Liver biopsy showed non-caseous microgranuloma (H&E). Immunostaining using a panel of anti-pathogen antibodies failed to detect the causative pathogens in the lesion.

Visceral leishmaniasis

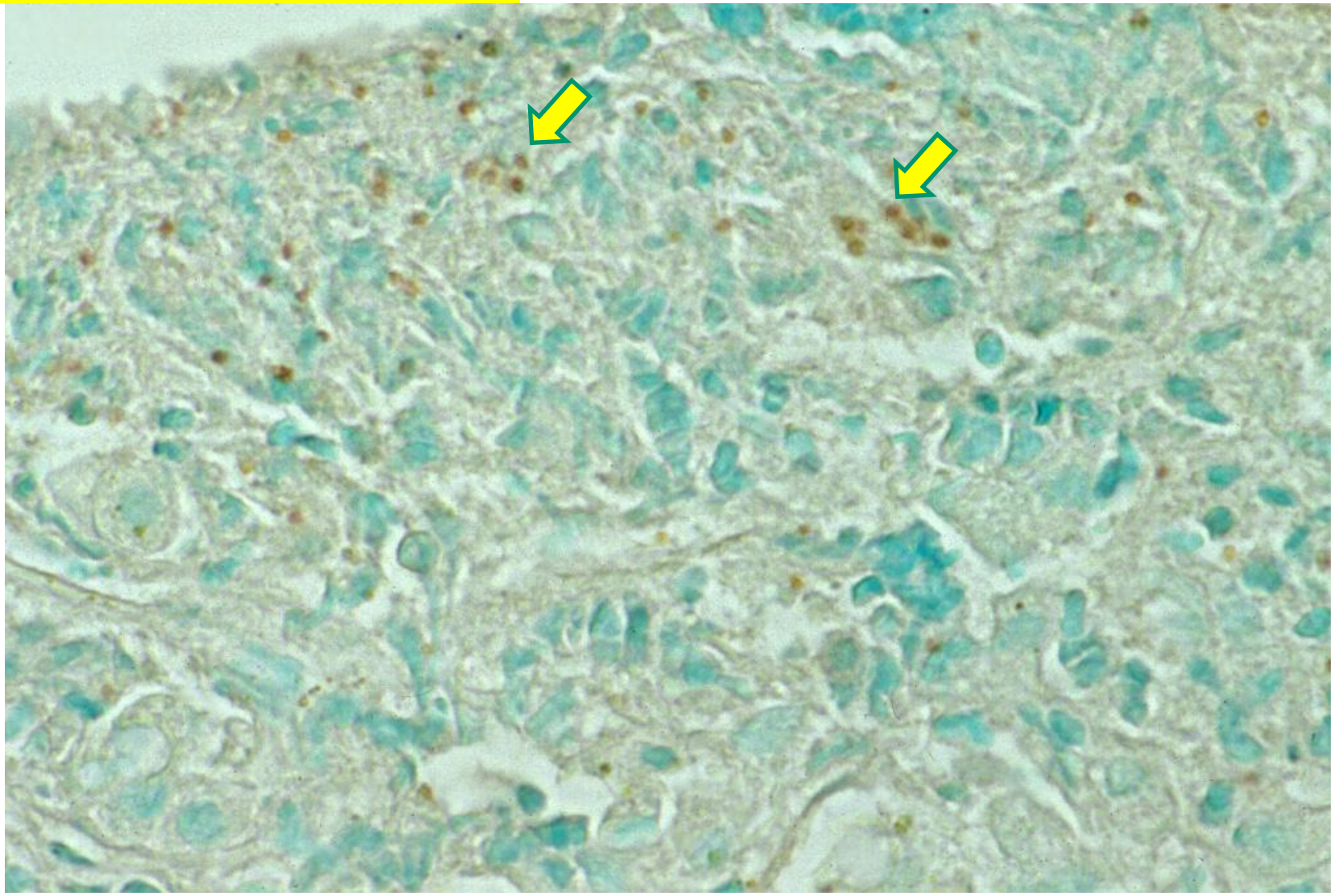

Red blood cell-sized protozoan parasites in the cytoplasm of epithelioid cells reacted with the diluted patient's own serum (arrows), and this was the key finding, leading to the final diagnosis of **visceral leishmaniasis** (**Kala azar**).

African-type cutaneous leishmaniasis

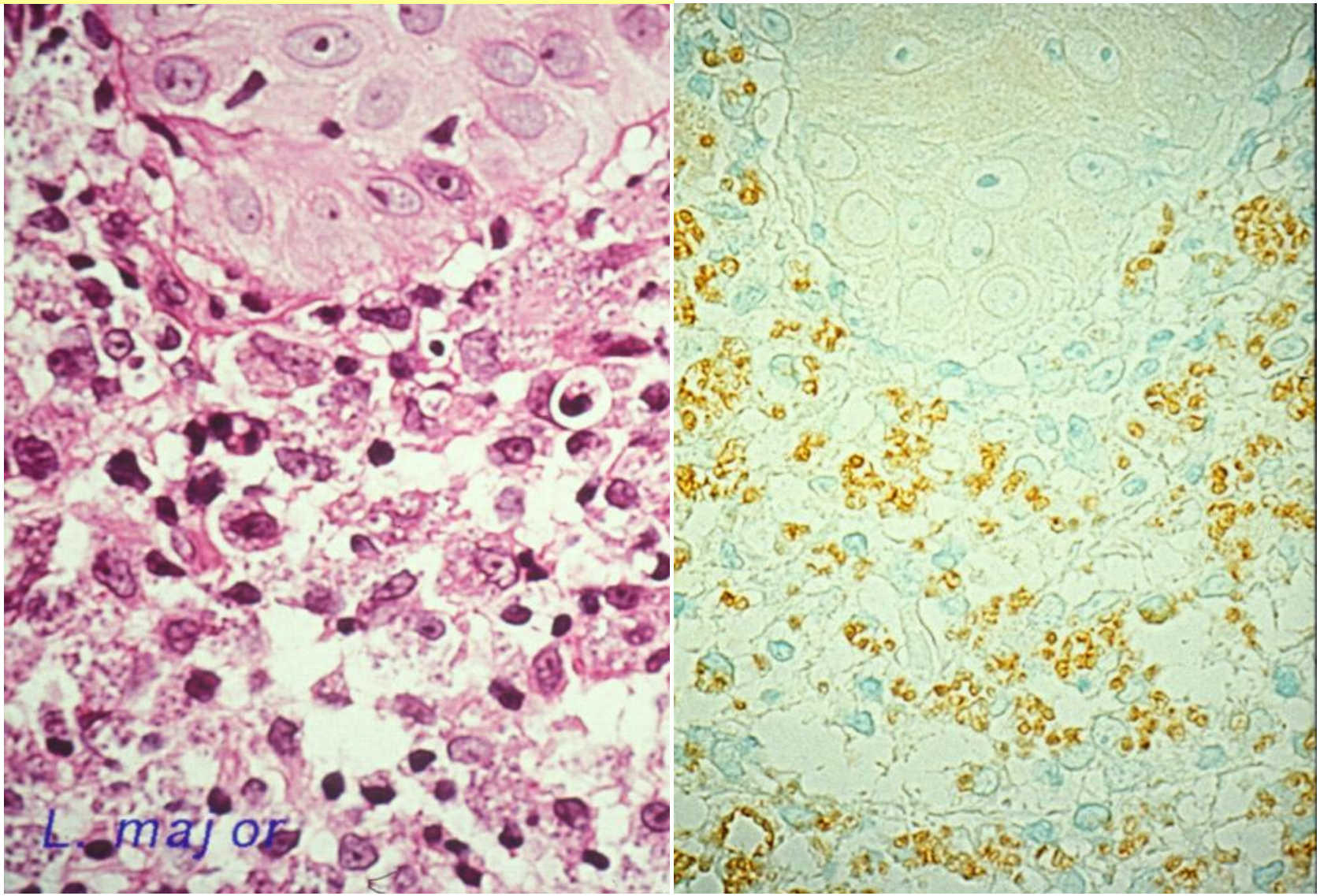

A Japanese plantation volunteer working for Mali Republic. Multiple skin ulcers were formed on the arms months later. The diagnosis of **cutaneous leishmaniasis** (*Leishmania major* infection) was confirmed with the reactivity to the diluted patient's own serum.

Acanthoamebic encephalitis (*Acanthoamoeba culbertsoni* infection)

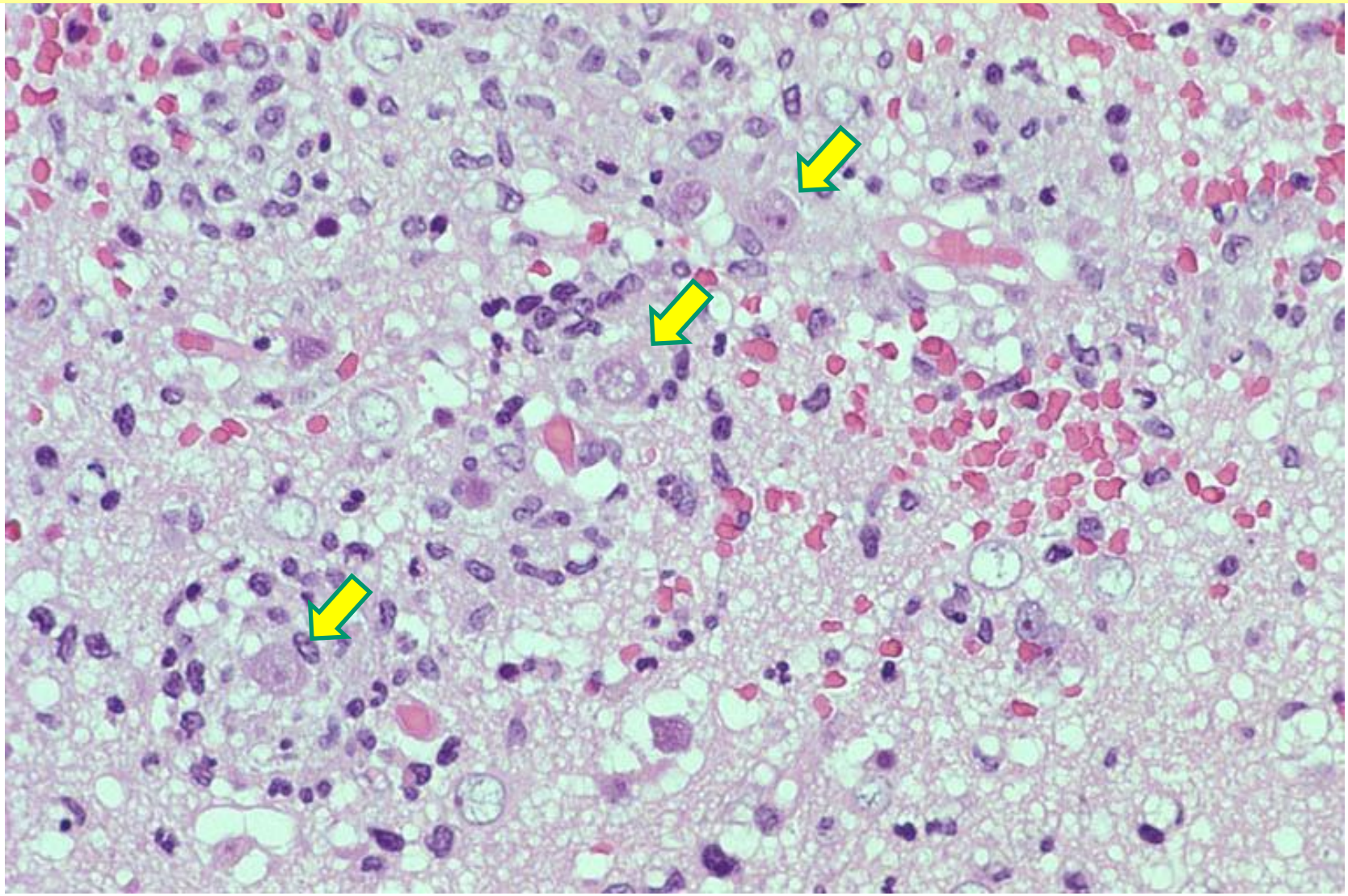

Acanthoamebic encephalitis. A 60 y-o male patient with alcoholic cirrhosis presented with progressive consciousness disturbance. Brain biopsy reveals granulomatous encephalitis with amebic trophozoites (arrows).

Acanthoamebic encephalitis (*Acanthoamoeba culbertsoni* infection)

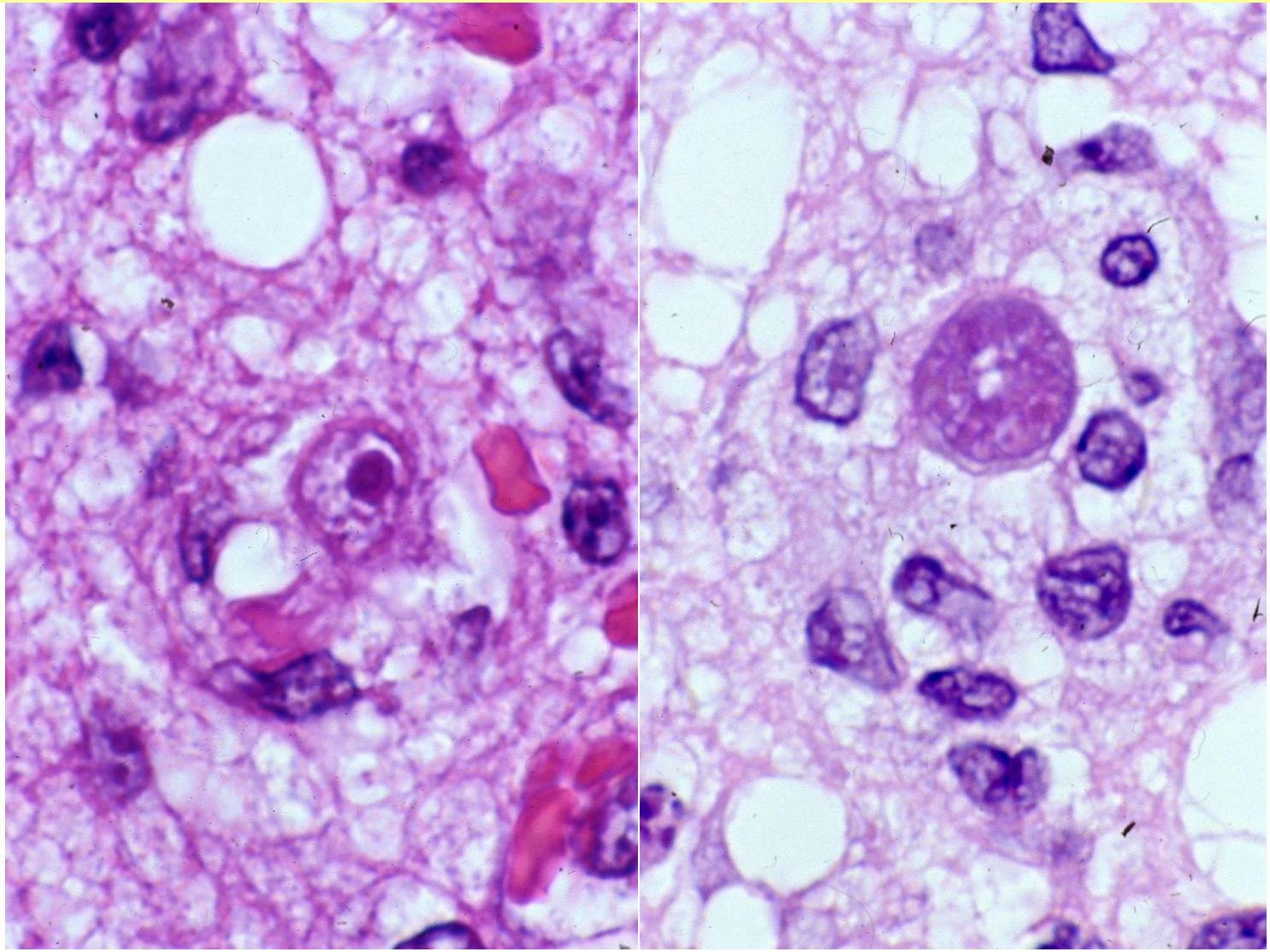

Acanthoamebic encephalitis. A 60 y-o male patient with alcoholic cirrhosis presented with progressive consciousness disturbance. Close examination of the brain biopsy reveals a trophozoite (left) and cyst (right) of the free-living amoeba (H&E).

Acanthoamebic encephalitis (*Acanthoamoeba culbertsoni* infection)

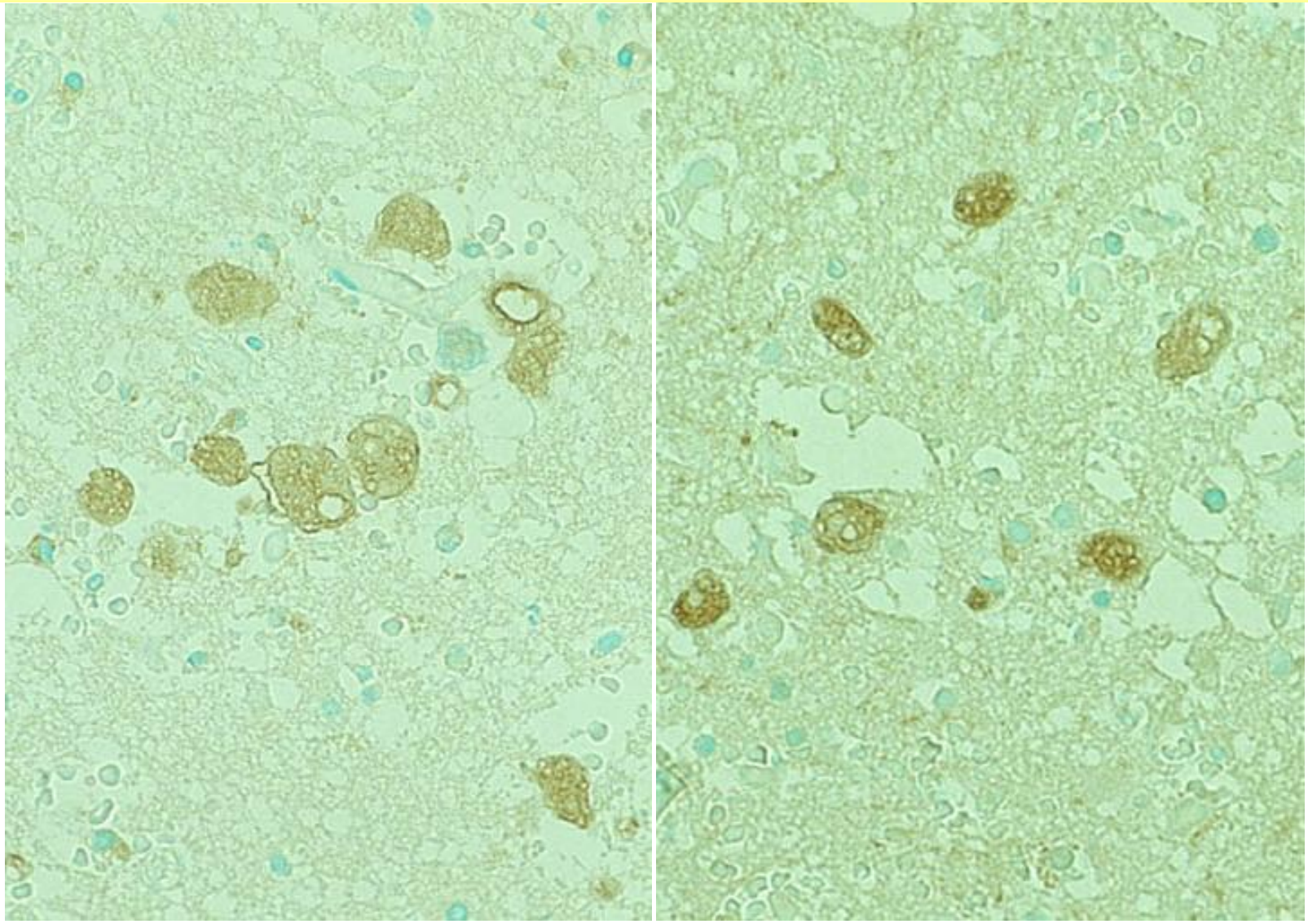

Acanthoamebic encephalitis. The diluted patient's own serum detects amebic pathogens in formalin-fixed, paraffin-embedded sections (left). A mouse antiserum against *Acanthoamoeba culbertsoni* was also immunoreactive (right).

Use of paraffin sections for ultrastructural study to identify viral pathogens

Ref.: Tsutsumi Y. Electron microscopic study using formalin-fixed and paraffin-embedded material, with special reference to observation of microbial organisms and endocrine granules. *Acta Histochem Cytochem 2018;* 51(2): 63-71. doi: 10.1267/ahc.18012

A 10-year-old Japanese boy, receiving BMT for recurrent ALL

CD34-positive stem cells isolated from HLA-mismatched father was transplanted.

One week later, diarrhea started, and hematochezia followed in 2 weeks.

Massive GI hemorrhage, 1 L/day, for 3 months to lead the patient to death.

No hematuria recorded.

At autopsy, acute GVHD observed histologically in the skin, liver and colon.

Viral intranuclear inclusions were seen in the jejunal intestinal mucosa and urinary bladder mucosa.

Dual DNA viral infections in the jejunum and urinary bladder

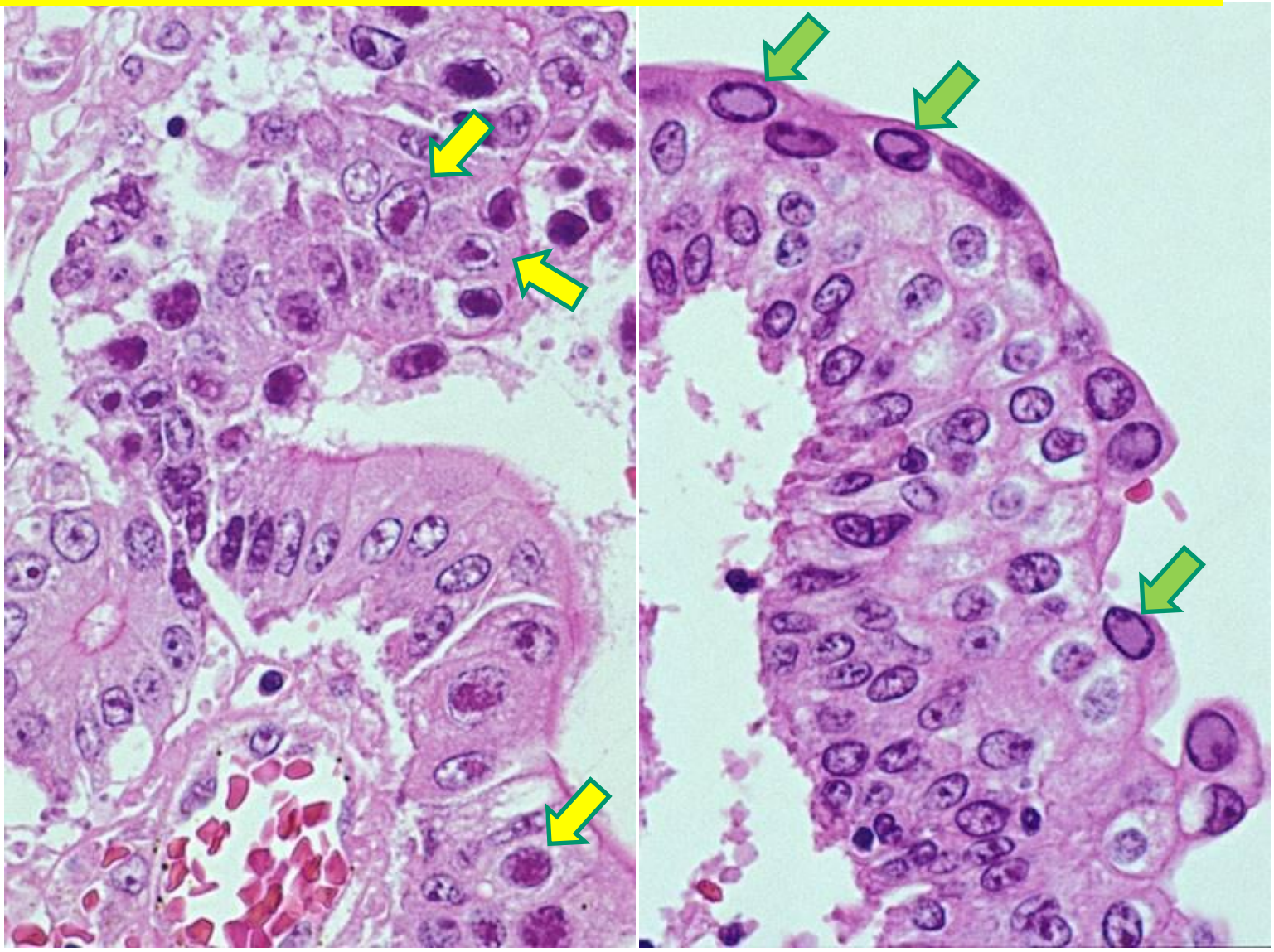

At autopsy, the epithelial cells possessed intranuclear viral inclusions. Left: jejunal mucosa with **adenovirus infection** (yellow arrows), right; umbrella cells of the urinary bladder mucosa with **BK virus infection** (green arrows).

Dual DNA viral infections in the jejunum and urinary bladder

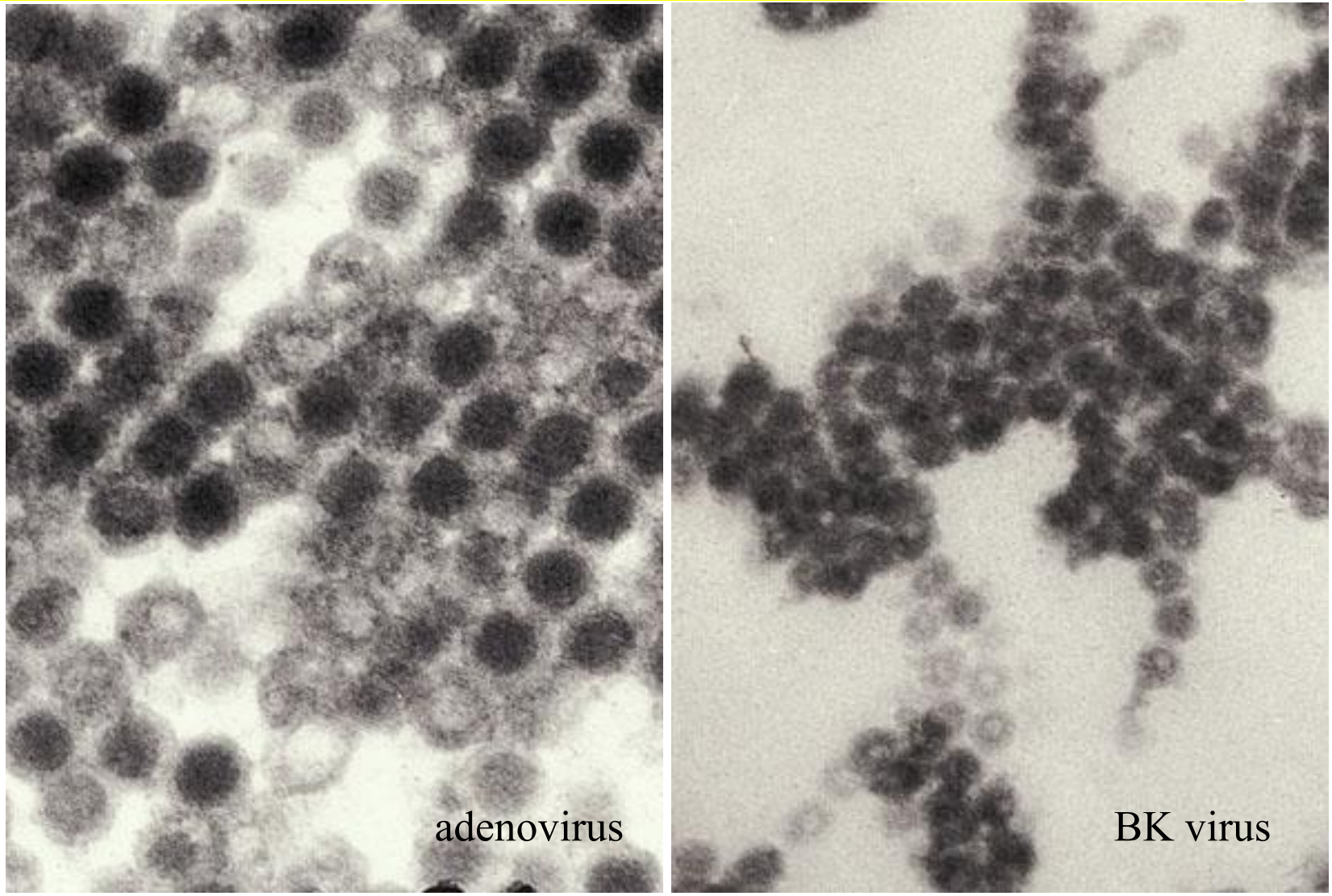

Ultrastructural visualization of viral infection in formalin-fixed, paraffin-embedded sections. **Adenovirus** virions seen in the jejunal epithelium (left) and **BK virus** virions seen in the urinary bladder mucosa (right).

Summary of the histologic findings

Small bowel epithelia contain intranuclear inclusion bodies.

Urinary bladder urothelia (umbrella cells) also reveal nuclear inclusion bodies.

The inclusions belonged to either full (smudge) type or Cowdry's type A.

Targeted ultrastructural studies were performed using H&E -stained paraffin sections.

The gut epithelia reveal enveloped, regularly arranged, 70 nm hexagonal particles.

The urothelia show unenveloped 40 nm round irregularly clustered particles.

Surprising!

Use of archival tissue specimens fixed in formalin for many years for demonstrating pathogens in paraffin sections

Hodgkin's disease autopsied by Thomas Hodgkin himself

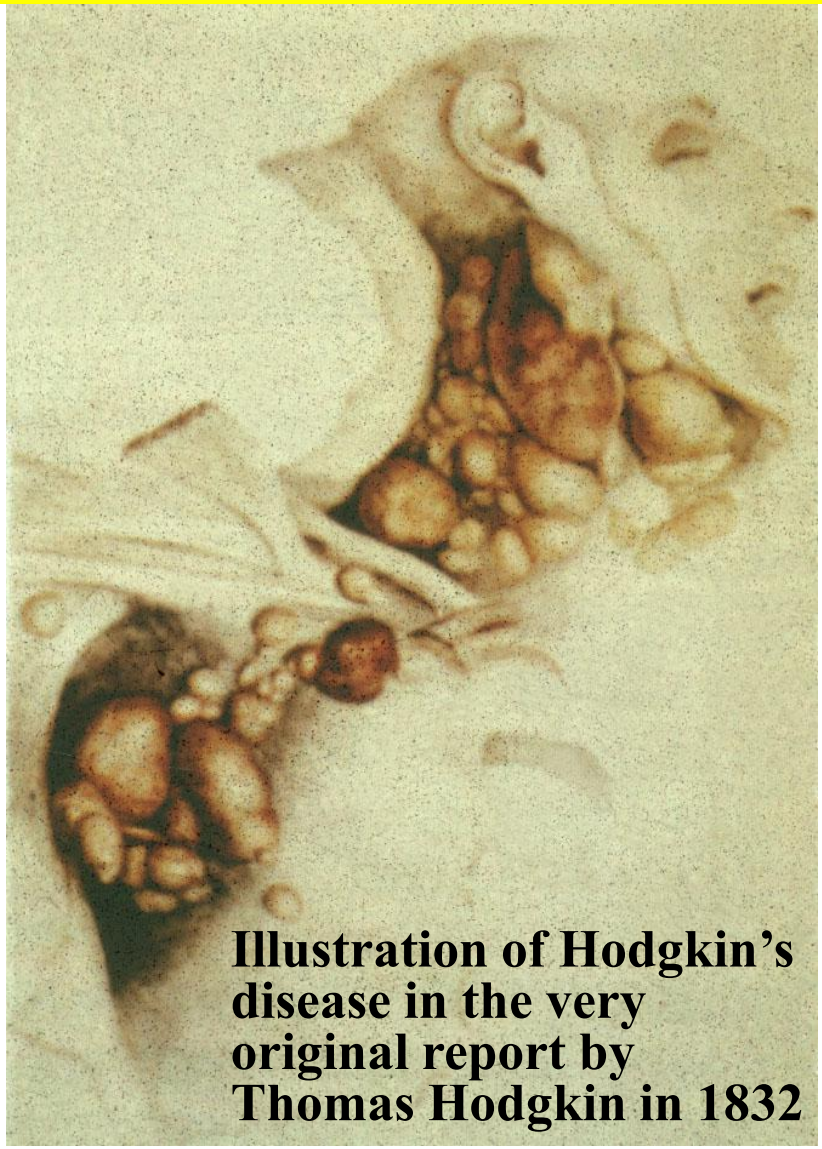

Illustration of the Hodgkin's disease in the very original paper reported by **Thomas Hodgkin** in 1832, and the specimens of Hodgkin's own autopsy cases exhibited in the Gordon Museum of Guy's Hospital, London

Hodgkin's disease autopsied by Thomas Hodgkin himself

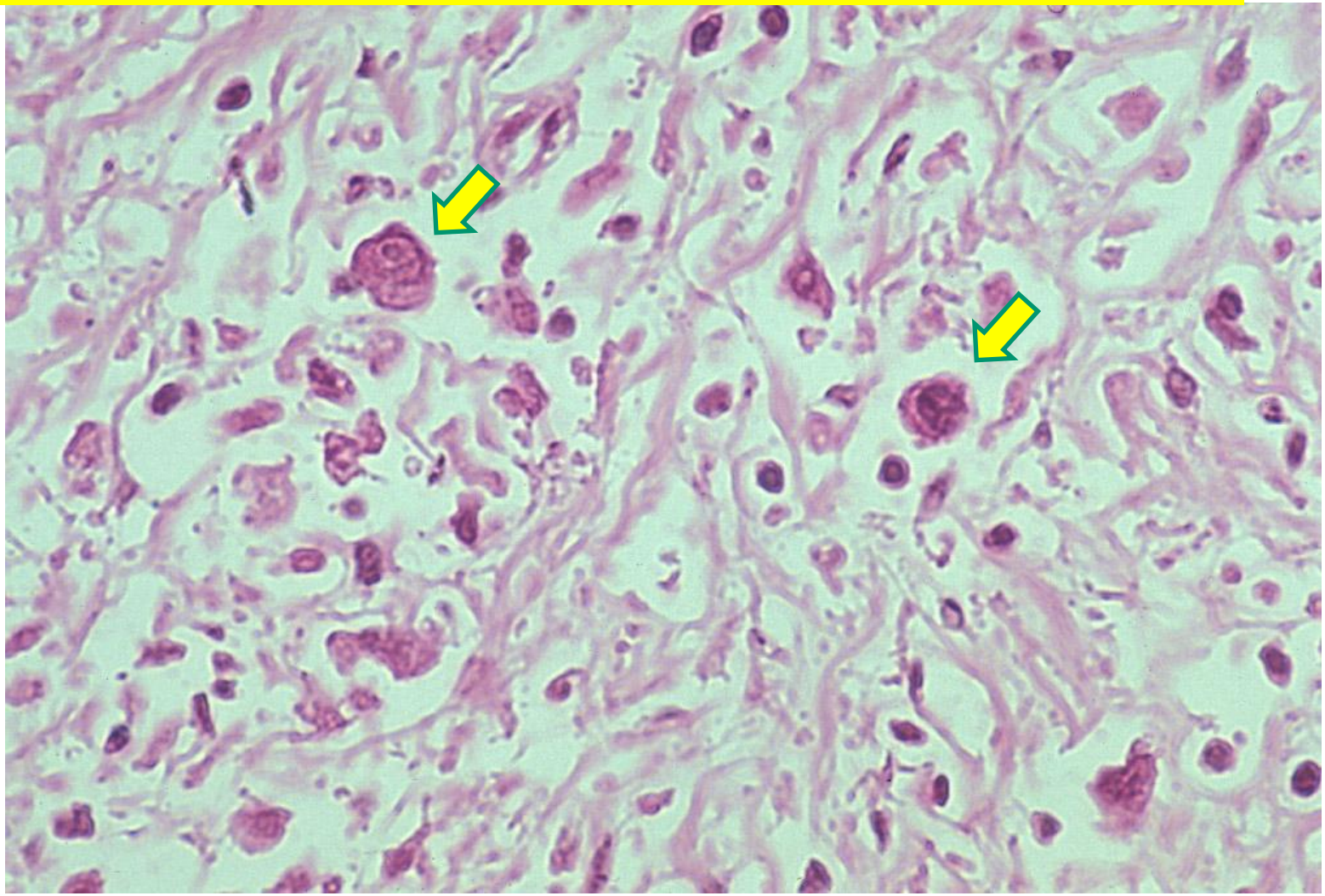

The unstained paraffin sections were given from the president of the Museum. The specimens were fixed in alcohol for 70 years and then in formalin for additional 90 years. The lymph node autopsied by **Thomas Hodgkin** himself was stained with H&E. Hodgkin cells are scattered (arrows).

Hodgkin's disease autopsied by Thomas Hodgkin himself

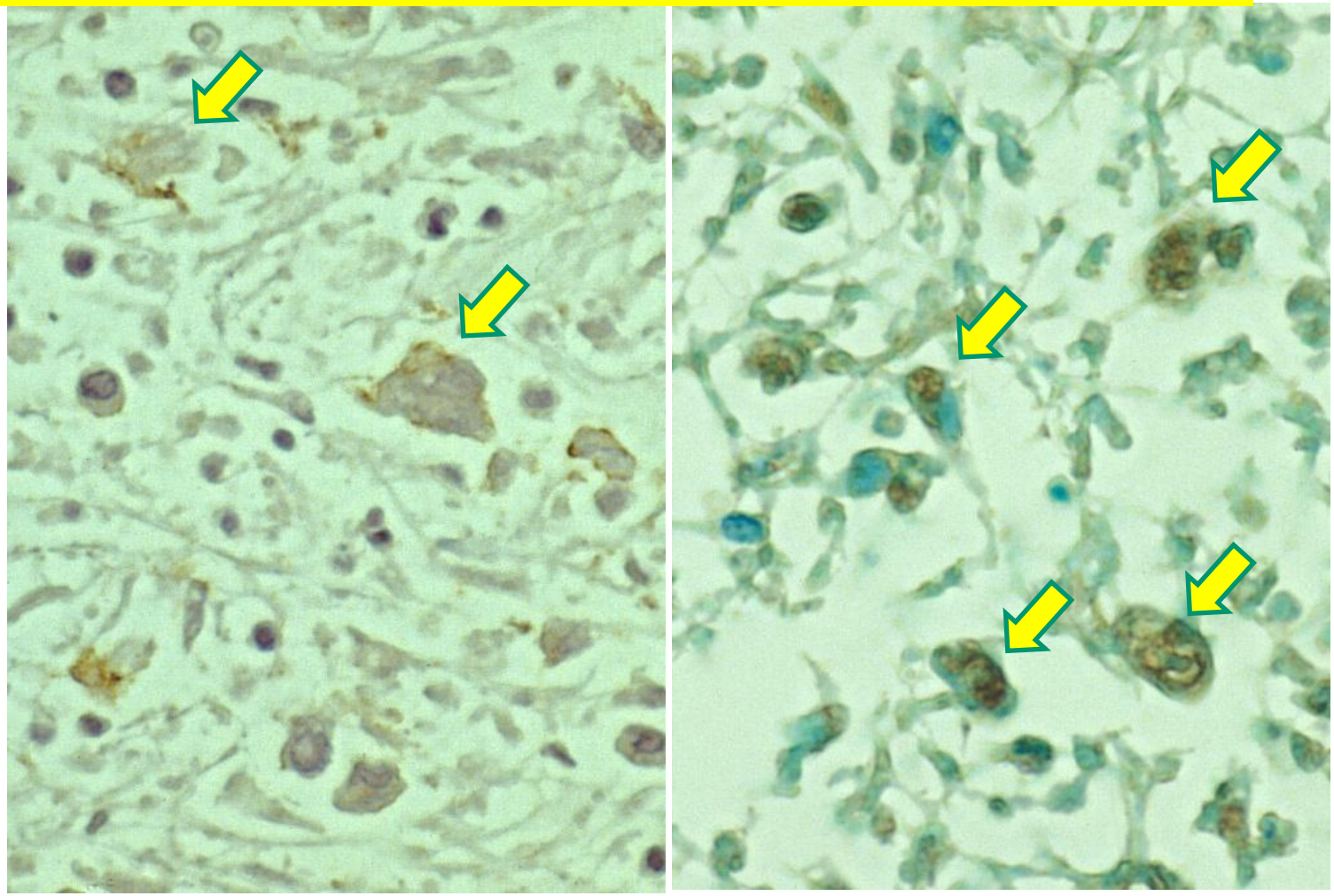

First, the single paraffin section was transferred to silane-coated glass slides with the cell transfer technique. Irrespective of an ultralong period of fixation, Hodgkin's markers were retained. See immunostaining for CD15 (Leu M1) (left) and *in situ* hybridization for EBER (right). **Ref.**: Tsutsumi Y. Demonstration of Epstein-Barr virus genome in archival paraffin sections of Hodgkin's lymphoma autopsied by Dr. Thomas Hodgkin nearly 170 years ago. Acta Histochem Cytochem 2003; 36: 511-514. doi: 10.1267/AHC.36.511

Detection of hepatitis virus B and C in archival autopsy specimens of liver cirrhosis

Two series included: a) Ten samples of liver cirrhosis autopsied during 1907 through 1930 and long fixed in formalin at Kyushu University, Fukuoka, and b) Twenty-two paraffin blocks of cirrhotic liver autopsied during 1940 through 1957 at Niigata University, Niigata. HBs antigen was immunostained using paraffin sections. HCV and its genotypes were identified by nested reverse transcription-polymerase chain reaction using total ribonucleic acid extracted from long-fixed tissue (Kyushu) or paraffin sections (Niigata). HBV was detected in eight (80%) of the Kyushu series, and in ten (45%) in the Niigata series. HCV genome was detected in two lesions in the respective series, and three belonged to genotype 1b and one to 2b. HBV was co-infected in three of four HCV-positive lesions. One lesion in the Niigata series with HCV genotype 1b without HBV co-infection showed fulminant transformation in cirrhotic liver. HBV infection was shown as early in 1907, and the oldest lesion with HCV infection was recorded in 1909.

Ref.: Tsutsumi Y, et al. Detection of hepatitis virus B and C in archival autopsy specimens of liver cirrhosis. *Biomed J Sci Tech Res* 2019. doi: 10.26717/BJSTR.2019.22.003757

PCR detection of HCV genome in archival cirrhotic specimens

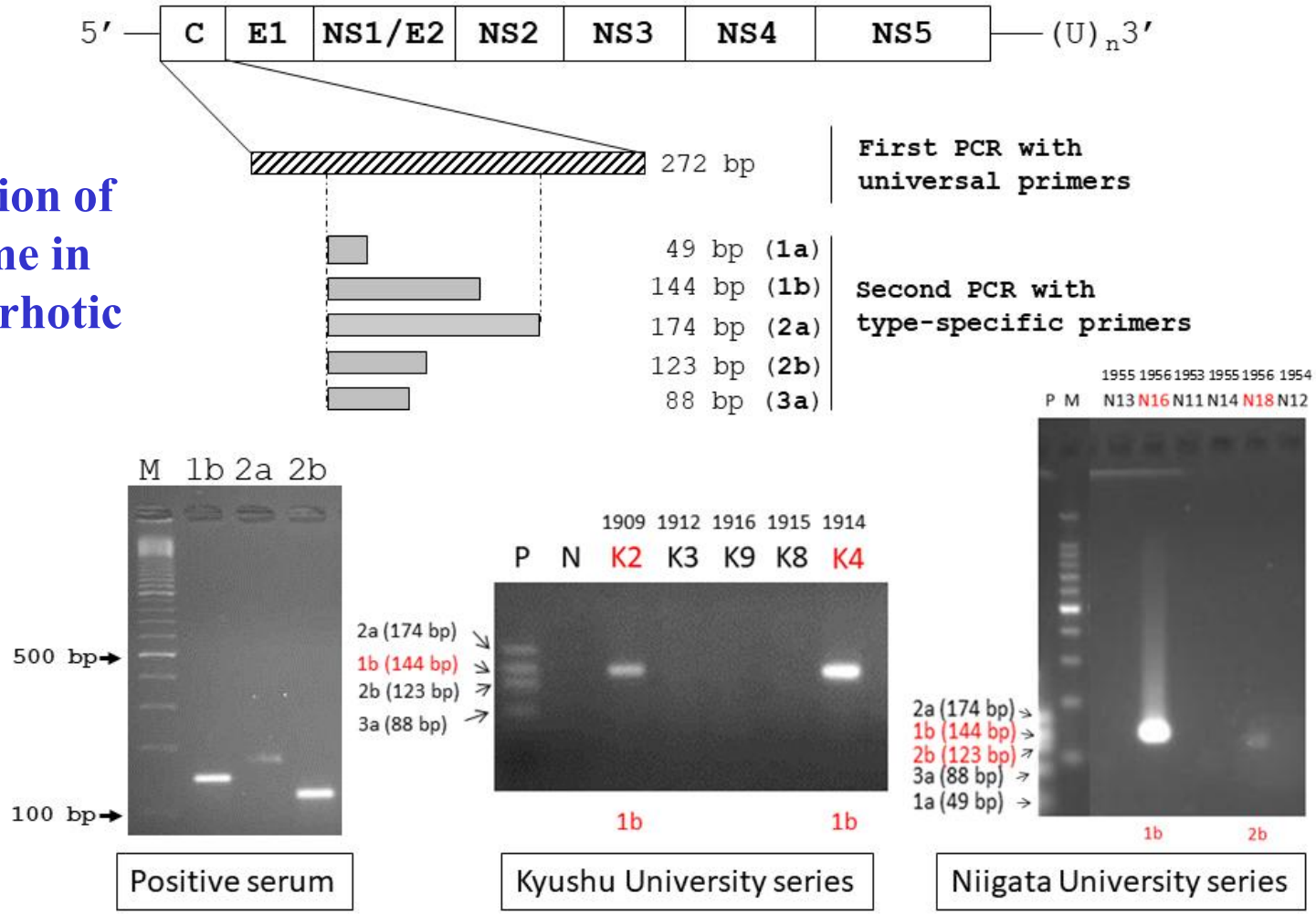

Schematic illustration of the genome organization of HCV and nested RT-PCR-mediated genotyping of HCV. The HCV genome structure and strategy of HCV genotyping are shown in the upper part (C: core region for nucleocapsid, E1-2: envelop glycoprotein regions, NS1-5: non-structural protein regions 1-5, M: molecular size markers). HCV-genotypes 1b (144 bp), 2a (174 bp) and 2b (123 bp) in human sera are visualized on the agarose gel (bottom left). HCV genotyping in the Kyushu University series (bottom center) and the Niigata University series (bottom right) are also illustrated. HCV genotype 1b was detected in three lesions (K2, K4 and N16), while one lesion (N18) contained genotype 2b. M: molecular size markers, P: positive controls, HCV genotypes 2a (174 bp), 1b (144 bp), 2b (123 bp), 3a (88 bp) and 1a (49 bp), N: negative control.

Immunohistochemical detection of HBs antigen in archival cirrhotic specimens

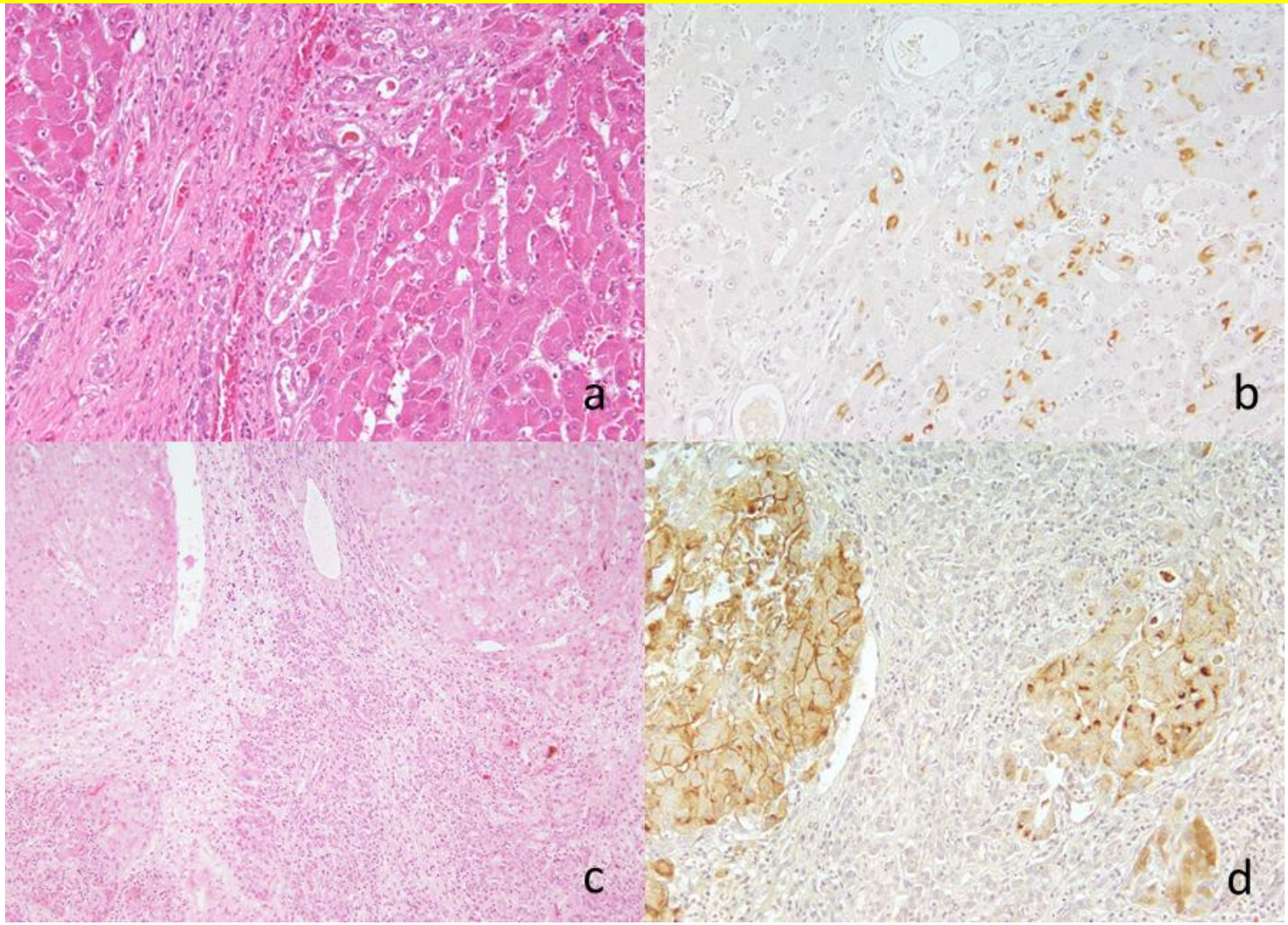

Cirrhotic microscopic appearance and HBs immunostaining in case K2 (a and b: HCV genotype 1b-positive) in the Kyushu University series and case N18 (c and d: HCV genotype 2b-positive) in the Niigata series. a and c: HE, b and d: immunostaining for HBs antigen using a monoclonal antibody HB024. **HBV infection** is observed in the cytoplasm (b) or on the plasma membrane (d) of hepatocytes in archival paraffin sections of liver cirrhosis.

Immunohistochemical detection of BCG antigens in caseous necrosis

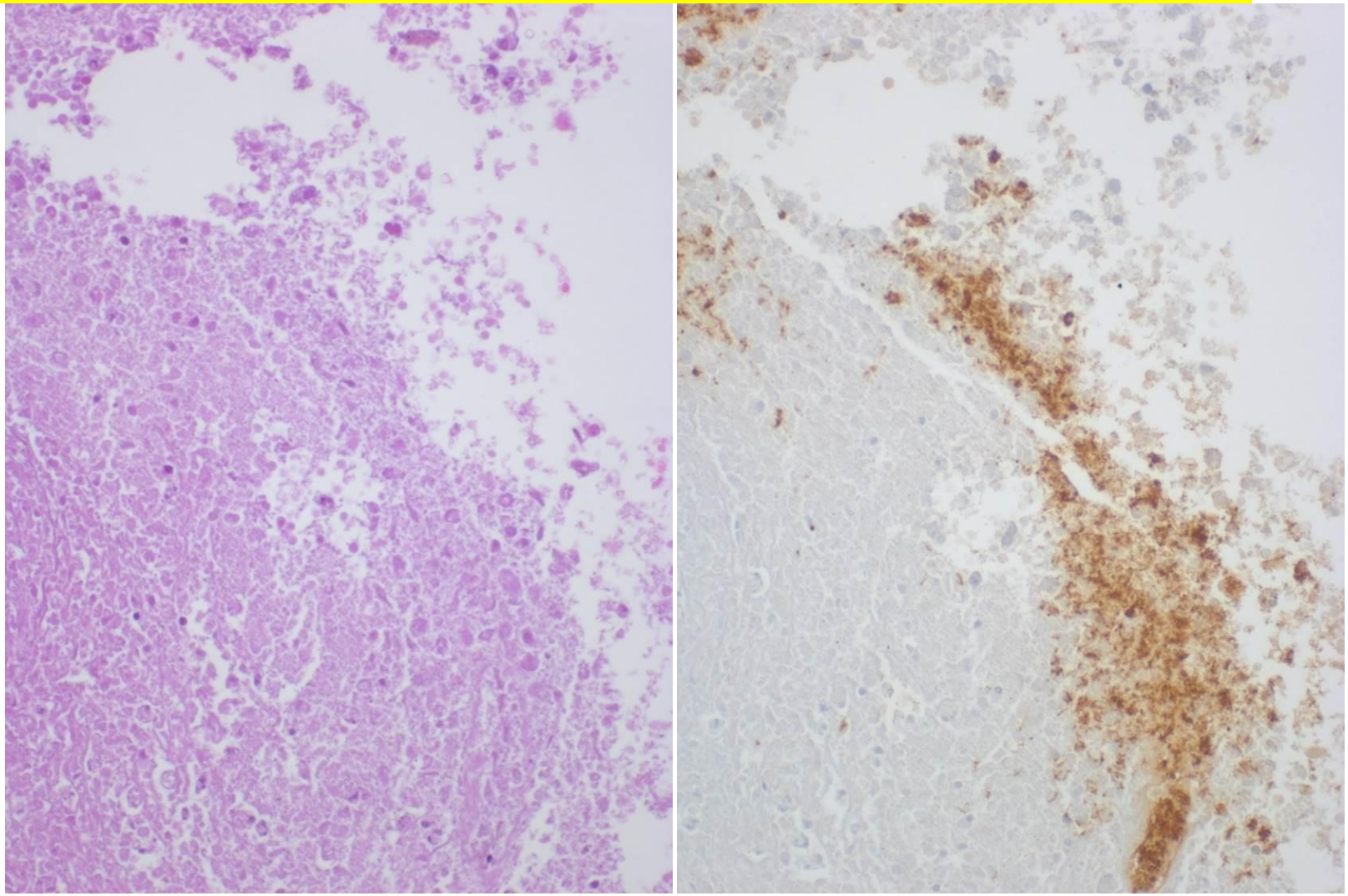

Lung tuberculosis in 1945, and fixed in formalin for 70 years. Caseous necrosis is shown in H&E (left). Immunostaining with BCG antiserum demonstrates mycobacterial antigens in paraffin sections (right).

Immunohistochemical detection of pneumococcal antigen in archival lobar pneumonia

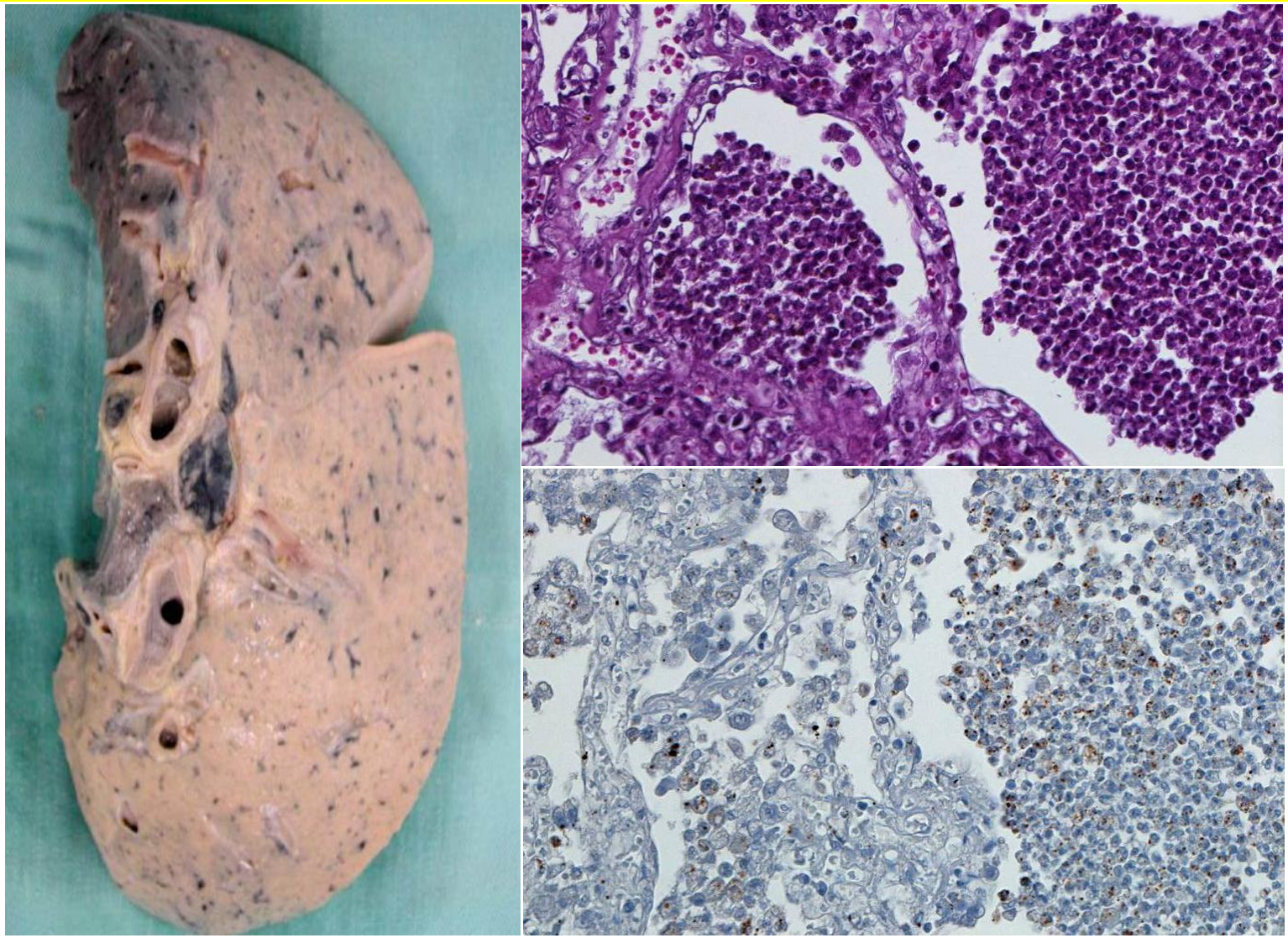

Lobar pneumonia fixed in formalin for 70 years. Left: gross appearance, right top: H&E, right bottom: Pneumococcus antigen. Pneumococcal antigen is detectable after long fixation in formalin.